CNS MYELINATION INVOLVES NONVESICULAR GLYCOLIPID TRANSPORT FROM ENDOPLASMIC RETICULUM TO PLASMA MEMBRANE IN OLIGODENDROCYTES

Jianping Wu

Graduate School of Systemic Neurosciences

LMU Munich

Dissertation at the
Graduate School of Systemic Neurosciences
Ludwig-Maximilians-Universität München

April, 2024

Supervisor
Prof. Dr. med Mikael Simons
Technical University of Munich
German Center for Neurodegenerative Diseases (DZNE)
LMU Munich

First Reviewer: Prof. Dr. med Mikael Simons
Second Reviewer: Prof. Dr. Angelika Harbauer
External Reviewer: Prof. Michael Hoppa

Date of Submission: 8th April 2024
Date of Defense: 9th July 2024

Table of Contents

Abstract

In the central nervous system (CNS), myelin is formed as oligodendrocytes wrap their plasma membrane multiple times around axons. Myelination, the process to generate myelin, requires a massive expansion of oligodendroglial plasma membrane. An outstanding question is how oligodendrocytes efficiently deliver lipids to the plasma membrane to facilitate myelination. Utilizing volume electron microscopy and immunohistochemistry, I demonstrated that mouse oligodendrocyte endoplasmic reticulum (ER) extends into developing myelin as tubules and is in close proximity to plasma membrane. Furthermore, tubular ER is highly correlated with myelination. Myelinating oligodendrocytes have elevated levels of tubular ER markers compared to premyelinating oligodendrocytes, suggesting oligodendrocytes increase the amount of tubular ER when they start to myelinate. When developmental myelination is complete, tubular ER is downregulated in white matter.

I hypothesized that lipids can be transferred directly from the ER to the plasma membrane at these contact sites. I focused on one lipid transfer protein abundant in myelin—glycolipid transfer protein (GLTP). Like tubular ER markers, GLTP is abundant in myelinating oligodendrocytes compared to premyelinating oligodendrocytes. I generated *Gltp flox* mouse lines and conditionally knocked out *Gltp* in oligodendrocytes by crossing the flox line with the *Cnp-Cre* mouse line. These conditional knockout (cKO) mice exhibit ER pathology in developing myelin, possibly due to lipid accumulation in the ER. Subsequently, these mice experience hypomyelination and degeneration. Myelin purified from cKO mice has a reduction in glycolipid, and primary oligodendrocytes with *Gltp* knockout and knockdown have a deficiency in glycolipid delivery to the cell surface, indicating that GLTP contributes to glycolipid transport during myelination.

In summary, my research suggests that non-vesicular lipid transport plays an important role in myelin development.

List of abbreviations

Abbreviation	Explanation
ABC transporters	ATP-binding cassette transporters
ATUM-SEM	automated tape collecting ultramicrotomy- scanning electron microscopy
BCAS1	breast carcinoma-amplified sequence 1
Cnp	2',3'-cyclic-nucleotide 3'-phosphodiesterase
CNS	central nervous system
cKO	conditional knockout
EM	electron microscopy
ER	endoplasmic reticulum
E-syt	extended synaptotagmin
GalCer	galactosylceramide
GFP	green fluorescent protein
GLTP	glycolipid transfer protein
GRAMD	glucosyltransferases, Rab-like GTPase activators and myotubularins domain
HEPES	4-(2-hydroxyethyl)-1-piperazineethanesulfonic acid
HexCer	hexosylceramide
HFA	hydroxy fatty acid
KO	knockout
LTP	lipid transfer protein
MAG	myelin-associated glycoprotein
MBP	myelin basic protein
MCS	membrane contact sites
Mospd2	motile sperm domain-containing protein 2
MS	mass spectrometry
MSMS	tandem mass spectrometry
NFA	normal fatty acid
NPC	Niemann-Pick type C
n.s.	not significant
OSBP	oxysterol-binding protein
ORP	oxysterol-binding protein (OSBP)-related protein
P14/28	postnatal day 14/28

PBS	phosphate-buffered saline
PC	phosphatidylcholines
PCA	Principal Component Analysis
PE	phosphatidylethanolamine
PFA	paraformaldehyde
PI	phosphatidylinositol
PITP	phosphatidylinositol transfer protein
PM	plasma membrane
PNS	peripheral nervous system
PS	phosphatidylserine
REEP5	receptor expression-enhancing Protein 5
RFP	red fluorescent protein
rpm	rotations per minute
RTN1	reticulon 1
RTN4	reticulon 4
SD	standard deviation
SDS-PAGE	sodium dodecyl sulfate – polyacrylamide gel electrophoresis
SEM	scanning electron microscopy
SMP	synaptotagmin-like mitochondrial-lipid binding protein
SNARE	soluble NSF attachment protein receptor
StART	steroidogenic acute regulatory transfer
TEM	Transmission electron microscopy
TMEM24	transmembrane protein 24
WT	wildtype

*For abbreviations of all lipid classes, please refer to “Box 1 Lipid nomenclature” in Section 3.6.

1. Introduction

1.1 Myelination, a fundamental process in the vertebrate nervous system

First emerging in jawed vertebrates, myelin represents a key innovation in vertebrate evolution (Ghosh et al., 2024). As a multilayered membrane wrapping around the axon (Fig 1.1), myelin acts as insulation comparable to the insulation material surrounding an electric wire, and can increase nerve conduction velocity by 20 to 200 times (Nave & Werner, 2021; Stadelmann et al., 2019). Additionally, myelin and myelin-generating cells offer metabolic support to axons, including the provision of pyruvate and lactate (Fünfschilling et al., 2012; Lee et al., 2012), and antioxidant defense (Mukherjee et al., 2020). Myelin is formed by oligodendrocytes in the central nervous system (CNS) and Schwann cells in the peripheral nervous system (PNS) (Nave & Werner, 2014). In this dissertation, I will focus on CNS myelin and myelination unless specified.

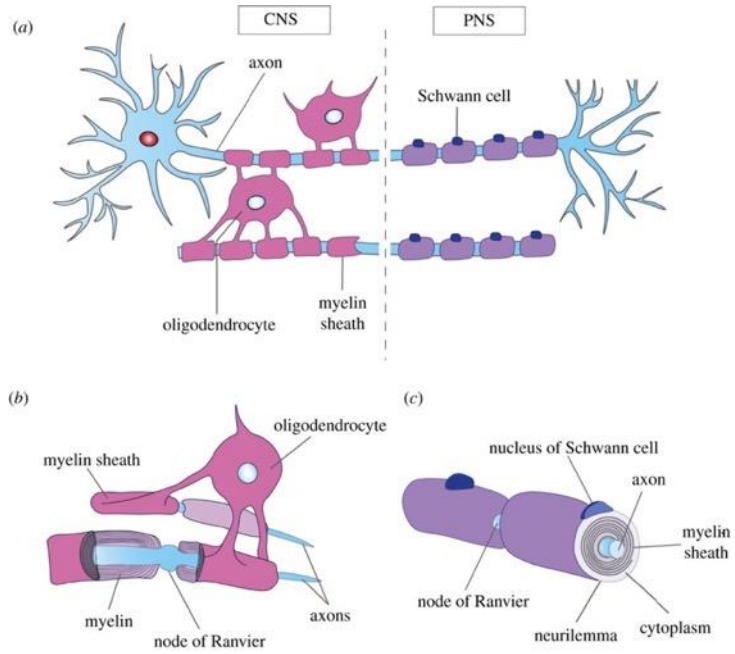

Figure 1.1 Myelination in the CNS and PNS. Oligodendrocytes in the CNS and Schwann cells in the PNS both ensheath axons to provide insulation. However, while oligodendrocytes can ensheath multiple axons, Schwann cells typically myelinate only one axon each, with the cell body lying adjacent to the myelin sheath. Figure taken from open access article (C. Z. Chen et al., 2021) DOI:https://doi.org/10.1098/rsob.200352

Myelination is a critical process that occurs not only during developmental stages but also in adulthood (Snaidero & Simons, 2017), where it is closely associated with learning and memory (Bonetto et al., 2021; Gibson et al., 2014; Hughes et al., 2018; McKenzie et al., 2014; Xin & Chan, 2020). In the context of some neurodegenerative diseases such as multiple sclerosis, the failure of remyelination drives disease progression (Fancy et al., 2011; Stadelmann et al., 2019). Therefore, it is essential to understand the molecular and cellular mechanism underlying myelination.

1.2 Myelination requires vast membrane expansion.

To generate myelin, an oligodendrocyte can wrap its plasma membrane around up to 50 axons (Chong et al., 2012; Hughes et al., 2018). It has been estimated that myelination requires oligodendrocytes to expand the plasma membrane up to many thousand folds (Pfeiffer et al., 1993). Remarkably, the majority of this vast expansion is achieved during development within just a few hours in zebrafish (Czopka et al., 2013) and two weeks in mouse (Djannatian et al., 2023; Foran & Peterson, 1992; Omoto et al., 2010; Snaidero & Simons, 2014). As a result, myelination requires oligodendrocytes to operate with exceptional efficiency in generating membranes, particularly lipids, since lipids account for 70-80% of the myelin membrane's dry weight (Aggarwal et al., 2011). This makes oligodendrocyte one of the most powerful lipid-producing cells in the human body.

Vesicular trafficking plays a crucial role in the expansion of the plasma membrane (Pfenninger, 2009). Recent studies have highlighted its significance in myelination, revealing that vesicular transport mediated by SNARE proteins VAMP2, VAMP3, and VAMP7 are essential for oligodendrocyte development and myelin formation (Fekete et al., 2023; Feldmann et al., 2011; Lam et al., 2022; Pan et al., 2023).

However, based on the 3D structure of myelin, I envisioned an additional layer to the story.

1.3 A 3D perspective on myelination

Myelination involves intricate cellular behavior of oligodendrocytes (Edgar et al., 2021; Meschkat et al., 2022; Nawaz et al., 2015; Snaidero & Simons, 2014; Snaidero et al., 2014, 2017; Zuchero et al., 2015). The process is illustrated in Fig 1.2, which includes three views: the 3D view (middle), the cross-sectional view (bottom left) and

the unwrapped view (upper right). Firstly, an oligodendrocyte extends its process to grow around an axon (Fig 1.2 A). At the end of one wrap, the growing front enters underneath the existing wrap and keeps growing while the outer wraps start to compact (Fig 1.2 B-D), by zippering the cytoplasmic leaflets of plasma membrane (Fig 1.3). However, this compaction is partial, leaving certain areas uncompact to form the cytoplasmic channels, which serve as a highway for transportation of essential materials from oligodendroglial cell body to myelin's growing front. This growing front, when viewed in the cross-sections of developing myelin (Fig 1.2 B-D bottom left), is the uncompact compartment known as inner tongue, situated between the myelin and the axon.

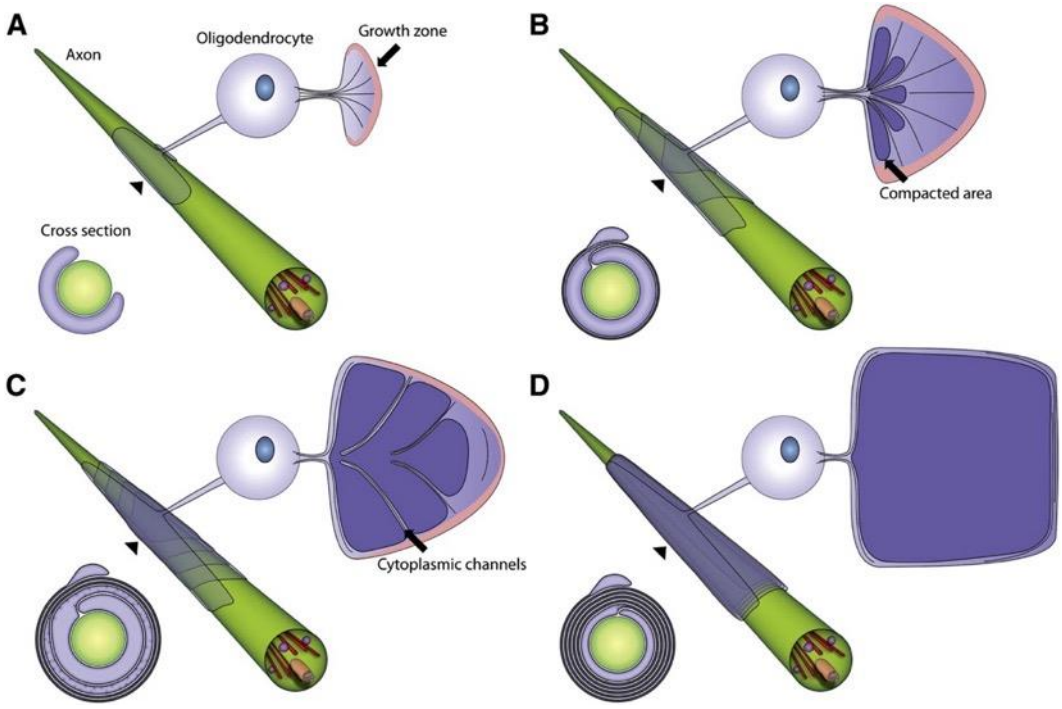

Figure 1.2 Model for myelin ensheathment with 3D (middle), unwrapped (upper right), and cross-sectional views (bottom left). The unwrapped view illustrates the sheath's geometry and development, including cytoplasmic channels (arrow in C) linking the cell body to the growth zone (pink area). Dark violet indicates the compacted myelin. The 3D view depicts ensheathment around the axon, and cross-sections display varying compaction levels throughout growth. Figure taken from (Snaidero et al., 2014), with permission from the publisher Elsevier, license number 5743700289301.

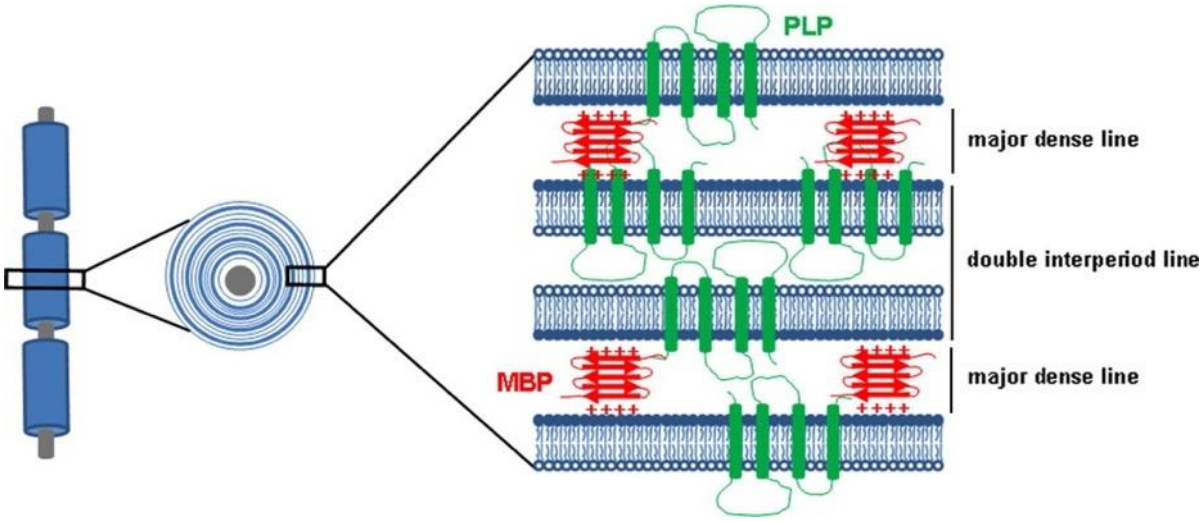

Figure 1.3 Structure of compact myelin. Compact myelin is formed when oligodendroglial cytosolic protein MBP mediates the alignment of intracellular leaflets of plasma membrane and the expulsion of cytoplasm, resulting in the formation of the major dense line, while plasma membrane protein PLP mediates juxtaposition of the bilayer membrane's extracellular leaflets, creating the double intraperiod line. Figure taken from (Baron & Hoekstra, 2010), with permission from the publisher ELSEVIER BV, license number 1462821-1.

Considering this 3D structure of developing myelin, vesicular trafficking poses a significant challenge: it would require transporting lipids from the ER to the Golgi apparatus located within the cell body and proximal processes, followed by formation of vesicles at the Golgi and their transport through the cytoplasmic channels to myelin, and the eventual fusion of these vesicles with target membranes (Alberts et al., 2017; Bonifacino & Glick, 2004; Feldmann et al., 2011; Jahn & Scheller, 2006; Trajkovic et al., 2006). Furthermore, given that cytoplasmic channel is highly curved and narrow, vesicular trafficking in myelin faces even greater challenges compared to axonal vesicular transport, which is already known to be complex.

In summary, vesicular trafficking is a multi-step, relatively slow and challenging process. It raises the question whether it could be complemented by a more straightforward pathway, specifically, a direct transfer of lipids from the ER to the plasma membrane during myelin development. Theoretically, this route is feasible since the majority of myelin lipids are synthesized in the ER and bypass the need for Golgi processing.

1.4 Nonvesicular Lipid transport

It has been shown that lipids can be transported in a nonvesicular manner between two membranes. The potential routes are summarized in Fig 1.4 (Prinz, 2010). Among these, the most documented route is the transport by lipid transfer proteins at membrane contact sites (Fig 1.4C). Different organelles can come together in close proximity to a distance of less than 30nm without fusing, often tethered by molecules. Such a short distance facilitates a class of proteins, known as lipid transfer proteins, to transfer lipids between membranes. A variation of this transport mechanism is the bridge-like transfer (Fig 1.4D), exemplified by VPS13, which forms a hydrophobic tunnel and facilitates bulk transport for a wide spectrum of lipids at membrane contact sites, making it a potentially crucial mechanism for membrane expansion (Melia & Reinisch, 2022). Transient hemifusion could also be an effective method for bulk lipid transport; however, the feasibility of this route is highly controversial. For the remaining mechanisms, additional evidence is required to confirm their physiological relevance.

Nonvesicular lipid transport can facilitate bulk transport of lipid, thereby contributing to membrane expansion, such as neurite growth (Gallo et al., 2020; Petkovic et al., 2014), and the membrane biogenesis of autophagasome (Maeda et al., 2019; Osawa et al., 2019; Valverde et al., 2019), mitochondria and chloroplast (Reinisch & Prinz, 2021). Yet, whether oligodendrocytes employ nonvesicular lipid transport for membrane expansion remains unclear.

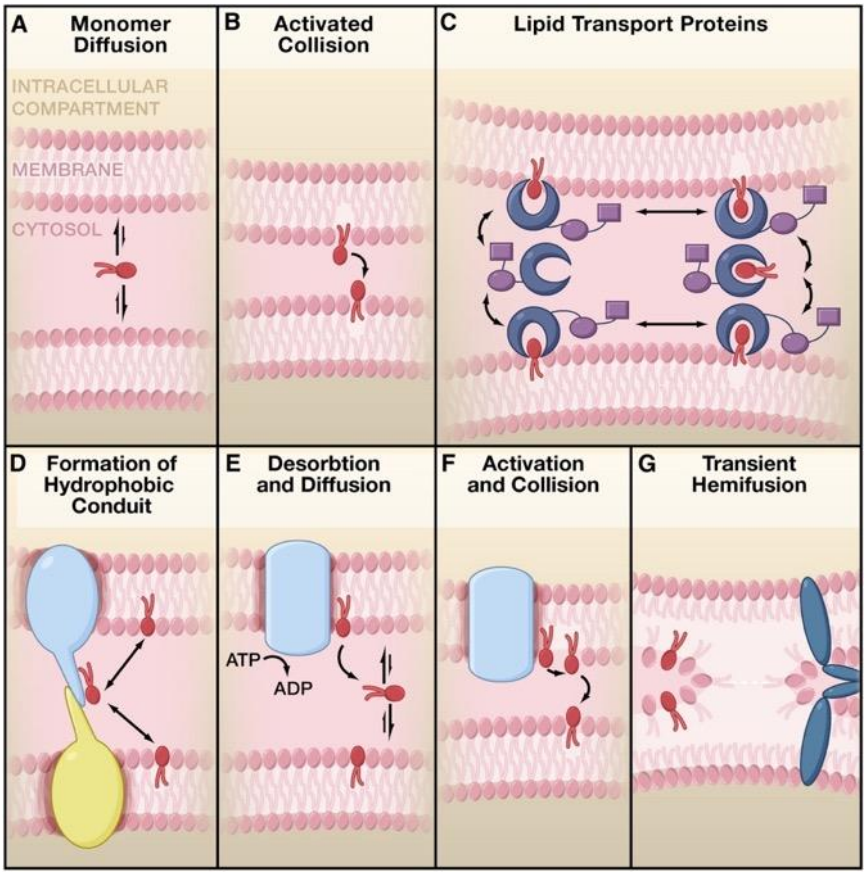

Figure 1.4 Possible routes of nonvesicular lipid transport.

Lipids can move between membranes without proteins' aid in two ways: (A) by diffusing as monomers through the aqueous phase or (B) when two membranes collide.

(C-G) illustrate mechanisms dependent on proteins. (C) Lipid transfer proteins (LTPs) can transfer lipids between membranes of different organelles. LTPs have a hydrophobic pocket (blue) and, often targeting domains (purple) that may direct lipid transfer to particular membranes by binding to certain lipids or proteins. Lipids may be transferred or exchanged at membrane contact sites where two membranes are apposed to each other. In addition, proteins or protein complexes can facilitate nonvesicular lipid transport by (D) creating a tunnel for lipid diffusion between membranes, (E) enhancing lipid detachment from a membrane, (F) activating lipids before membranes collide, or (G) inducing temporary membrane hemifusion.

Figure taken from (Prinz, 2010) with permission from the publisher Elsevier, license number 5747690781232

Nonvesicular lipid transport also occurs between ER-plasma membrane (Saheki & De Camilli, 2017). In fact, the first evidences supporting nonvesicular transport came from studies on ER-to-plasma membrane transport (Prinz, 2010): A wide range of lipids synthesized on the ER, including glycerophospholipids, sterols and monoglycosylceramides, have been shown to reach the plasma membrane when vesicular transport is blocked (Table 1) (Baumann et al., 2005; Halter et al., 2007; Kaplan & Simoni, 1985a; Urbani & Simoni, 1990; Vance et al., 1991). Furthermore,

ER-to-plasma membrane nonvesicular transport exhibit significant capacity, as the transfer rate of various lipids remains unaffected even when vesicular trafficking is inhibited (Kaplan & Simoni, 1985a, 1985b; Sleight & Pagano, 1983; Warnock et al., 1994). In recent years, with the advancements and increased accessibility of electron and light microscopy techniques, ER-plasma membrane contacts have been documented across various cell types. This has strengthened the evidence supporting the feasibility and importance of ER-to-plasma membrane nonvesicular transport.

Table 1: Lipid classes that can reach plasma membrane in the absence of vesicular trafficking.

Lipid classes	References
Sterols	(Heino et al., 2000; Kaplan & Simoni, 1985b; Urbani & Simoni, 1990)
Phosphatidylcholine (PC)	(Kaplan & Simoni, 1985a)
Phosphatidylethanolamine (PE)	(Sleight & Pagano, 1983; Vance et al., 1991)
Glucosylceramide	(Warnock et al., 1994)
Galactosylceramide (GalCer)	(Halter et al., 2007)

1.5 Potential nonvesicular lipid transport for myelination

For cultured oligodendrocytes, blocking exocytic SNAREs leads to smaller cells that are nonetheless capable of forming myelin-like sheets (Fig 1.5) (Lam et al., 2022). Although inhibiting protein transport significantly impedes these cells' development—evidenced by a reduction in mature oligodendrocyte markers like myelin basic protein (MBP) (Lam et al., 2022)—the analysis of Galactosylceramide (GalCer), a major myelin lipid, on the plasma membrane indicates that GalCer still reaches the plasma membrane and tends to accumulate over time. This points to the potential involvement of a nonvesicular pathway, at least for GalCer.

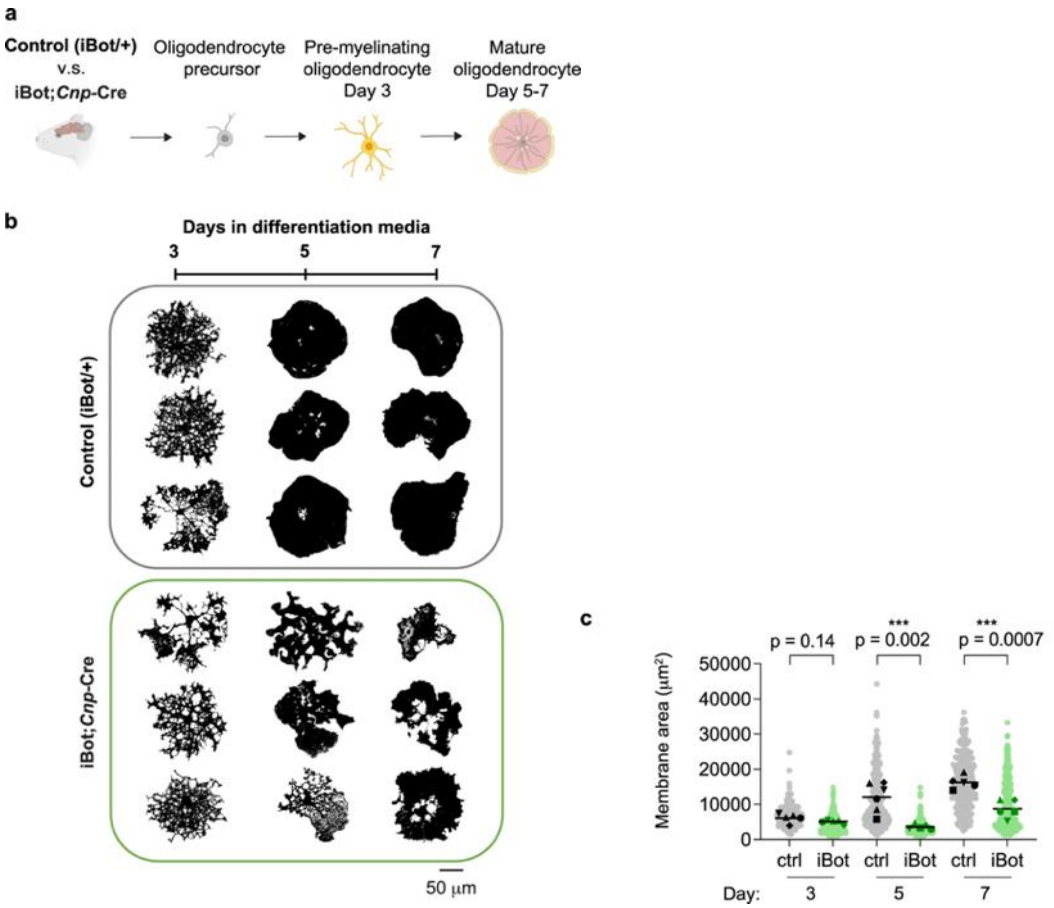

Figure 1.5 Oligodendroglial plasma membrane GalCer under exocytosis inhibition (iBot; *Cnp-Cre*). Figure taken from an open access article (Lam et al., 2022) DOI https://doi.org/10.1038/s41467-022-33200-4

Oligodendrocytes also express a number of lipid transfer proteins (Sharma et al., 2015; Y. Zhang et al., 2014), such as cholesterol transporter NPC1 and NPC2 (Prinz, 2010), glycolipid transfer proteins (GLTP) (Mishra et al., 2020) and bridge-like lipid transfer proteins (Braschi et al., 2022).

1.6 Glycolipid transfer protein (GLTP)

A particularly intriguing candidate for further study is GLTP, which is significantly more abundant in oligodendrocytes than in other cell types within the CNS. GLTP is known to transfer glycolipids, including GalCer, between liposomes *in vitro* (Mishra et al., 2020). Myelin contains large amount of glycolipids, primarily GalCer, which is synthesized in the ER, and a small quantity of its derivative, sulfatide, which is synthesized in the Golgi apparatus (Norton & Poduslo, 1973). Interestingly, in cell line studies, GalCer transport persists in the absence of vesicular trafficking and *Gltp* overexpression stimulates GalCer transport (Halter et al., 2007). Furthermore, GLTP

is upregulated during the progression of myelin development in wildtype mice (C. Zhang et al., 2023), while in contrast, is downregulated in hypomyelinated mutants, along with UGT8, the enzyme responsible for GalCer synthesis (Yang et al., 2019). Taken together, these findings suggest that GLTP plays an important role in myelin development.

1.7 Hypothesis and aims of the study.

With the above-mentioned background knowledge, I formulated my hypothesis as follows: Oligodendroglial lipids are transferred directly from the ER to plasma membrane in a nonvesicular manner to contribute to myelin membrane biogenesis. If this hypothesis holds true, two key phenomena should be observable: firstly, the ER would extend into the developing myelin, making contacts with the expanding oligodendroglial plasma membrane. Secondly, lipid transfer proteins would operate at these contact sites, facilitating the transport of lipids. Based on this hypothesis, I have structured the aims of my study as follows:

Aim 1: To determine the presence of the ER in developing myelin. Surprisingly, despite the growth zone of myelin (i.e., the inner tongue) being a critical site for essential reactions of myelination and crucial for understanding the process, its detailed contents, particularly the organelles present, remain unexplored. I intend to examine the developing myelin in mice using volume electron microscopy, the benchmark technique for organelle characterization, supplemented by immunohistochemistry.

Aim 2: To analyze the distance between the ER and plasma membrane in developing myelin. The application of electron microscopy techniques will facilitate the measurement of such distance.

Aim 3 (Provided that findings from Aims 1 and 2 support my hypothesis): To investigate the involvement of lipid transfer proteins, specifically GLTP, in myelination. First, I plan to confirm GLTP's abundance and examine its subcellular localization. Subsequently, I aim to assess GLTP's impact on myelin development by generating a mouse mutant lacking GLTP and exploring whether GLTP operates at ER-plasma membrane contact sites.

2. Material and Methods

2.1 Generation of *Gltp* knockout (KO) and *Gltp flox* mice

To create *Gltp* KO and *Gltp* flox mice, CRISPR/Cas9-mediated genome editing was performed in mouse zygotes, as described previously (Wefers et al., 2023). Briefly, zygotes at the pronuclear stage were collected from matings between C57BL/6J males and superovulated C57BL/6J females (Charles River). These embryos were treated by pronuclear microinjection with a CRISPR/Cas9 ribonucleoprotein (RNP) solution targeting the *Gltp* gene, consisting of SpCas9 protein (IDT), crRNA (IDT), tracrRNA (IDT), and mutagenic long single-stranded DNA (lssDNA). The LssDNA included 200 nucleotides of homology arms and two loxP sites flanking exon 2 (ENSMUSE00000190151) of the *Gltp* gene (264 bp upstream and 487 bp downstream, respectively). After microinjection, the zygotes were implanted into pseudopregnant CD-1 foster mice. Founder mice exhibiting the desired genetic modifications—either an exon 2 deletion or both loxP sites incorporation in cis—were bred with C57BL/6J mice to establish pure lines. The fidelity of genetic alterations in F1 progeny was confirmed through a combination of restriction fragment length polymorphism (RFLP) analysis, Sanger sequencing, and quantitative PCR for gene copy numbers. To exclude off-targets, CRISPOR online tool (Concordet & Haeussler, 2018) was utilized to predict potential off-target sites, which were PCR-amplified and verified by Sanger sequencing. Only mice free of unintended genetic modifications were chosen for further breeding.

2.2 Mouse experiments

All mice were handled according to the institutional guidelines sanctioned by the Animal Welfare and Use Committee of the Government of Upper Bavaria. Mice were group-housed in individually ventilated cages (IVC) in a specific pathogen-free and temperature-controlled (21 ± 2°C) facility on a 12-hr light/dark cycle, with free access to food and water. Experiments involved both male and female mice, with cohorts being sex-matched for comparisons. The study utilized C57BL/6j mice as the wildtype group. The *Cnp-Cre* mouse strain, generously provided by Department Nave of the Max Planck Institute for Multidisciplinary Sciences, was kept heterozygous through backcrossing with C57BL/6j mice. In crossing of *Cnp-Cre* X *Gltp flox*, the *Cre* was

always from maternal source. All *Cnp-Cre* samples examined in this study are heterozygous for the *Cnp-Cre* gene.

2.3 Cell line and plasmid

U2OS cells (ATCC HTB-96), a kind gift from Christian Behrends laboratory at SyNergy Munich, were cultured in DMEM medium with 10% FBS and 1X penicillin-streptomycin at 37°C with an atmosphere of 5% CO2. Transfections were performed using Lipo3000 (Invitrogen). The plasmid "pCMV-UGT8-FusionRed" is constructed by Gibson assembly (NEB), assembling three fragments from 5' to 3': (1) pCMV from Addgene plasmid #36412; (2) mouse Ugt8 cDNA (synthesized as gblock fragment by IDT); (3) FusionRed from Addgene plasmid #54778. Because UGT8 is a Type I ER membrane protein, it is designed to fuse with a non-cytotoxic fluorescence protein, FusionRed, at its C-terminal.

2.4 Primary antibodies

Antibodies	**Source**	**Application**
Rat anti-MBP	Abcam ab7349	1:500 for IHC/ICC
chicken anti-MBP	Thermo PA1-10008	1:500 for IHC/ICC
anti-Rtn4	Abcam ab47085	1:500 for IHC/ICC
anti-Reep5	Proteintech 14643-1-AP	1:500 for IHC/ICC
anti-BCAS1	Santa Cruz sc136342	1:400 for IHC
anti-MAG-Alexa647	Santa Cruz sc-166849 AF647	1:100 for IHC 1h at room temperature
anti-Rtn1	Sigma HPA044249	1:250 for ICC
anti-Sec61b	Sigma HPA049407	1:400 for ICC
anti-KDEL	Enzo ADI-SPA-827-D	1:250 ICC
anti-GLTP	Sigma ATA-HPA056461-100	1:300 for IHC/ICC with antigen retrieval, 1:500 for Western Blot
anti-GalCer	Merck MAB342	1:1500 for ICC
anti-GalCer-Alexa488	Merck MAB342A4	1:100 for ICC
anti-UGT8	Proteintech 17982-1-AP	1:500 for ICC
anti-CD140a	Biolegend 135902	1:300 for primary culture isolation

2.5 siRNA for oligodendrocyte culture

Cell permeable siRNAs were purchased from Horizon/Dharmacon, as the "SMARTpool" format (a mixture of four siRNA): nontargeting (D-001910-10-20), mouse *Rtn4* (E-059578-00-0010), mouse *Gltp* (E-058085-00-0010). 100x stock solution was prepared according to manufacturer's instruction. The siRNA was added to the cells when switching to differentiation medium, with a final concentration of 1 µM, and incubated for 3 days.

2.6 Transmission and scanning electron microscopy

Optic nerve and spinal cord tissue were dissected and immersion fixed (P14) or perfusion fixed (P28) in 4% PFA (EM-grade, Science Services), 2.5% glutaraldehyde (EM-grade, Science Services), 2 mM calcium chloride in 1xPBS, pH 7.4 (Science Services) for 24h. Short (2-3 mm) pieces of the optic nerve and the 1 mm thick spinal cord slices were incubated in the same fixative for another 24h and stored in 0.1 M cacodylate buffer at 4°C. We applied a rOTO en bloc staining protocol including postfixation in 2% osmium tetroxide (EMS), 1.5% potassium ferricyanide (Sigma) in 0.1 M sodium cacodylate (Science Services) buffer (pH 7.4) (Kislinger et al., 2020). The contrast was enhanced by incubation in 2% thiocarbohydrazide (Sigma) for 45 min at 40°C. The tissue was washed in water and incubated in 1% aqueous osmium tetroxide, washed and further contrasted by overnight incubation in 1% aqueous uranyl acetate at 4°C and 2h at 50°C. Samples were dehydrated in an ascending ethanol series and infiltrated with the epoxy-araldite resin LX112 (Ladd Research). Blocks were cured for 48h at 60°C, trimmed (EM TRIM, Leica) and sectioned at 100 nm thickness using a 35° ultra-diamond knife (Diatome) on an ultramicrotome (UC7, Leica). Sections were collected onto 1x0.5 cm carbon nanotube tape strips (Science Services) for scanning EM (SEM) analysis or onto formvar-coated copper grids (Plano) for transmission EM (TEM). For SEM imaging the samples on tape were attached to adhesive carbon tape (Science Services) on 4-inch silicon wafers (Siegert Wafer) and grounded by adhesive carbon tape strips (Science Services). EM micrographs were acquired on a Crossbeam Gemini 340 SEM (Zeiss) with a four-quadrant backscatter detector at 8 kV using ATLAS5 Array Tomography (Fibics). Medium lateral resolution images (100-200 nm) allowed the identification of regions of interest that were in turn reimaged at 4-10 nm lateral resolution. TEM micrographs for higher resolution representations were acquired on a JEM 1400plus (JEOL) equipped

with a XF416 camera (TVIPS) and the EM-Menu software (TVIPS). Image analysis was performed in Fiji (Schindelin et al., 2012)

2.7 Volume electron microscopy

For volume EM analysis of myelinated axons in the optic nerve we applied Automated Tape Collecting Ultramicrotomy (ATUM) (Kislinger, Niemann, et al., 2023). The blocks were trimmed at a 45° angle on four sides using a trimming machine (EM TRIM, Leica). Serial sections were taken with a 35° ultra-maxi diamond knife (Diatome) at a nominal cutting thickness of 50 nm on the ATUMtome (Powertome, RMC). Sections were collected onto freshly plasma-treated carbon coated Kapton tape (kindly provided by Jeff Lichtman and Richard Schalek). Plastic tape stripes were assembled onto adhesive carbon tape (Science Services) attached to 4-inch silicon wafers (Siegert Wafer) and grounded by adhesive carbon tape strips (Science Services). ATUM-SEM acquisition was performed on an Apreo S2 SEM (Thermo Fisher Scientific) with the T1 detector using the Maps2 (Thermo Fisher Scientific) software. The tissue was hierarchically imaged as previously described(Kislinger et al., 2020). Target regions were identified and acquired at high resolution (4x4x50 nm). Serial section data were aligned by a sequence of automatic and manual processing steps in Fiji TrakEM2 (Kislinger, Fabig, et al., 2023; Schindelin et al., 2012).

2.8 EM analysis

The VAST software was used for manual segmentation(Berger et al., 2018) and rendered in Blender(Brito, 2018) for three-dimensional visualization.

Organelle identification followed the detailed protocol (Park, 2023) with inputs from Martina Schifferer (SyNergy EM hub, Munich, Germany) and Shujun Cai (Southern University of Science and Technology, Shenzhen, China). Organelles were categorized into three groups: ER, mitochondria and others. The ER is characterized as a continuous structure, while mitochondria are distinguished by their inner and outer membranes (cristae), which were absent in developing myelin. The 'others' category encompasses endosomes, vesicles, and organelles of uncertain identity. Endosomes are typically ball-shaped with a light lumen; among these, multivesicular bodies (MVBs) are a special type that contain small vesicles. The Golgi apparatus is identified by its ribbon-like appearance, featuring interconnected stacks, and surrounding small vesicles. In this dataset, some membrane structures of unclear identity might

represent the Golgi, which were potentially missed due to the ATUM-SEM's technical limitation with a z-resolution of 50nm. Nonetheless, if these structures are indeed Golgi, they are relatively rare.

G-ratio and inner tongue diameter were measured semi-automatedly using MyelTracer(Kaiser et al., 2021). Outfolding and paranodes are excluded for quantification. Axon, inner and outer edge of myelin are recorded. Diameter of each compartment is calculated as $2X\sqrt{area/\pi}$. G-Ratio is calculated as $\sqrt{\frac{inner\ myelin\ area}{outer\ myelin\ area}}$, i.e. the ratio of inner to outer myelin diameter. Notably this is an updated definition of g-ratio, as opposed to the ratio of axon diameter to outer myelin diameter, so that I can take into account of inner tongues present in developing myelin. Inner tongue diameter is calculated as inner myelin diameter - axon diameter.

2.9 Immunohistochemistry

The mice were anesthetized with isoflurane, followed by transcardial perfusion with PBS and then 4% paraformaldehyde (PFA). Subsequently, brains and spinal cords underwent postfixation in 4% PFA for 4h and overnight, respectively. The tissues were immersed in 30% sucrose in PBS until they sank, then embedded in Tissue-Tek O.C.T., frozen on dry ice, and stored at -80°C. The frozen tissues were cut to 14-µm coronal sections using a Leica CM 1900 cryostat. Sections were rinsed with PBS containing and permeabilized in 0.3% Triton X-100 for 15min (for brain) or 1h (for spinal cord). For GLTP staining, antigen retrieval was performed for 20min sodium citrate buffer (pH 6) in 80°C using water bath. Sections were incubated in blocking solution (1% FBS, 1% fish gelatin, and 1% bovine calf serum in PBS) for 1h at room temperature and if mouse primary antibodies are used, Fab fragments are added for another 1h. Primary antibodies, diluted in 10% blocking solution, were added, and incubated overnight at 4°C. On the following day, after washing with PBS, sections were incubated with secondary antibodies for 1h at room temperature, followed by washing, staining with 2 µg/ml Hoechst 33342, and mounting with ProLong gold antifade mounting medium (Thermo P36934).

2.10 Primary oligodendrocyte culture

Oligodendrocyte progenitor cells were prepared from postnatal day 7 to day 9 mouse cortices by immunopanning(Emery & Dugas, 2013). Briefly, cortices were dissociated

to single-cell suspension, which was passed through two negative-selection plates coated with BSL1 to remove microglia. The remaining cell suspension was then incubated in a positive-selection plate coated with anti-CD140a antibodies. The attached cells were collected by accutase and cultured on poly-L-lysine-coated coverslips in proliferation medium containing Dulbecco's modified Eagle's medium (DMEM; Thermo Fisher Scientific, catalog no. 41965), Sato Supplement, B-27 Supplement, GlutaMAX, Trace Elements B, penicillin–streptomycin, sodium pyruvate, insulin, N-acetyl-L-cysteine, D-biotin, forskolin, ciliary neurotrophic factor (CNTF), platelet-derived growth factor (PDGF) and neurotrophin-3 (NT-3). The culture is differentiated by replacing the above-mentioned proliferation medium's PDGF and NT-3 with T3.

2.11 Immunocytochemistry

Cells were fixed by 4% PFA in room temperature for 10min, washed with PBS and stored in PBS containing azide at 4°C. For staining, cells were permeabilized with PBS-0.1% Triton X-100 for 30 sec. For GLTP staining, antigen retrieval was performed for 10min sodium citrate buffer (pH 6) at 70°C using water bath. Blocking solution (1% FBS, 1% fish gelatin, and 1% bovine calf serum in PBS) is applied for 30 min before incubating with primary antibody in PBS-10% blocking solution at 4°C overnight. The following day, the cells are stained with secondary antibdodies for 1h at room temperature, followed by Hoechst 33342 for 10min and mounted with ProLong glass antifade mounting medium (Thermo P36980). For GalCer measurement, cells are first incubated with blocking solution, stained with mouse anti-GalCer antibody with 10% blocking solution for 1h at room temperature, then anti-mouse Alexa 555 for 1h at room temperature, permeabilized with 0.1% Triton X-100 for 30 sec, blocked again, and stained overnight with chicken anti-MBP (or other primary antibody) in PBS-10% blocking solution at 4°C overnight. The following day, the cells were stained with anti-chicken-Alexa 647 and anti-GalCer conjugated with Alexa 488 for 1h in room temperature, and lastly stained with Hoechst 33342(Sigma B2261) and mounted with mounting medium.

2.12 Fluorescence imaging and analysis

All florescence images were acquired by the point scanning confocal microscope Zeiss LSM 900 equipped with Airyscan 2 module, and Plan-Apochromat 63×/1.2 oil

immersion objective, C-Apochromat 40x/1.1 water immersion objective, Plan-Apochromat 20x/0.8 objective, Plan-Neofluar 10x/0.3 objective. Images were analyzed using Fiji(Schindelin et al., 2012).

2.13 Western Blot Analysis

Individual P14 mouse brains were homogenized using a sonicator. The resulting whole-brain lysates were loaded at 12 µg per lane onto a 12% TGX^{TM} precast gel (BioRad #4561046). Following separation by SDS-PAGE, proteins were transferred onto a nitrocellulose membrane. The membrane was then blocked in 3% BSA in PBS-Triton for 30min at room temperature, followed by overnight incubation with primary antibodies in PBS at 4°C. After washing, the membrane was incubated with HRP-conjugated secondary antibodies in PBST for 1h at room temperature. Subsequently, targeted proteins were detected using Pierce ECL substrate (Thermo Fisher #32106), and visualized using an Odyssey Fc imager from LI-COR.

2.14 Myelin isolation

Myelin was isolated from mouse brain and spinal cord (P14) or mouse brain only (P28), using one animal for each sample. The protocol with two rounds of sucrose density centrifugation and osmotic shocks is as previously described(Gouna et al., 2021), with some modifications. The ultracentrifugation was done using an SW41 Ti rotor. The tissues were homogenized with a sonicator in a solution containing 10 mM Hepes pH 7.4 and 0.32 M sucrose. The homogenized tissue was layered on 0.32/0.85M sucrose gradient and centrifuged at 25,000 rpm for 35 min with low deceleration and acceleration. The crude myelin fraction was recovered from the interface, resuspended in ice-cold distilled water, and centrifuged at 25,000 rpm for 18 min. The hypo-osmotic shock was applied to the pellet two more times and pellets were collected at 10,000 rpm for 18 min. The pellet from the last step was dissolved in Hepes buffer containing 0.32 M sucrose, then all the centrifugation steps and hypo-osmotic shocks were repeated one more round. Eventually, the purified myelin pellet was resuspended in 1 ml PBS and stored at −20°C.

2.15 Lipidomics

Each sample is myelin from one animal. Mass spectrometry-based lipid analysis was performed by Lipotype GmbH (Dresden, Germany) as described(Michał A Surma et al., 2021). Lipids were extracted using a chloroform/methanol procedure(Ejsing et al.,

2009). Samples were spiked with internal lipid standard mixture containing: cardiolipin 14:0/14:0/14:0/14:0 (CL), ceramide 18:1;2/17:0 (Cer), diacylglycerol 17:0/17:0 (DAG), hexosylceramide 18:1;2/12:0 (HexCer), lyso-phosphatidate 17:0 (LPA), lyso-phosphatidylcholine 12:0 (LPC), lyso-phosphatidylethanolamine 17:1 (LPE), lyso-phosphatidylglycerol 17:1 (LPG), lyso-phosphatidylinositol 17:1 (LPI), lyso-phosphatidylserine 17:1 (LPS), phosphatidate 17:0/17:0 (PA), phosphatidylcholine 15:0/18:1 D7 (PC), phosphatidylethanolamine 17:0/17:0 (PE), phosphatidylglycerol 17:0/17:0 (PG), phosphatidyl-inositol 16:0/16:0 (PI), phosphatidylserine 17:0/17:0 (PS), cholesterol ester 16:0 D7 (CE), sphingomyelin 18:1;2/12:0;0 (SM), triacylglycerol 17:0/17:0/17:0 (TAG) and cholesterol D6 (Chol). After extraction, the organic phase was transferred to an infusion plate and dried in a speed vacuum concentrator. The dry extract was re-suspended in 7.5 mM ammonium formiate in chloroform/methanol/propanol (1:2:4; V:V:V). All liquid handling steps were performed using Hamilton Robotics STARlet robotic platform with the Anti Droplet Control feature for organic solvents pipetting. Samples were analyzed by direct infusion on a QExactive mass spectrometer (Thermo Scientific) equipped with a TriVersa NanoMate ion source (Advion Biosciences). Samples were analyzed in both positive and negative ion modes with a resolution of Rm/z=200=280000 for MS and Rm/z=200=17500 for MSMS experiments, in a single acquisition. MSMS was triggered by an inclusion list encompassing corresponding MS mass ranges scanned in 1 Da increments(Michal A Surma et al., 2015). Both MS and MSMS data were combined to monitor CE, Chol, DAG and TAG ions as ammonium adducts; LPC, LPC O-, PC and PC O-, as formiate adducts; and CL, LPS, PA, PE, PE O-, PG, PI and PS as deprotonated anions. MS only was used to monitor LPA, LPE, LPE O-, LPG and LPI as deprotonated anions, and Cer, HexCer, and SM as formiate adducts. Data were analyzed with in-house developed lipid identification software based on LipidXplorer(Herzog et al., 2011, 2012). Data post-processing and normalization were performed using an in-house developed data management system. Only lipid identifications with a signal-to-noise ratio >5, and a signal intensity 5-fold higher than in corresponding blank samples were considered for further data analysis.

2.16 Statistical analysis

Statistical Analysis were performed using Microsoft Excel 2016 and GraphPad Prism 10. Volcano Plot (Fig. 6a) additionally used Lipid Map statistical tool(Fahy et al., 2007;

Ni et al., 2023). Missing values of lipidomics are filled as 0. For mouse analysis, mean value per mouse was calculated and presented as a single data point.

2.17 Use of artificial intelligence (AI) tools

The text of this dissertation is revised with assistance from ChatGPT 4, where I wrote initial drafts and utilized the AI for suggestions on phrasing and clarity. I selectively incorporated suggestions and ensured the accuracy and integrity of the dissertation's contents.

3. Results

3.1 Tubular ER is enriched in developing myelin and contacts the plasma membrane.

The investigation began by examining the presence of the ER in developing myelin, focusing on mice at the postnatal day 14 (P14), a stage when active myelination occurs. A volume electron microscopy dataset from P14 mouse optic nerve was acquired using ATUM-SEM (Automated Tape-collecting Ultramicrotome-Scanning Electron Microscopy) (Kasthuri et al., 2015). Based on the continuity, shape, lumen, and membrane appearance (Heinrich et al., 2021; Park, 2023; Terasaki, 2018), the ER was identified and segmented within the inner tongue, the growing front of myelin (Fig. 3.1a, Movie 1, Fig. 3.1b). The 3D reconstruction revealed an ER network composed primarily ER tubes within the inner tongue. Occasionally, the ER appeared “lumenless” (arrow Fig. 3.1b), reminiscent of the thin ER reported in neuron (Hoffmann et al., 2021; Wu et al., 2017). Quantitative analysis of membrane-bound organelles in three mice at P14 highlighted the ER as the predominant organelle within the inner tongue, with at least one ER present in 82% of examined inner tongues (Fig 3.1c, d, e). Conversely, mitochondria, which are typically prevalent, were absent. The occurrence of ER surpassed that of all other types of membrane-bound organelles, which collectively accounted for 20%, including multivesicular bodies (Fig. 3.1e, f). Despite the spatial constraints of the inner tongue, a significant portion of this area was allocated to the ER by oligodendrocytes, with the ER within the inner tongue occupying more space than that within axons (Fig. 3.1g). The presence of the ER in developing myelin was verified by immunohistochemistry performed on spinal cord cross-sections from P14 mice, which showcased the myelin marker MBP forming distinct rings indicative of myelin structures. Markers for tubular ER, specifically receptor expression-enhancing protein 5 (REEP5) and reticulon 4 (RTN4) (Gia K Voeltz et al., 2006; H. Zhang & Hu, 2016), were detected as puncta on MBP+ rings (Fig. 3.2a). Analysis from three mice indicated that 82% of MBP-positive rings exhibited overlapping REEP5 puncta, and 73% displayed RTN4 puncta (Fig. 3.2b). Moreover, the oligodendrocyte ER was identified in close proximity to the plasma membrane in developing myelin (Fig. 3.3a), with 83% of ER-plasma membrane distances measuring less than 20nm, a

distance feasible for nonvesicular lipid transport (Scorrano et al., 2019; G K Voeltz et al., 2024). Because some inner tongues contain multiple ER, the minimum distance in each inner tongue is more striking, with 94% of ER-plasma membrane distances less than 20 nm.

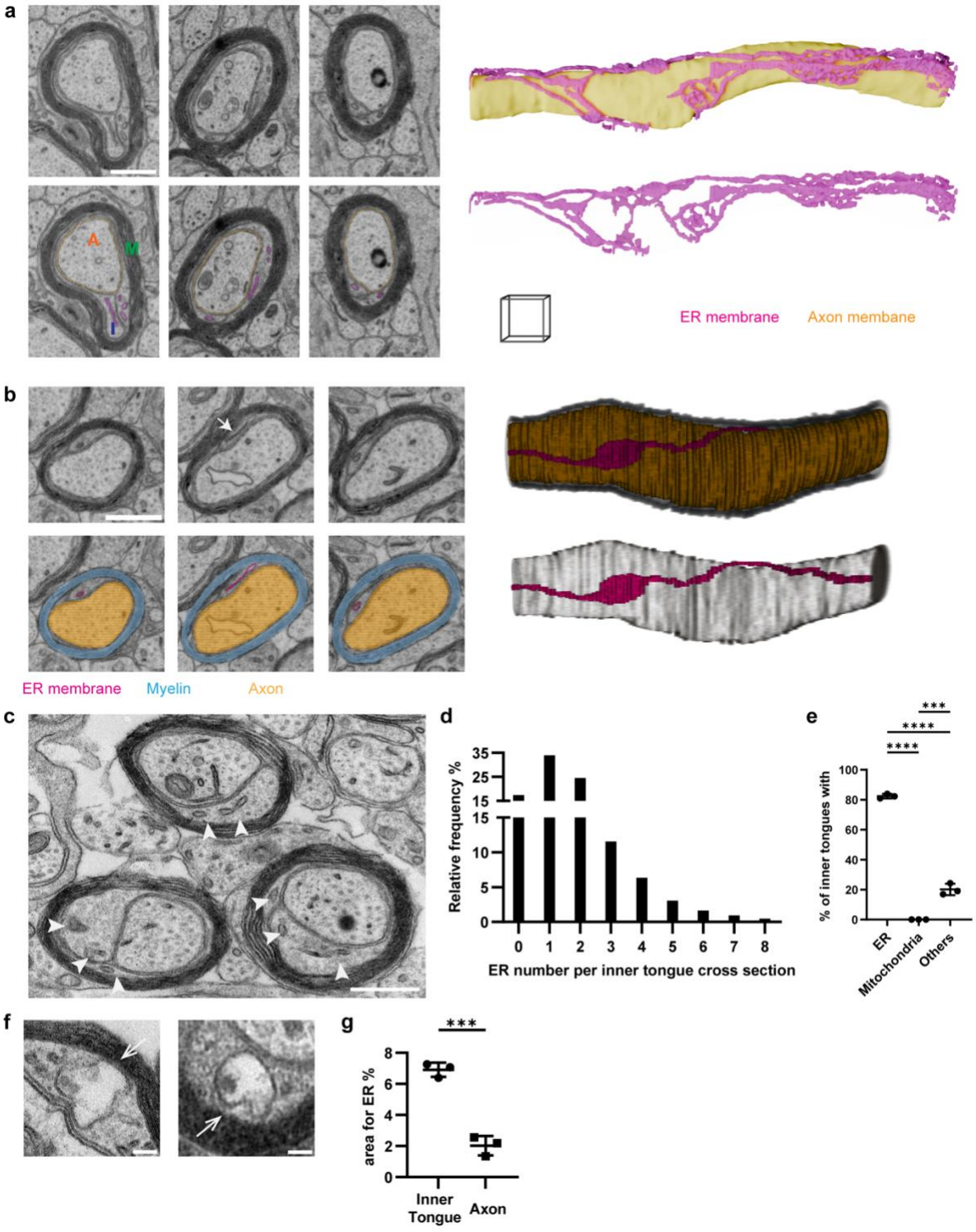

Fig. 3.1 | Tubular ER in developing myelin revealed by electron microscopy

a Volume EM (ATUM-SEM) analysis of developing myelin from postnatal day 14 (P14) mouse optic nerve. Different compartments are marked on the bottom left image: axon (A), myelin (M) and inner tongue (I). ER membrane (magenta) and axon membrane (yellow) are segmented. 3D reconstruction of ER network is shown together with (upper) or without (bottom) axonal membrane, from an 11.25 µm-thick stack (226 slices with 50 nm interval, scale cube 1x1x1 µm). **b** Another 3D reconstruction of ER in the inner tongue. From a 4.5µm-thick stack (91 slices with 50 nm interval). Arrow in 2nd EM example: "lumenless" ER. Magenta: ER membrane; Blue: Myelin; Yellow: Axon. **c** Representative image of the TEM dataset for quantification of membrane-bound organelles in the inner tongue. Arrow heads: ER. **d** The distribution of ER number per inner tongue cross section, quantified from 425 inner tongue cross sections of three mice. **e** Ratio of inner tongues containing specified organelles. Quantification of (c) showing mean ± SD, ER: 82.36 ± 1.51, mitochondira: 0, others: 20.13 ± 3.80 (n=3 wildtype P14 mice, One-way ANOVA followed by Tukey's post-hoc test). **f** Examples of other membrane-bound organelles (arrows), many being multivesicular body. **g** ER occupies 6.91±0.45% area of inner tongue and 2.02±0.62% area of axon (mean ± SD). (n=3 wildtype P14 mice, Two-tailed unpaired t-test). Scale bars: 0.5 µm (a, b, c), 0.1 µm (f). *: $P \leq 0.05$, **: $P \leq 0.01$, ***: $P \leq 0.001$, ****: $P \leq 0.0001$

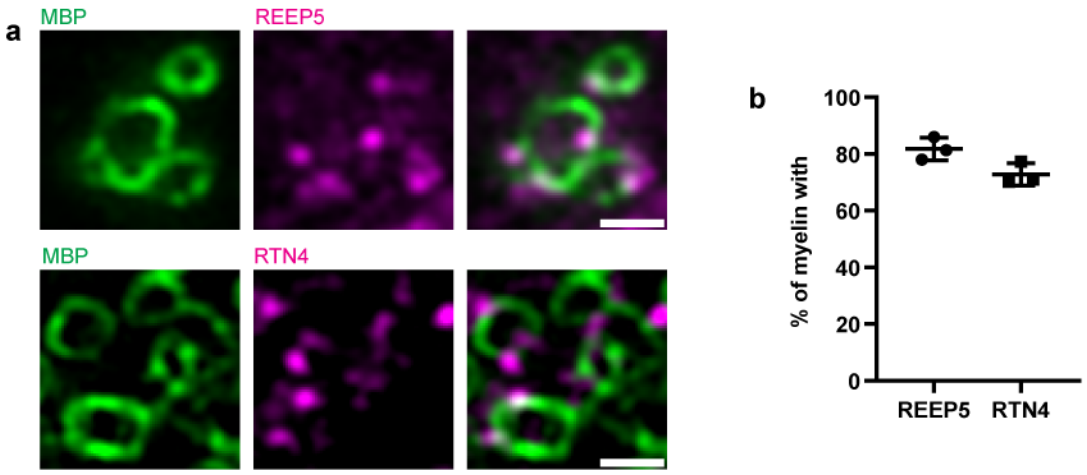

Fig. 3.2 Tubular ER in developing myelin revealed by immunohistochemistry

a Immunohistochemistry of developing myelin from P14 mouse spinal cord shows tubular ER markers (REEP5 and RTN4) appear as puncta and overlap with myelin (MBP). **b** Ratio of myelin (MBP^+ ring) overlapping with specified tubular ER. Quantification of (a) showing mean ± SD, REEP5: 81.80 ±3.97, RTN4: 72.79 ± 3.91 (n=3 wildtype P14 mice). Scale bars: 1 µm (a).

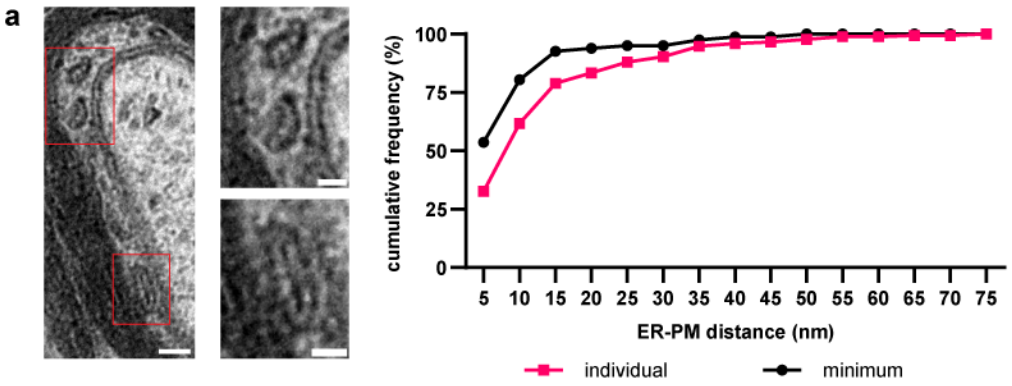

Fig. 3.3 Tubular ER contacts plasma membrane in developing myelin

a An example with zoom-in views shows short distance between the oligodendroglial ER and plasma membrane in developing myelin, and distribution of ER's distance to plasma membrane. Distribution of individual ER's distance to plasma membrane is shown by magenta squares: 62% ≤ 10 nm, 83% ≤ 20 nm, 90% ≤ 30 nm (n=175 ER-plasma membrane distance from three wildtype P14 mice) and distribution of minimum distance in a given inner tongue is shown by black dots: 80% ≤ 10 nm, 94% ≤ 20 nm, 95% ≤ 30 nm (n=82 inner tongues from three wildtype P14 mice). Scale bars: 100 nm (a left), 50 nm (a zoom-in)

3.2 Tubular ER is associated with active myelination.

To investigate if the expression patterns of tubular ER markers are aligned with active myelin development, immunohistochemistry was performed, utilizing antibodies against BCAS1 and MAG to mark premyelinating and actively myelinating oligodendrocytes (Fard et al., 2017). P14 mouse cortex was analyzed. Within the cortex (Fig. 3.4a, b), myelinating oligodendrocytes (BCAS1+MAG+, marked by arrows) exhibited increased levels of the tubular ER markers REEP5 and RTN4 compared to their premyelinating counterparts (BCAS1+MAG-, marked by arrowheads). Data from three P14 mice indicated that a significant majority, 93% for REEP5 and 82% for RTN4, of myelinating oligodendrocytes displayed elevated expression of these markers (Fig. 3.4c). Conversely, premyelinating oligodendrocytes have lower levels of these tubular ER proteins, implying an upregulation of tubular ER proteins concurrent with the onset of myelination. Similar patterns were observed in the cerebellum (Fig. 3.4d, e, f).

In 6-month-old mice, where myelin is mature, a decline in tubular ER within white matter regions was observed in comparison to P14 mice (Fig. 3.5a, b). Analysis of three mice from each time points highlighted a significant decrease of the tubular ER

fluorescence signal, normalized by the myelin marker MBP signal (Fig. 3.5c, d). This observation could be explained by the previously reported finding that the size of the inner tongue decreases as myelination completes. Presumably, the ER in the inner tongue withdraws from the myelin as the inner tongue undergoes closure. To confirm, EM analysis was performed on wildtype mice at postnatal day 28 (P28), a period corresponding to a late stage of developmental myelination. Most myelin sheaths lacked inner tongues or have narrow inner tongues, and the ER was rarely observed (Fig. 3.5e)

In addition, cultured mouse oligodendrocytes were utilized to investigate the subcellular distribution of various ER subdomains. Markers SEC61b and KDEL, indicative of rough ER and ER sheets, respectively (Farías et al., 2019), were predominantly found in the cell body. In contrast, tubular ER markers RTN4 and RTN1 (H. Zhang & Hu, 2016) were distributed more broadly. The calculation of the peripheral to cell body signal ratio demonstrated a predominance of tubular ER over other ER forms, indicating that oligodendrocytes preferentially extend their ER as tubules towards the growing front (Fig. 3.6a).

Furthermore, the requirement of tubular ER for myelination was explored. Knocking down Rtn4 via RNA interference in primary oligodendrocytes led to a marked reduction in cell size (Fig. 3.6b, c), underscoring the critical role of tubular ER in membrane expansion.

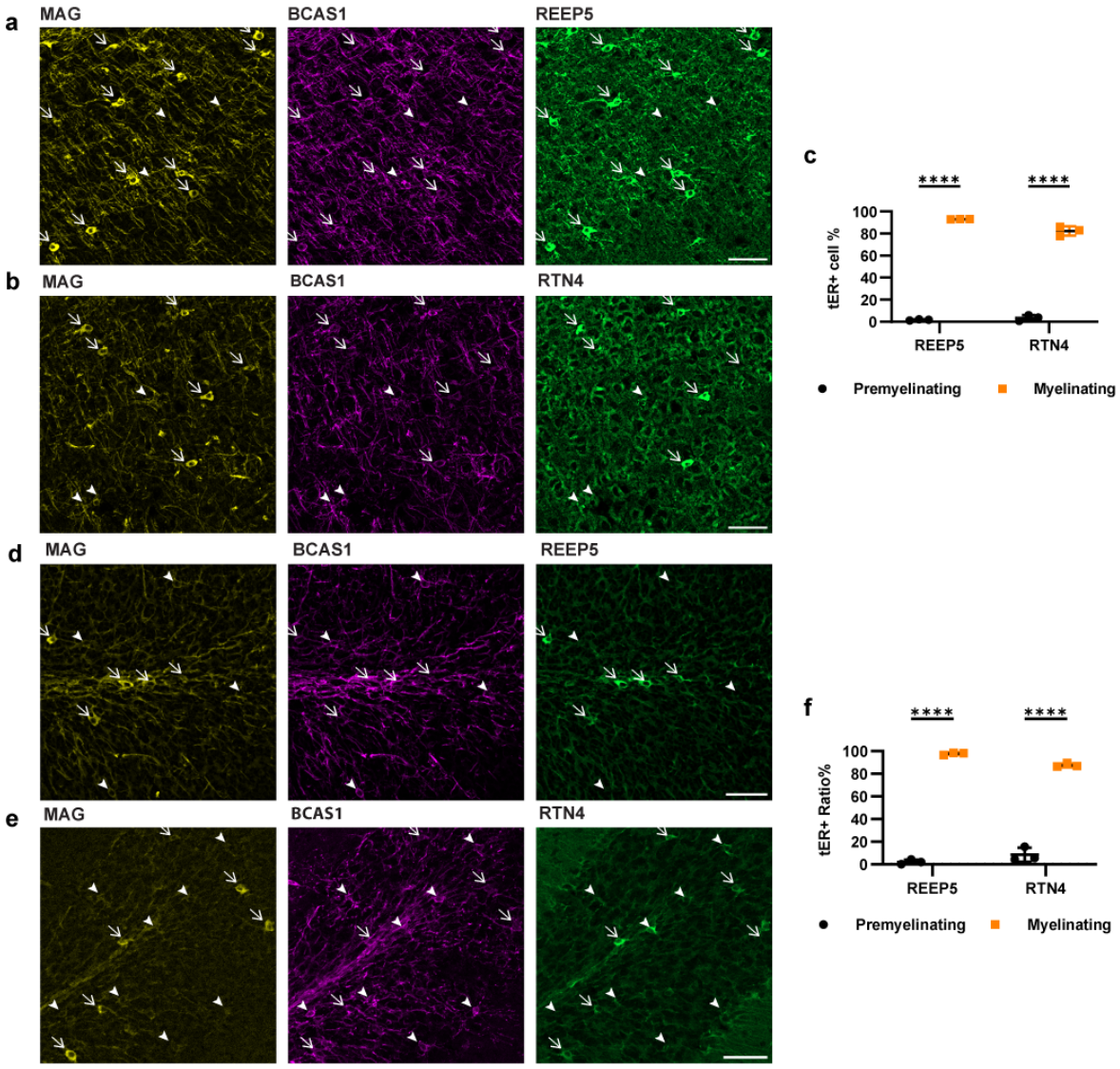

Fig. 3.4 | Tubular ER is more abundant in myelinating than premyelinating oligodendrocytes

a, b, d, e Immunohistochemistry of P14 mouse cortex (a, b) and cerebellum (d, e). Arrow heads: premyelinating oligodendrocytes ($MAG^{-}BCAS1^{+}$); arrows: myelinating oligodendrocytes ($MAG^{+}BCAS1^{+}$). **c** Quantification of (a) and (b) showing mean ± SD, 1.65 ± 0.55% or 3.54 ± 2.60% premyelinating cells are REEP5+ or RTN4+, 93.04 ± 0.25% or 82.34 ± 4.16% myelinating cells are REEP5+ or RTN4+. (n=3 wildtype P14 mice, Two-way ANOVA followed by Sidak's multiple comparison test). **f** Quantification of (d) and (e) from three P14 mice, showing mean ± SD, 2.04 ± 2.09% or 8.40 ± 6.19% premyelinating cells are REEP5+ or RTN4+, 97.79 ± 1.03% or 87.48 ± 1.68% myelinating cells are REEP5+ or RTN4+. (n=3 wildtype P14 mice, Two-way ANOVA followed by Sidak's multiple comparison test). Scale bars: 50 µm (a, b, d, e). *: $P \leqslant 0.05$, **: $P \leqslant 0.01$, ***: $P \leqslant 0.001$, ****: $P \leqslant 0.0001$

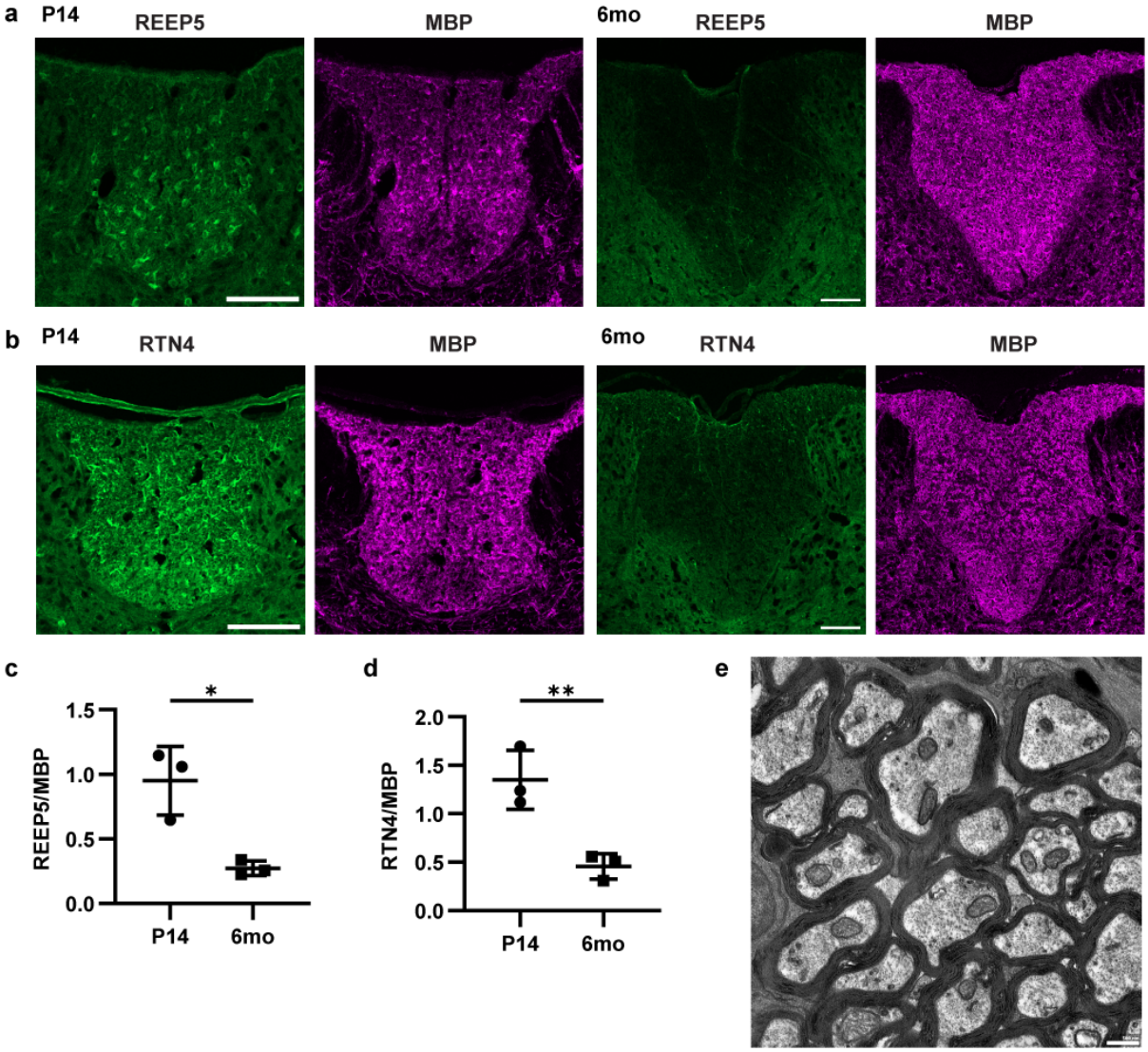

Fig. 3.5 | Tubular ER is absent in mature myelin

a, b Immunohistochemistry of P14 and adult (6mo) mouse thoracic spinal cord, focusing on dorsal white matter **c, d** Quantification of (a) and (b), respectively: tubular ER (REEP5 or RTN4) fluorescence signal normalized by myelin (MBP) signal, in dorsal white matter of thoracic spinal cord, showing mean ± SD, (f) P14: 0.95±0.27, 6-month-old: 0.27±0.06 (g) P14: 1.35±0.30, 6-month-old: 0.46±0.13 (n=3 wildtype mice for each time point, Two-tailed unpaired t-test) **e** TEM analysis of wildtype P28 optic nerve. Scale bars: 100 µm (a, b), 500 nm (e). *: P ⩽ 0.05, **: P ⩽ 0.01, ***: P ⩽ 0.001, ****: P ⩽ 0.0001

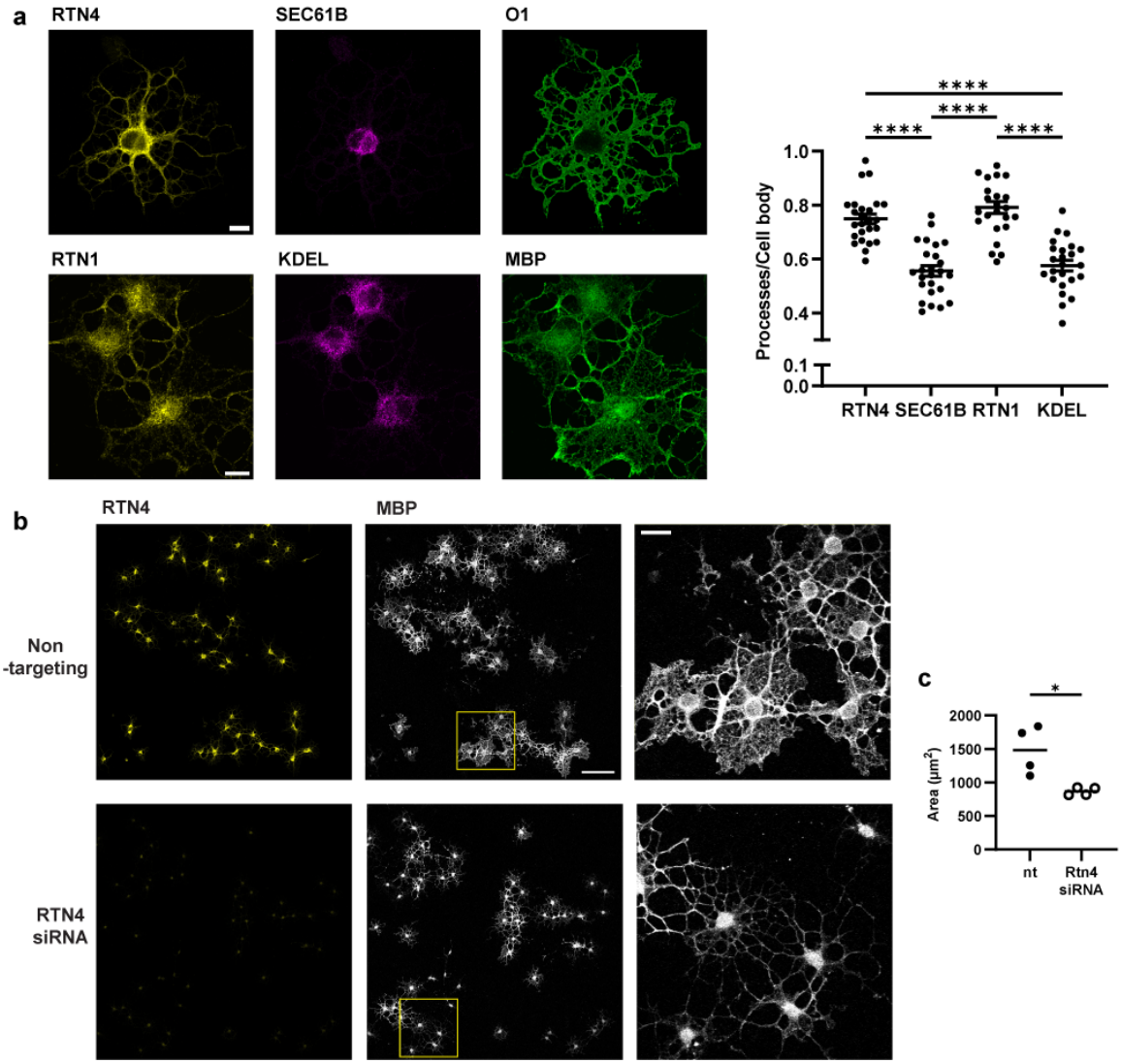

Fig. 3.6 | Tubular ER supports plasma membrane expansion in cultured oligodendrocytes

a Left: Immunocytochemistry of primary oligodendrocyte culture for tubular ER markers (RTN4 and RTN1), rough ER marker SEC61B, ER sheet marker KDEL(Farías et al., 2019) and oligodendrocyte marker O1 and MBP for outlining the cells. Right: The ratio of fluorescence signals from different ER subtypes at the cellular processes to that at the cell body, showing mean ± SD, KDEL: 0.58±0.10, RTN1: 0.79±0.11, SEC61B: 0.56±0.10, RTN4: 0.75±0.09 (n=24 cells for KDEL/RTN1, 25 cells for SEC61B/RTN4, one-way ANOVA followed by Tukey's post-hoc test) **b** *Rtn4* knockdown in oligodendrocyte culture. **c** Quantification of area based on MBP fluorescence signal from four independent replicates, showing mean ± SD, non-targeting siRNA: 1483±359.8, *Rtn4* siRNA: 868.1±60.03. (n=4 technical replicates, Two-tailed unpaired t-test) Scale bars: 10 µm (a), 100 µm (b), 20 µm (b zoom in) *: P ⩽ 0.05, **: P ⩽ 0.01, ***: P ⩽ 0.001, ****: P ⩽ 0.0001

3.3 Glycolipid transfer protein (GLTP) is associated with active myelination

To explore the possibility of nonvesicular lipid transport from the ER to the plasma membrane during myelin development, an in-depth re-analysis of published transcriptome and proteome databases was performed. Glycolipid transfer protein (GLTP) was identified as a good candidate (Sharma et al., 2015; Y. Zhang et al., 2014). GLTP stands out as a highly abundant and specific transcript in oligodendrocytes according to an RNA-Seq (Fig. 3.7a). Further investigation through immunohistochemistry solidified GLTP as a protein abundant within oligodendrocytes and myelin. This was supported by co-staining with BCAS1 and MAG, which indicated a more pronounced presence of GLTP in oligodendrocytes undergoing myelination compared to those in premyelinating stages (Fig. 3.8a, b). Additionally, it was observed that GLTP expression decreased as the myelin reached maturity (Fig. 3.8c, d). A zoom-in view of P14 myelin showed focal staining of GLTP within myelin (Fig. 3.8e), indicating GLTP is present in the inner tongue.

Moreover, immunocytochemical analysis on mouse primary oligodendrocytes showed that GLTP is localized to the oligodendroglial cell body, the processes as well as the growing front, which is akin to neuronal growth cones (Fig. 3.8f).

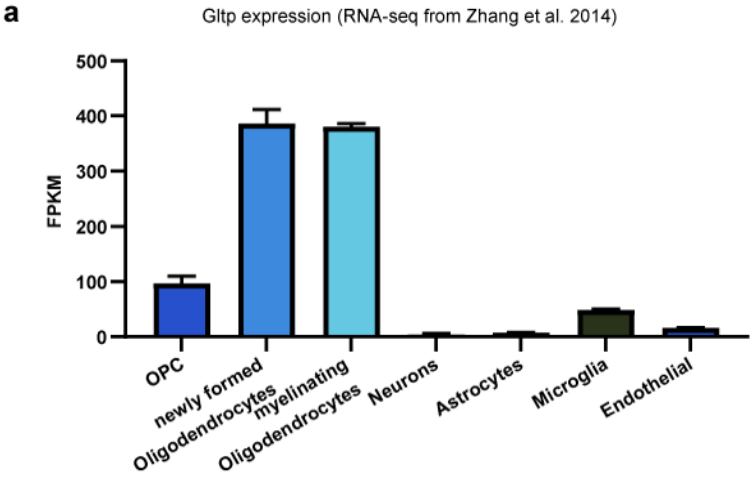

Fig. 3.7 | Glycolipid transfer protein (GLTP) is associated with active myelination

a RNA-seq analysis from Zhang et al. J. Neuroscience 2014. FPKM reads (two replicates per cell type) OPC: 88.495447, 105.799478; newly formed oligodendrocytes 368.317293, 404.231063; myelinating oligodendrocytes: 375.889082, 384.631206; neurons: 3.025255,

5.900611; astrocytes: 7.211993, 7.877303; microglia: 49.882491, 47.164643; endothelial cells: 15.936901, 16.717767.

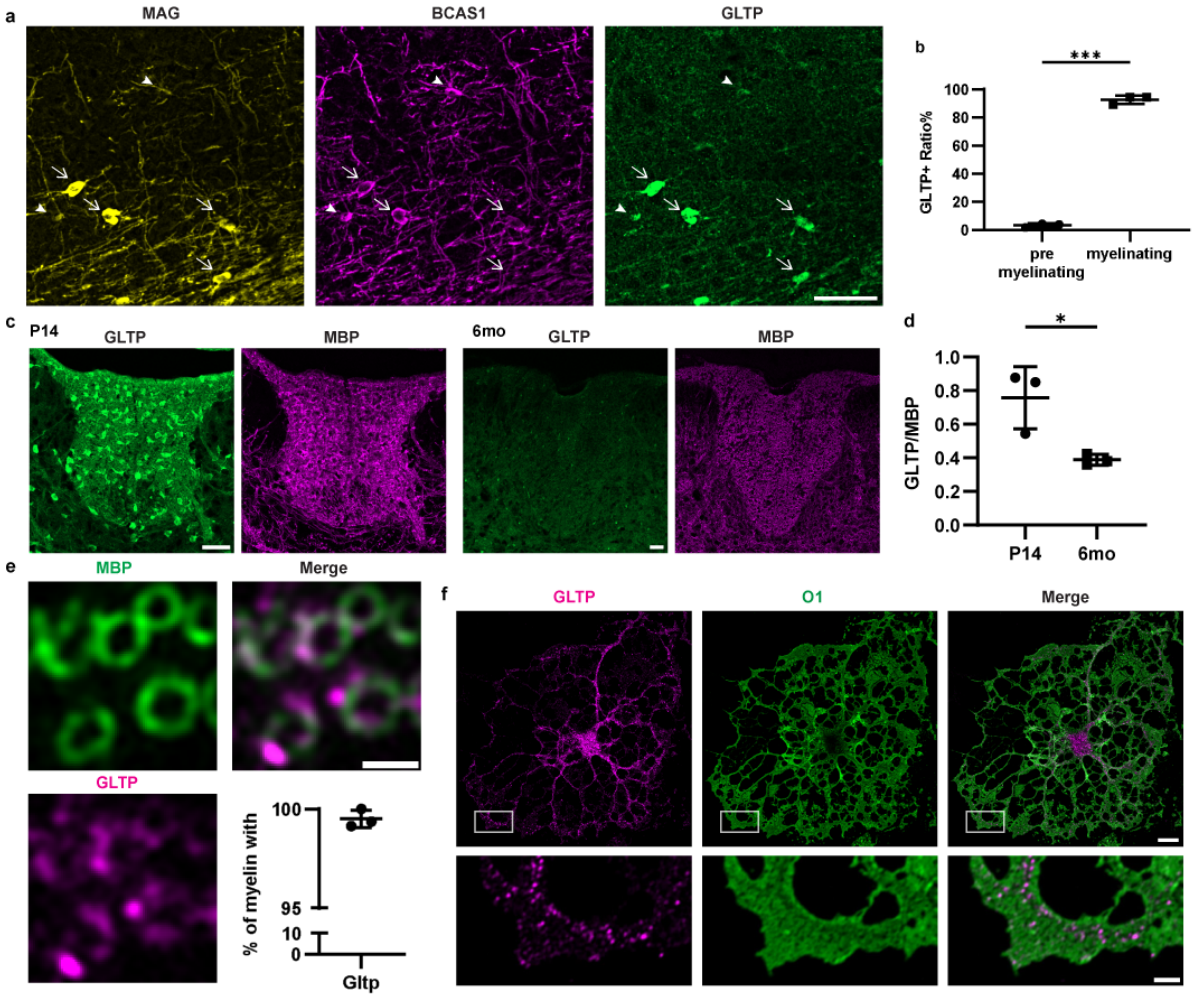

Fig. 3.8 | Glycolipid transfer protein (GLTP) is associated with active myelination

a Immunohistochemistry of P14 mouse cortex. Arrow heads: premyelinating oligodendrocytes ($MAG^{-}BCAS1^{+}$); arrows: myelinating oligodendrocytes ($MAG^{+}BCAS1^{+}$). **b** Quantification of (a) showing mean ± SD, 3.33 ± 1.36% premyelinating cells are GLTP+, 92.62 ± 3.08% myelinating cells are GLTP+ (n=3 wildtype P14 mice, Two-tailed pair t-test) **c** Immunohistochemistry of P14 and adult mouse thoracic spinal cord, focusing on dorsal white matter. **d** quantification of GLTP fluorescence signal normalized by myelin (MBP) signal, in dorsal white matter of thoracic spinal cord, showing mean ± SD, P14: 0.76±0.19, 6-month-old: 0.39±0.03 (n=3 wildtype mice for each time point, Two-tailed unpair t-test). **e** zoom-in view of P14 spinal cord and ratio of myelin (MBP^{+} ring) overlapping with GLTP, showing mean ± SD, 99.51 ± 0.44% myelin overlaps with GLTP (n=3 wildtype P14 mice). **f** Immunocytochemistry of primary oligodendrocytes. Magenta: GLTP; Green: oligodendrocyte marker O1 for outlining the cell. Scale bars: 50 µm (a), 100 µm (c), 1 µm (e), 10 µm (f upper), 2 µm (f bottom). *: $P \leqslant 0.05$, **: $P \leqslant 0.01$, ***: $P \leqslant 0.001$, ****: $P \leqslant 0.0001$

3.4 *Gltp* mutant has ER pathology in myelin at P14

The hypothesis that GLTP is responsible for transferring GalCer from ER to plasma membrane was tested through the creation of *Gltp*-deficient mouse models. To this end, a whole-body *Gltp* knockout (KO) model and a floxed *Gltp* model (Fig. 3.9a) were developed, leveraging the resources of the DZNE facility. The universal *Gltp* KO results in embryonic lethality, necessitating a focus on the conditional KO model, created by breeding *Gltp* floxed mice with *Cnp-Cre* mice(Lappe-Siefke et al., 2003) to drive the oligodendrocyte-specific gene deletion. *Gltp* cKO (*Cnp-Cre, Gltp* $^{fl/fl}$) exhibited diminished GLTP expression in both Western blot and immunohistochemistry analyses (Fig. 3.9b, c). Immunohistochemistry further verified the effective deletion of *Gltp* from oligodendrocytes across various brain regions.

Firstly, *Gltp* cKO mice were analyzed by EM at P14. Although these mice could form compact myelin, their myelin displayed unusual membrane ring structures (Fig 3.10a for spinal cord, Fig. 3.10b for optic nerve). These structures were observed across various brain regions in different *Gltp* cKO mice but were absent in the *Cnp-Cre* control littermates, as confirmed by examining over 1500 myelin cross-sections per condition (Fig 3.10c). Variations in the thickness of these rings were observed (Fig 3.10a zoom-in), with some displaying fewer wraps (marked by an arrow), others more wraps (marked by an arrowhead), and a subset presenting with a comet tail-like extension (marked by a star). Furthermore, such ring formations were also identified in the outer tongue (marked by double arrowhead, Fig. 3.10a zoom-in), within the cytoplasm of the cell body (Fig. 3.10d) and on the nuclear envelope (Fig. 3.10e). Volume electron microscopy (ATUM-SEM) unveiled that these rings were long tubes, traceable for up to 11 µm (Movie 2). 3D reconstruction indicated these tubes originated from the ER, first transitioning into a "lumenless" ER, and eventually rolling up to form a tube (Fig. 3.10f, Movie 3, 4). Analysis further revealed that myelin containing these rings typically showed a reduction or absence of ER. Specifically, in regions where rings were present in the inner tongue, there was merely a 40% probability of detecting ER, in contrast to inner tongues without such rings, which exhibited a normal likelihood of ER observation, aligning with wild-type patterns (Fig. 3.10g).

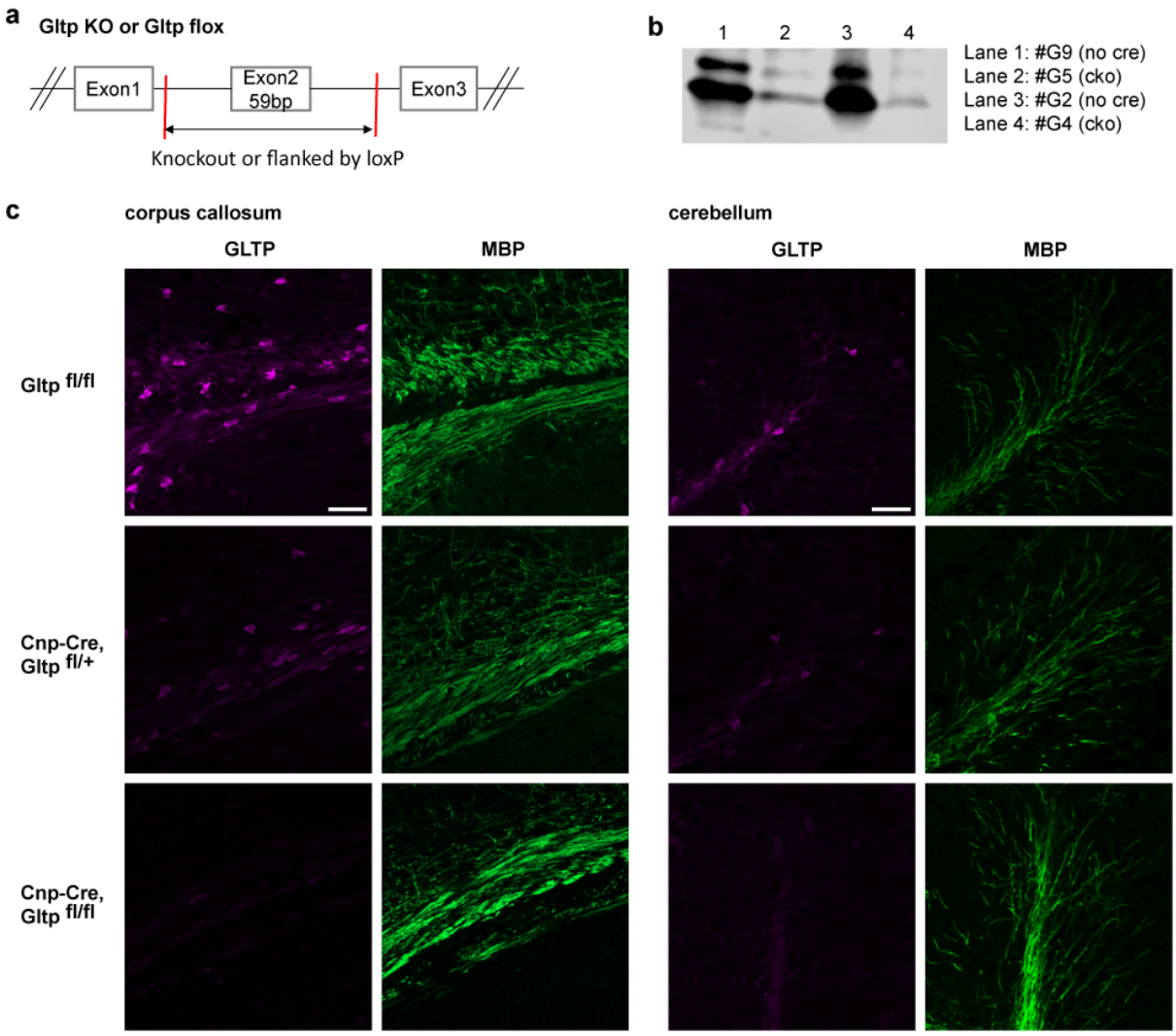

Fig. 3.9 | Design and verification of *Gltp* mutants

a Design of *Gltp* knockout (KO) or *Gltp flox* mouse lines. **b** Western Blot analysis of whole brain lysate from four P14 mice, 12 µg protein per lane. **c** Immunohistochemistry of corpus callosum and cerebellum from P14 WT (*Gltp* $^{fl/fl}$), het (*Cnp-Cre, Gltp* $^{fl/wt}$) and cKO (*Cnp-Cre, Gltp* $^{fl/fl}$) Scale bars: 50 µm (c).

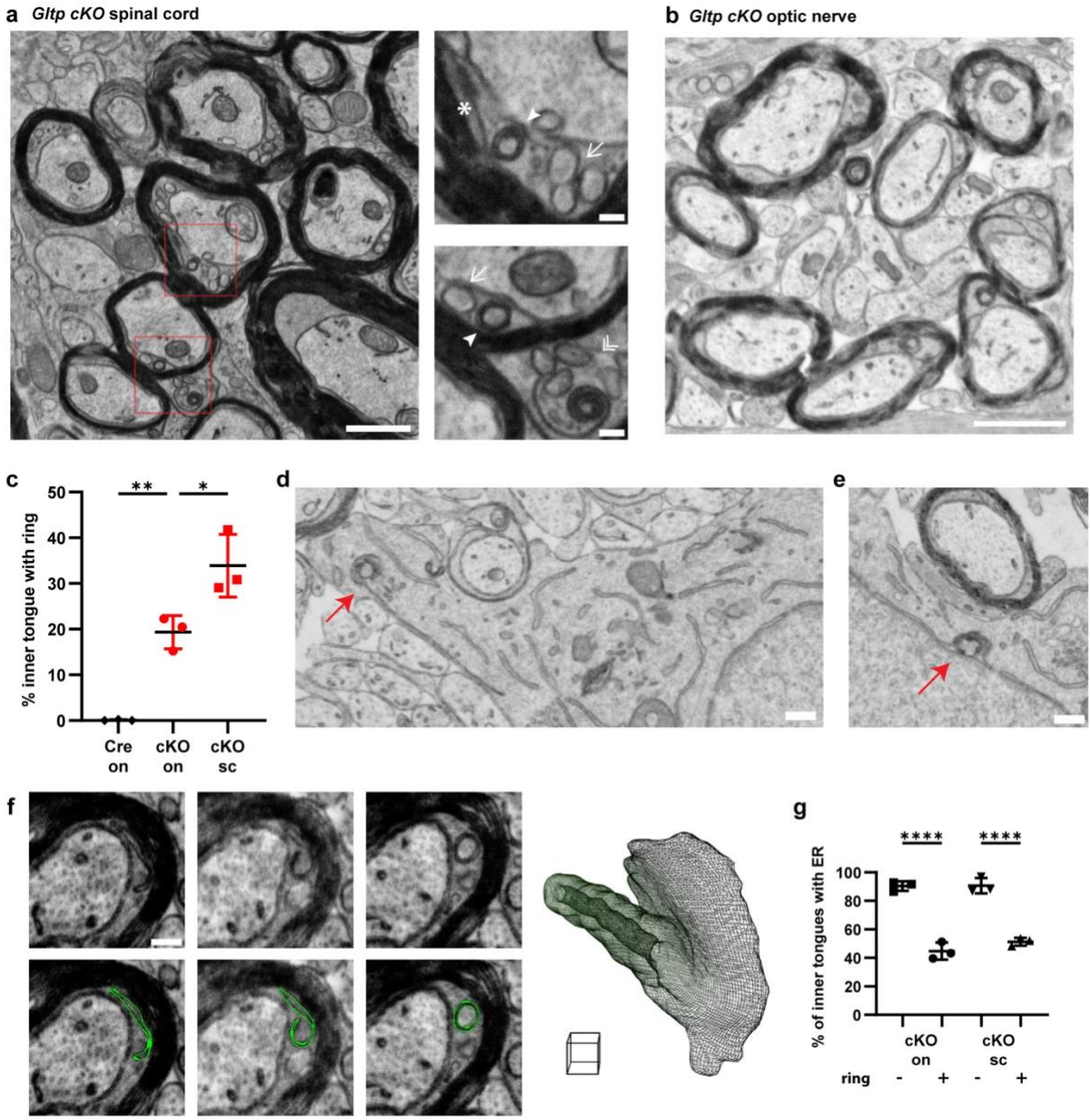

Fig. 3.10 | *Gltp* mutant has ER pathology in myelin at P14

a Membrane rings in inner tongue at spinal cord of P14 *Gltp* cKO (*Cnp-Cre, Gtlp*$^{flox/flox}$). Arrows: thin rings; arrowheads: thick rings; Star: a comet tail-like structure associated with the ring; double arrowheads: rings in the outer tongue **b** Membrane rings in inner tongue at optic nerve of cKO (*Cnp-Cre, Gltp* $^{fl/fl}$). **c** Ratio (mean ± SD) of inner tongue containing rings: 0.08±0.13% of inner tongues in optic nerve of *Cnp-Cre* (Cre on), 19.34±3.65% in optic nerve of *Cnp-Cre, Gtlp*$^{flox/flox}$ (cKO on), 33.90±6.87% in spinal cord of *Cnp-Cre, Gtlp*$^{flox/flox}$ (cKO sc) (n=3 mice for each condition, from 436+537+543 inner tongues of "Cre on", 508+525+531 of "cKO on", 589+585+664 of "cKO sc", One-way ANOVA followed by Tukey's post-hoc test) **d** Ring (red arrow) at cell body of oligodendrocyte. **e** Ring (red arrow) at nuclear envelop of oligodendrocyte. **f** Volume EM of optic nerve from *Gltp* cKO. Ring membrane is segmented in green, and 3D reconstruction of ring from a 1.5 µm-thick stack (31 slices with 50nm interval), from dark green to light green across the stack. Scale cube: 1x1x1 µm. **g** Amount of ER

decrease in the presence of rings, suggested by the ratio (mean ± SD) of inner tongue containing the ER: 90.34±3.33% of ring- vs. 44.69±6.01% of ring+ inner tongues in optic nerve of *Cnp-Cre, Gtlp*$^{flox/flox}$ (cKO on), 90.67±5.47% of ring- vs. 51.31±2.78% of ring+ inner tongues in spinal cord of *Cnp-Cre, Gtlp*$^{flox/flox}$ (cKO sc) (n=3 mice for each condition, One-way ANOVA followed by Sidak's multiple comparisons test) Scale bars: 1 µm (a), 150 nm (a zoom-in view), 1 µm (b), 100 nm (d, e), 200 nm (f). *: P ≤ 0.05, **: P ≤ 0.01, ***: P ≤ 0.001, ****: P ≤ 0.0001

3.5 *Gltp* mutant exhibits hypomyelination and degeneration at P28

To understand the effects of *Gltp* knockout and the development of membrane rings on myelination, a later time point P28 was examined. At this stage, *Gltp* cKO exhibited hypomyelination, as evidenced by a reduced g-ratio (inner myelin diameter divided by outer myelin diameter) compared to *Cre* littermates (Fig. 3.11a, b, c).

Additionally, myelin inner tongues of the *Gltp* cKO mice were noticeably swollen (Fig. 3.11d), a condition likely stemming from the pathological effects induced by the presence of membrane rings. Moreover, degeneration increases in the *Gltp* cKO (Fig. 3.11e, f). Despite of these changes, the proportion of axons that were myelinated were not significantly reduced in the *Gltp* cKO mice, suggesting that the knockout of GLTP and the membrane rings do not hinder the onset of myelin biogenesis (Fig. 3.11g).

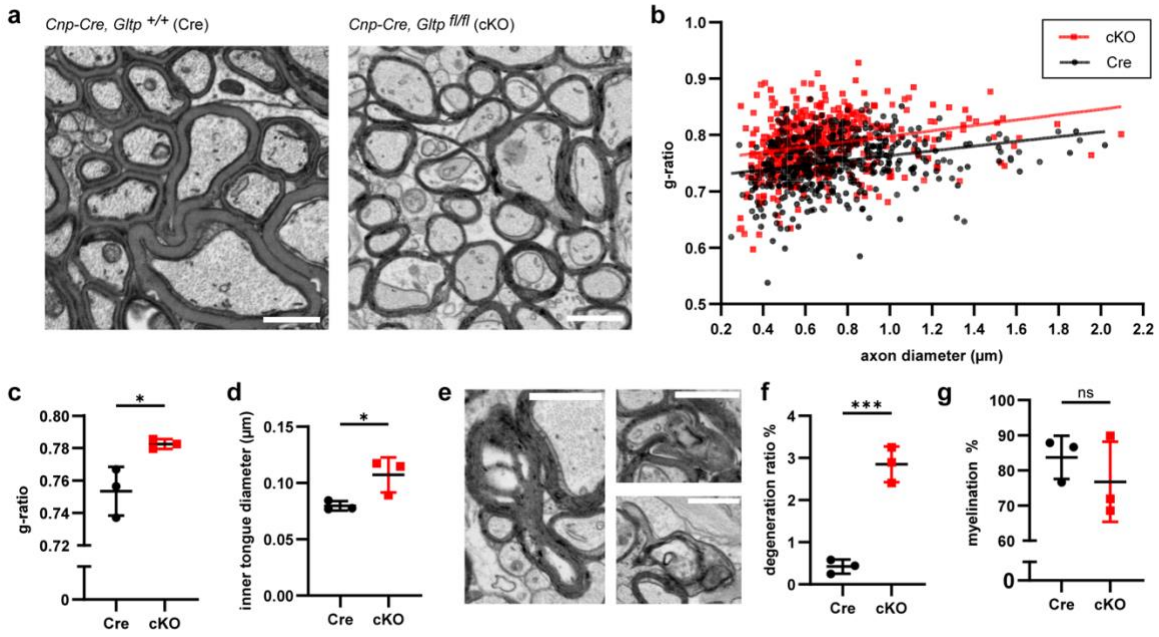

Fig. 3.11 | *Gltp* mutant exhibit hypomyelination and degeneration

a Optic nerve of *Gltp* cKO and Cre control mice at P28. **b, c** g-ratio (a measurement of myelin thickness defined as inner diameter of myelin divided by outer diameter), quantification from three mice for each condition. (b) shows g-ratio of individual myelin relative to the enwrapped axon's diameter. (**c**) shows the mean of myelin g-ratio from each mouse, showing mean of the cohort ± SD, Cre: 0.754±0.015, cKO: 0.783±0.003 (n=3 mice for each condition, Two-tailed unpaired t-test) **d** mean of inner tongue diameter from three mice for each condition, showing mean of the cohort ± SD, Cre: 0.080±0.004 µm, cKO: 0.107±0.016 µm. (n=3 mice for each condition, Two-tailed unpaired t-test) **e** examples of degenerations **f** Ratio of degeneration, showing mean of the cohort ± SD, Cre: 0.424±0.170%, cKO: 2.852±0.425% (n=3 mice per condition, Two-tailed unpaired t-test) **g** Percentage of axons that are myelinated, showing mean of the cohort ± SD, Cre: 83.720±6.148%, cKO: 76.780±11.43% (n=3 mice per condition, Two-tailed unpaired t-test). Scale bars: 1 µm (a and e) *: P ⩽ 0.05, **: P ⩽ 0.01, ***: P ⩽ 0.001, ****: P ⩽ 0.0001

3.6 Delivery of glycolipid to myelin is impaired in *Gltp* mutants

To elucidate whether GLTP is essential for glycolipid transport during the myelination process, myelin was isolated from individual *Gltp* cKO and *Cre* control mice at two distinct developmental stages, employing a standard two-round sucrose density gradient centrifugation technique (Erwig et al., 2019). This preparatory step was followed by a shortgun lipidomics analysis to examine the lipid composition in detail, with the nomenclature for the lipidome detailed in Box 1 for clarity.

Principal Component Analysis (PCA) on the lipid species composition of different samples revealed clear separations among the four conditions (Fig. 3.12f). A volcano plot generated from multiple t-tests comparing the *Gltp* cKO and *Cre* control mice underscored significant lipidomic alterations, with the top 10 downregulated and upregulated lipid species listed (Fig. 3.12a, b, c). Hexosylceramide (HexCer) constitute the majority of downregulated lipids. Unfortunately, the lipidomics analysis cannot distinguish GalCer and glucosylceramide: the two were detected together as HexCer. The reduction in HexCer species was especially pronounced for those with normal fatty acids (NFA), whereas HexCer species with 2-hydroxy fatty acids (HFA) did not exhibit significant fluctuations in the *Gltp* cKO mice (Fig. 3.12d), a phenomenon that may be explained by the compensatory upregulation of HFA-glucosylceramide in GalCer-deficient mutants (Bosio et al., 1996; Coetzee et al., 1996).

Further grouping of lipid species into classes and subsequent analysis via two-way ANOVA followed by Tukey's post-hoc test revealed that *Gltp* cKO mice exhibited altered myelin lipid composition. This alteration manifested as a decrease in HexCer and ether-linked phosphatidylethanolamine (PE O-), alongside an increase in cholesterol and variable changes in phosphatidylserine (PS) levels (Fig. 3.12e). Further lipidomics report can be found in Fig. 3.13a-p.

To corroborate the lipidomics outcomes, the delivery of GalCer was evaluated using anti-GalCer antibodies in a 2D oligodendrocyte culture system capable of generating myelin-like MBP-positive sheets. This assay involved immunocytochemical measurement of extracellular and intracellular GalCer, before and after permeabilization with Triton X-100, respectively (Fig. 3.12g). Observations indicated a diminished extracellular to intracellular GalCer ratio in oligodendrocytes derived from *Gltp* cKO mice, pointing to a disruption in GalCer delivery (Fig. 3.12g, h). Furthermore, a complementary gene disruption approach, siRNA, was adopted to validate this deficit in GalCer transport (Fig. 3.12g, i). The specificity of the anti-GalCer antibody, *Gltp* knockout and knockdown efficiency in primary oligodendrocyte culture were confirmed (Fig. 3.13q-s).

Box 1: Lipid nomenclature

(1) List of reported lipid classes

Some lipid classes (eg. PC) were detected by MSMS mode to obtain subspecies details. In this mode, the lipid was fragmented so the acyl chain composition of the lipid molecule is identified.

Lipid class	Full name	Structure detail level
Cer	Ceramide	species
Chol	Cholesterol	species
DAG	Diacylglycerol	subspecies
HexCer	Hexosylceramide	species
LPA	lyso-Phosphatidate	species
LPC	Lyso-phosphatidylcholine	species
LPE	Lyso-phosphatidylethanolamine	species
LPE O-	Lyso-Phosphatidylethanolamine (-ether)	species
LPI	Lyso-Phosphatidylinositol	species
LPS	Lyso-Phosphatidylserine	species
PA	Phosphatidate	subspecies
PC	Phosphatidylcholine	subspecies
PC O-	Phosphatidylcholine (-ether)	subspecies
PE	Phosphatidylethanolamine	subspecies
PE O-	Phosphatidylethanolamine (-ether)	subspecies
PG	Phosphatidylglycerol	subspecies
PI	Phosphatidylinositol	subspecies
PS	Phosphatidylserine	subspecies
SM	Sphingomyelin	species

(2) Lipid species nomenclature

Lipid species are annotated according to their molecular composition as:

Head group <sum of the carbon atoms in the hydrocarbon moiety>:<sum of the double bonds in the hydrocarbon moiety >;<sum of hydroxyl groups>.

For example, HexCer 42:0:2 denotes a Hexosylceramide species with a total of 42 carbon atoms, 0 double bond, and 2 hydroxyl groups in the ceramide backbone.

Lipid subspecies annotation contains additional information on the fatty acid chains and their positions on the glycerol backbone, when known. For instance, PE 18:0;0_22:1;0 refers to a phosphatidylethanolamine molecule with stearic acid (18:0;0) and docosenoic acid (22:1;0), without distinguishing between the sn-1 and sn-2 positions for these acyl groups (indicated by underscore "_"). Conversely, PE O-16:1;0/22:1;0 refers to a plasmalogen form of phosphatidylethanolamine, where a plasmenyl chain with 16 carbon atoms and one double bond (O-16:1;0) is ether-linked to the sn-1 position of the glycerol backbone, and a docosenoic acid (22:1;0) is esterified to the sn-2 position of the glycerol backbone (a slash "/" is used to show that the positions of the fatty acid chains on the glycerol can be distinguished).

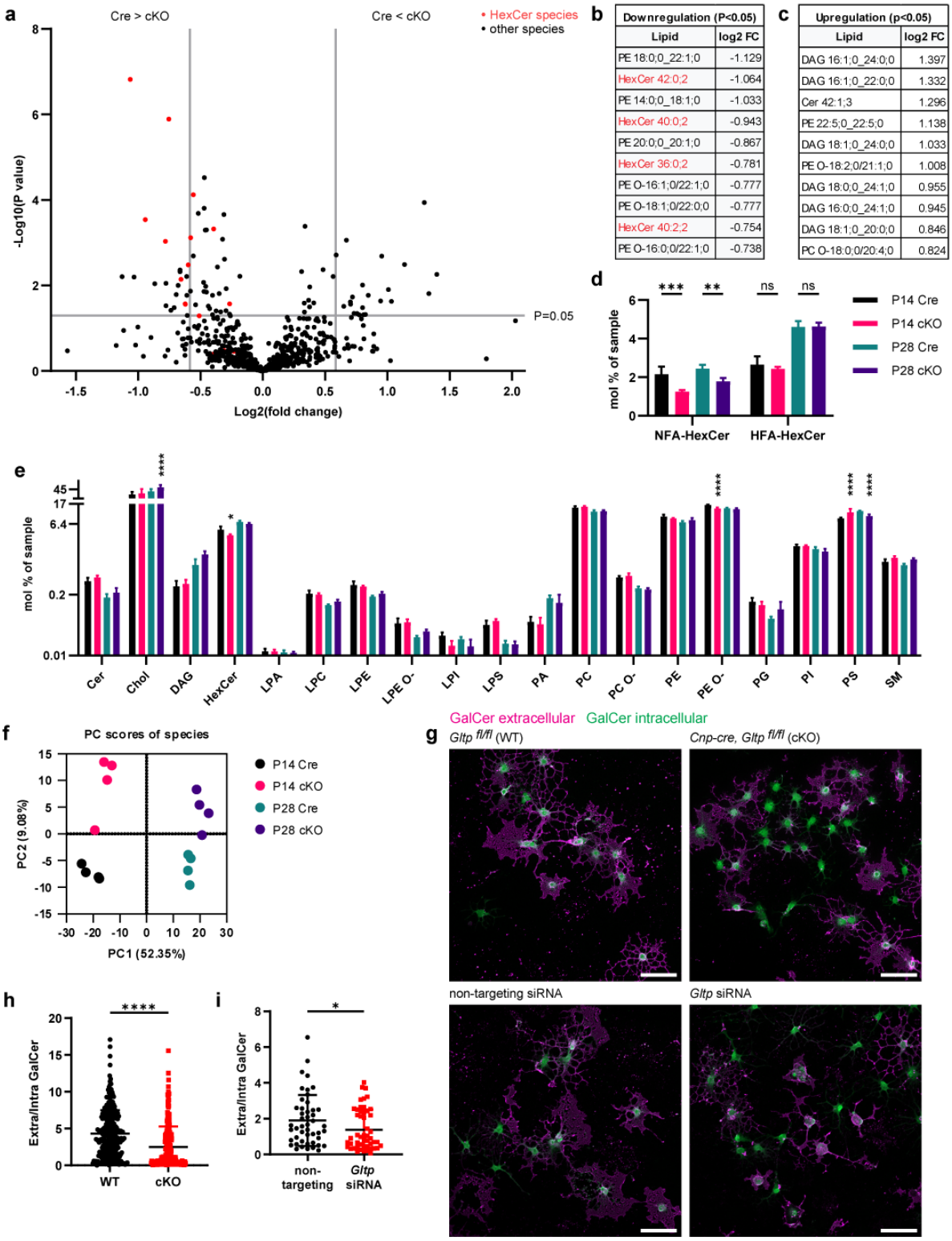

Fig. 3.12 | Delivery of glycolipid to myelin is impaired in *Gltp* mutant

a-f Lipidomics analysis of myelin purified from *Gltp* cKO (*Cnp-Cre Gltp*$^{flox/flox}$) and Cre control (*Cnp-Cre*) mice (n=4 mice for each genotype/time point). (a) Volcano plot shows differentiated regulated lipid species in cKO vs. Cre control. Vertical lines mark -/+ 1.5 fold change. Data points above horizontal line have p-value <0.05. Data were grouped based on genotype (Cre and cKO), and transformed to log2 for two-tailed Welch's t-test. (b) and (c) Top 10

downregulated and upregulated lipid species sorted by fold changes. (d) Relative amount of HexCer containing normal fatty acid (NFA) or 2-hydroxy fatty acid (HFA), showing mean± SD, P14-Cre-NFA: 2.15±0.39%, P14-cKO-NFA: 1.25±0.08%, P28-Cre-NFA: 2.44±0.19%, P28-cKO-NFA: 1.78±0.17%, P14-Cre-HFA: 2.65±0.44%, P14-cKO-HFA: 2.42±0.11%, P28-Cre-HFA: 4.61±0.3%, P28-cKO-HFA: 4.62±0.2%. (Two-way ANOVA followed by Tukey's post-hoc tests). (e) Relative amount of various lipid classes, showing mean ± SD. Color code is the same as in (d). (Two-way ANOVA followed by Tukey's post-hoc test. Stars indicate significant changes compared to the control of same age. Descriptive statistics and raw data are available in supplementary information) (f) Principal Component Analysis (PCA) of lipid species from the samples. Each sample is myelin from one animal. **g** Mouse primary oligodendrocyte's extracellular(magenta) and intracellular(green) GalCer signal obtained before and after Triton X-100. **h** Quantification of WT and KO cells from three mice for each condition, showing mean ± SD, WT (*Gltp* $^{fl/fl}$): 4.32 ± 3.18, cKO (*Cnp-Cre, Gltp* $^{fl/fl}$): 2.50±2.78. (n=286 for WT, n=265 for cKO, Two-tailed unpaired t-test). P value is calculated by Student's t-test. **i** Quantification of non-targeting and GLTP siRNA, showing mean ± SD, non-targeting siRNA: 1.90±1.43, *Gltp* siRNA: 1.38±1.13. (n=47 for nt, n=50 for siRNA, Two-tailed unpaired t-test) Scale bars: 50 μm (f) *: P ⩽ 0.05, **: P ⩽ 0.01, ***: P ⩽ 0.001, ****: P ⩽ 0.0001

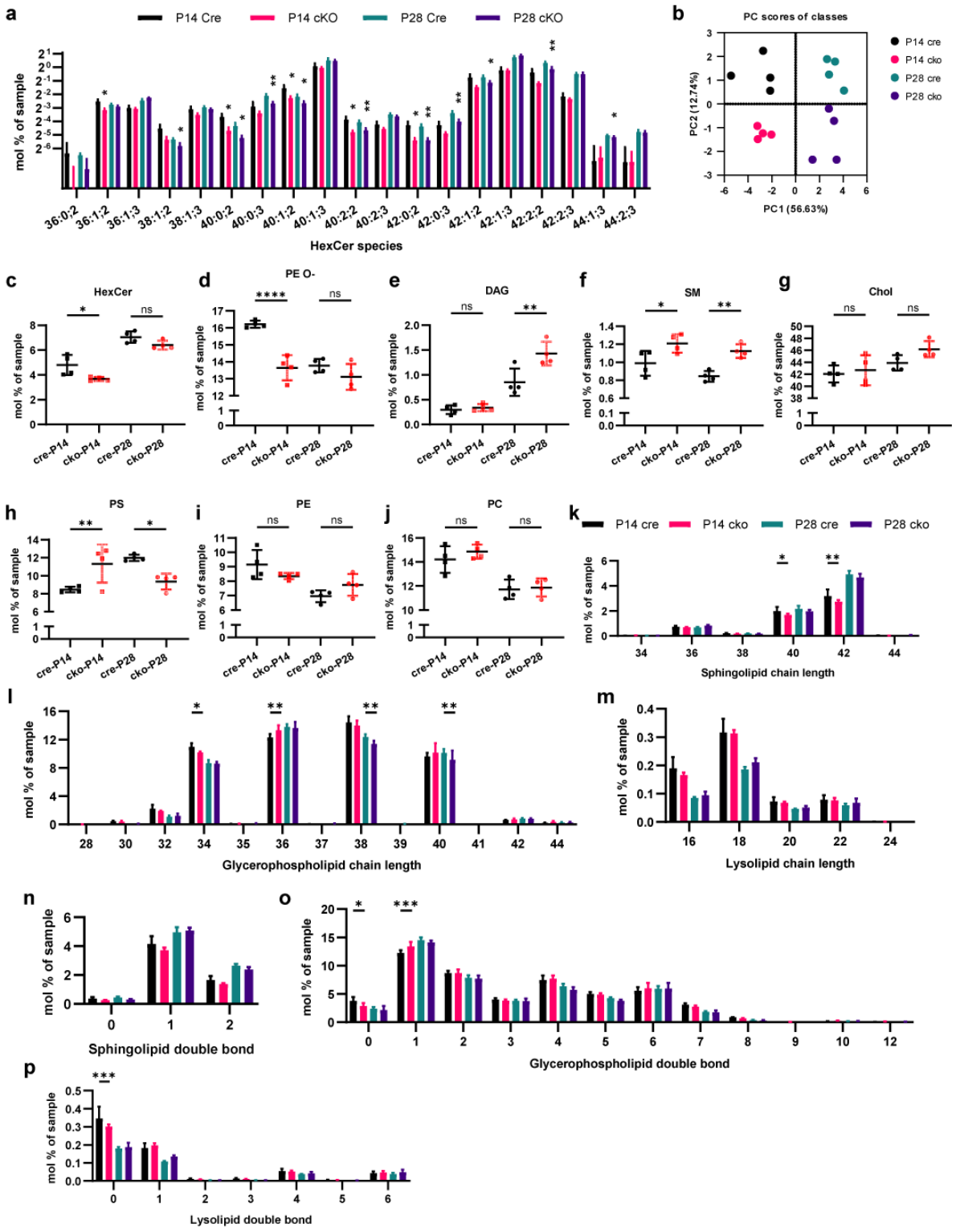
a
P14 Cre
P14 cKO
P28 Cre
P28 cKO
mol % of sample
HexCer species
b
PC scores of classes
P14 cre
P14 cko
P28 cre
P28 cko
PC2 (12.74%)
PC1 (56.63%)
c
HexCer
d
PE O-
e
DAG
f
SM
g
Chol
cre-P14
cko-P14
cre-P28
cko-P28
h
PS
i
PE
j
PC
k
Sphingolipid chain length
l
Glycerophospholipid chain length
m
Lysolipid chain length
n
Sphingolipid double bond
o
Glycerophospholipid double bond
p
Lysolipid double bond

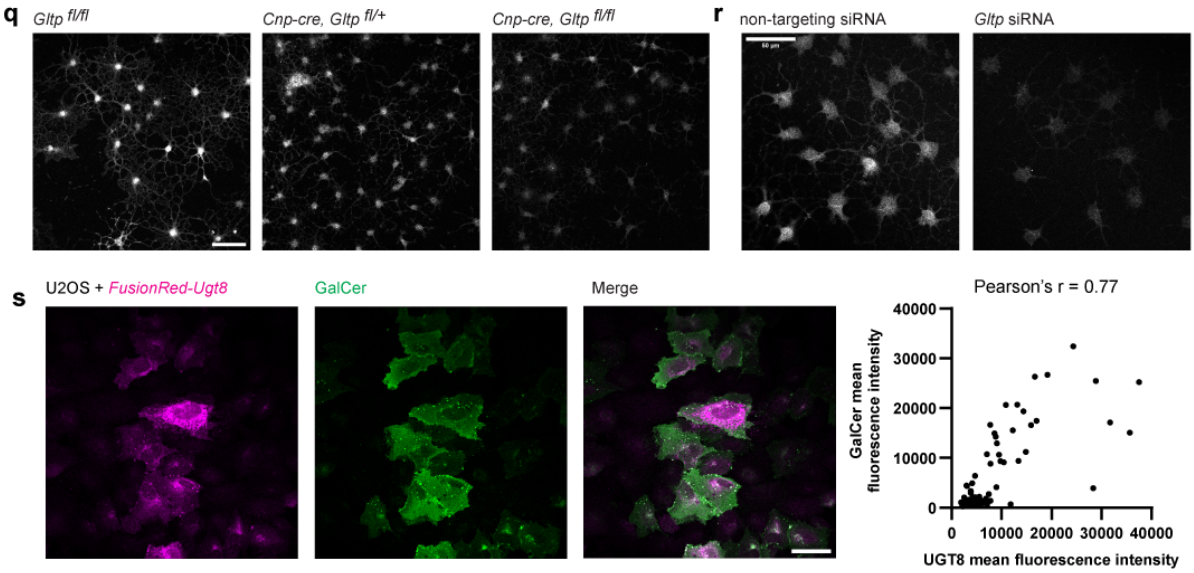

Fig. 3.13 | Delivery of glycolipid to myelin is impaired in *Gltp* mutant

a Relative amount of different GalCer species, showing mean ± SD. P value is calculated from two-way ANOVA followed by Tukey's post-hoc test. **b** Principal Component Analysis of the samples based their lipid classes. **c-j** One-way ANOVA of major lipid classes in myelin (instead of Two-way ANOVA in Fig. 6d), showing mean ± SD. P value is calculated from one-way ANOVA followed by Tukey's post-hoc test. **k-m** Chain length of different functional classes, showing mean ± SD. P value is calculated from two-way ANOVA followed by Tukey's post-hoc test. **n-p** Double bond of different functional classes, showing mean ± SD. P value is calculated from two-way ANOVA followed by Tukey's post-hoc test. **q** Validation of Gltp knockout oligodendrocyte culture. **r** Validation of Gltp knockdown oligodendrocyte culture. **s** Validation of anti-GalCer antibody. The GalCer signal is high in cells overexpressing UGT8, the enzyme responsible for GalCer synthesis, and correlation of GalCer and UGT8. Data points represent measurement from individual cells (n=96). Scale bars: 50 µm (q, r, s) Descriptive statistics and raw data for lipidomics are available in supplementary information. *: $P \leqslant 0.05$, **: $P \leqslant 0.01$, ***: $P \leqslant 0.001$, ****: $P \leqslant 0.0001$

3.7 Supplementary movies

The following movies were uploaded to the cloud. Key frames or maximum intensity projections were shown in figures.

Movie 1: Volume EM (ATUM-SEM) stack for 3D reconstruction in Fig 3.1a. 11.25 µm-thick (226 slices with 50 nm interval), from P14 wildtype mouse optic nerve.

Movie 2: Volume EM (ATUM-SEM) stack revealed the ring structure is a long tube (arrow), 11 µm-thick (222 slices with 50 nm interval), from P14 *Gltp* cKO mouse optic nerve. Scale bar 500nm.

Movie 3: Volume EM (ATUM-SEM) stack of rolling-up ring in myelin inner tongue, 1.5 µm-thick (31 slices with 50 nm interval), from P14 *Gltp* cKO mouse optic nerve. Related to Fig 3.10f. Scale bar 100nm.

Movie 4: Volume EM (ATUM-SEM) stack of rolling-up ring in oligodendrocyte cell body, 2.1 µm-thick (43 slices with 50 nm interval), from P14 *Gltp* cKO mouse optic nerve. Related to Fig 3.10d. Scale bar 100 nm.

4. Discussion

4.1 The working model

4.1.1 Transport of GalCer in developing myelin

I proposed a model in which GLTP facilitates nonvesicular transport of GalCer to support myelination (Fig. 4.1a). GalCer is synthesized through the addition of galactose to ceramide, a process mediated by the enzyme UDP-galactose:ceramide galactosyltransferase encoded by the *Ugt8* gene in mouse. The enzymatic domain of UGT8 is located at the lumen of the ER. Consequently, GalCer is initially formed in the luminal leaflet, but it has rapid access to the cytoplasmic leaflet (Burger et al., 1996; Xavier Buton et al., 2002; X Buton et al., 1996; van Meer, 2011). GLTP facilitates the transfer of GalCer from the ER to myelin, a specialized domain of oligodendroglial plasma membrane, where a yet-to-be-identified machinery transports GalCer from the intracellular leaflet to the extracellular leaflet. In this scenario, GalCer in the intracellular leaflet of plasma membrane remains low, creating a gradient and establishing the transfer direction as ER-to-plasma membrane. But eventually, the intracellular leaflet also accumulates a significant amount of GalCer, which may be beneficial, serving as molecular glue like MBP and contributing to the formation of major dense line. This explains the swollen inner tongue observed in P28 *Gltp* cKO.

In *Gltp* knockout (Fig. 4.1b), GalCer is accumulated in both lumenal leaflet and cytoplasmic leaflet of the ER. Headgroups of GalCer have been shown to interact with each other via carbohydrate-carbohydrate interaction, potentially involving hydrogen bonds and hydrophobic interactions, leading to the adherence of GalCer bilayers in vitro (Boggs, 2014; Kulkarni et al., 1999). As a result, GalCer in the intracellular leaflet aids in zipping up the ER, leading to the observed “lumenless” ER. Additionally, due to the accumulation of GalCer at the cytoplasmic leaflet, the ER adopts a rolled-up configuration. The ER is known to be prone to roll up when its membrane can interact, as seen, for instance, with nonmonomeric GFP on the ER (Snapp et al., 2003). I propose that *Gltp* mutant resembles this case. The observed rings in the mutant further support the idea that GalCer is localized to both leaflets of the ER.

The “lumenless” ER is also observed in wildtype and I think this is the site for active GalCer synthesis (Fig 3.1b). But in wildtype, because the GalCer on cytoplasmic leaflet of ER is actively transported away, the ER never rolls up.

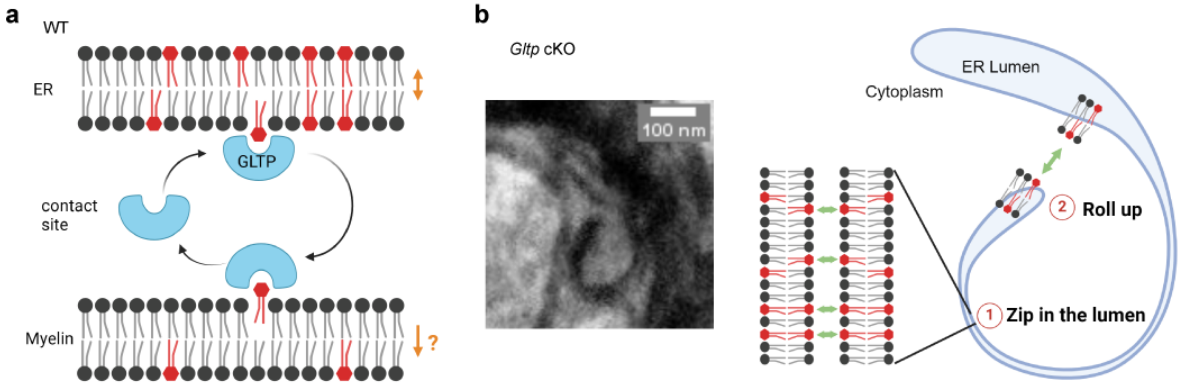

Fig. 4.1 | Graphical illustration of model showing transport of GalCer in developing myelin.

a In wild type myelin, GLTP transfers GalCer (red) from the ER to myelin, a specialized domain of oligodendroglial plasma membrane. Double-head arrow indicates GalCer reach an equilibrium in ER. Single-head arrow indicates that a yet-to-be-identified machinery transports GalCer to the extracellular leaflet of plasma membrane, keeping GalCer low in the intracellular leaflet of myelin membrane, creating a gradient and establishing the transfer direction as ER-to-plasma membrane. **b** Ring formation in *Gltp* cKO occurs in two steps. Step 1: GalCer attract each other and zip up the ER from the lumen. Step 2: GalCer accumulating in cytoplasmic leaflet of ER make the ER to roll up. Created with BioRender.com

4.1.2 The existence of tether

Tethering molecules are required for the formation of all membrane contact sites reported so far. In developing myelin, what bridges the ER and plasma membrane into close proximity? GLTP is a cytosolic protein that can interact with VAP-A (Tuuf et al., 2009), an ER transmembrane protein involved in the formation of various ER-organelle contact sites (Balla et al., 2019). VAP-A forms a dimer (Subra et al., 2023). GLTP can work at VAP-A mediated ER-plasma membrane contact site if one VAP-A subunit binds to a plasma membrane protein while the other binds to GLTP. But it is also possible that myelin is a special case in which nonvesicular lipid transport occurs without a tether. The inner tongue, being a small compartment, allows the ER to be consistently close to the plasma membrane. Observations along the inner tongue reveal a continuous proximity between the ER and the plasma membrane.

This suggests that myelin might resemble the situation of a test tube with high-concentration liposomes, where transfer can occur without a tethering mechanism.

4.1.3 Potential floppases

In my working model, GalCer is moved from the intracellular leaflet to the extracellular leaflet on plasma membrane. There are two classes of proteins that can move lipids in this direction: scramblases and floppases. Scramblases move a variety of lipids in both directions. Asymmetric lipid distribution between leaflets is essential for cellular homeostasis (Doktorova et al., 2020), which also applies to myelin – for instance, phosphatidylserine normally resides in the intracellular leaflet of myelin, and when exposed to the extracellular leaflet by scramblases, it shows the “eat me” signal (Djannatian et al., 2023). Therefore, the involvement of floppases is more likely. Floppases facilitate the movement of lipids from the intracellular to the extracellular leaflet and are usually ATP-binding cassette (ABC) transporters, which belong to a large protein family with approximately 50 members in the human genome. These transporters are capable of translocating substrates including lipids and small molecule drugs across cellular membranes. A number of ABC transporters are found in oligodendrocytes (Kim et al., 2008; Wolf et al., 2012).

ABCA2 is an abundant ABC transporter in oligodendrocytes (Tanaka et al., 2003) and is required for myelination in mouse (Mack et al., 2007; Sakai et al., 2007). This transporter is present at the endolysosomal systems. Interestingly, endosomal transport is known to take part in the remodeling of myelin membrane protein, such as proteolipid protein (PLP) (Baron et al., 2015; Feldmann et al., 2011; Winterstein et al., 2008). The possibility that this remodeling extends to lipids, specifically whether GalCer is sorted in the recycling endosome by ABCA2, warrants closer examination.

4.2 Alternative explanations of the results

While my findings support the role of GLTP in ER-to-plasma membrane nonvesicular lipid transport during myelination, the complexity of lipid dynamics suggests that other mechanisms may also contribute to the observed results. Below, I discuss several alternative explanations:

(1) GLTP transfers GalCer from ER to endosomes

Based on the previous section, an alternative route for GalCer transport could involve its movement from the ER to the endosomes before ultimately reaching plasma membrane. Endosomes are present in developing myelin(Almeida & Macklin, 2023; Krämer-Albers & Werner, 2023). Additionally, existing literatures have reported ER-endosome contact sites and the lipid transfer that occurs between them (Raiborg et al., 2015; Suzuki et al., 2024). Therefore, this alternative explanation presents a plausible route but requires further study for verification.

(2) GLTP as a shuttle

Like many lipid transfer proteins, GLTP could function as a shuttle. Biochemical studies have confirmed that lipid transfer proteins can transfer lipids between liposomes, while cell biology studies highlight the existence of membrane contact sites, suggesting that non-vesicular transport occurs at these locations. Fully bridging these two types of studies can be challenging, leaving the field open to the possibility that lipid transfer proteins might act as shuttles. In the case of myelin development, given the close proximity of the ER to myelin membrane, GLTP likely does not need to operate over long distances as a shuttle would. However, in adults, where myelin becomes more compact and space is constrained, GLTP emerges as a promising candidate for facilitating lipid turnover within myelin. This is especially relevant given recent suggestions that myelin still undergoes biogenesis in adulthood (Meschkat et al., 2022).

(3) GLTP affects vesicular trafficking

According to a recent study on HeLa cells (Nurmi et al., 2023), GLTP could also affect vesicular trafficking. However, this conclusion was drawn from a few images without quantification, where mutants appear very similar to controls. Moreover, even if this observation is statistically significant, it could indicate a secondary effect.

I have evidence suggesting this alternative explanation is unlikely. Firstly, as mentioned in the introduction, GalCer transport persists in the absence of vesicular trafficking in both cell lines and cultured oligodendrocytes. Secondly, my lipidomics analysis revealed HexCer as one of the few lipid classes that changed. The fact that

GLTP's influence is rather specific to certain lipid classes could argue for nonvesicular trafficking since vesicular trafficking is less selective toward lipids.

To further explore this alternative explanation, examining myelin membrane proteins could offer significant insights. Because proteins rely exclusively on vesicular trafficking, unlike lipids, which may utilize nonvesicular pathways, conducting a proteomics analysis of P28 myelin from *Gltp* cKO and *Cre* control appears to be a promising approach to clarify these mechanisms.

However, it's important to keep in mind the challenge of distinguishing direct from indirect influences. The *Gltp* cKO mutant in my study exhibits ER pathology, and with a compromised ER, cellular homeostasis—and consequently, vesicular trafficking—could be affected.

4.3 Lipid transport in myelination

4.3.1 Why nature chose galactosylceramide (GalCer) for myelin

It has been postulated that myelin membranes avoid incorporating negatively charged phospholipids at extracellular leaflets to prevent repulsion. Glycolipids, on the other hand, are not only not repulsive, but also attractive due to carbohydrate-carbohydrate interaction (Boggs, 2014). GalCer is one of the few glycolipids synthesized in the ER, so it is produced directly at the growing front and can be transferred directly to the myelin membrane. In contrast, the remaining glycolipids are synthesized in the Golgi apparatus and requires further trafficking to enter the myelin.

It is noteworthy that glucosylceramide is upregulated in *Cgt* mutant mice that are unable to convert ceramide to GalCer (Bosio et al., 1996; Coetzee et al., 1996). While this upregulation could be a compensatory mechanism, it is also possible that, in the wild type, ceramide is predominantly used for GalCer synthesis in the ER, leaving limited precursors for glucosylceramide synthesis in the Golgi.

4.3.2 Specialized lipid distribution in myelin

This study offers a potential explanation for the unsolved puzzle of differential distribution of GalCer and sulfatide in myelin. GalCer is localized to myelin, but once

sulfated in Golgi apparatus and converted to sulfatide, it is delivered to noncompact myelin fraction enriched with paranode (Maier et al., 2008), and plays a role in paranode formation (Honke et al., 2002). It has been long postulated these two lipids are delivered by different routes (Baron & Hoekstra, 2010; Hayashi & Su, 2004).

My findings shows that the ER extends into the inner tongue of myelin, positioning GalCer synthesis within the myelin sheath itself and facilitating its direct access to the internodal region. In contrast, the paranodal cytosolic space is significantly larger, enabling easier access for the Golgi apparatus and vesicular transport. This suggests that sulfatide is synthesized at the paranode or transported there via Golgi-derived vesicles, supporting the idea of separate lipid delivery mechanisms for internodal and paranodal regions.

4.3.3 Other nonvesicular transport for myelination

In this section, I will discuss additional nonvesicular transport families potentially involved in myelination based on three reviews (Y.-J. Chen et al., 2019; Hanna et al., 2023; Saheki & De Camilli, 2017), and list their gene expression in mouse oligodendrocytes relative to other brain cell types in Fig 4.3, based on the RNA-Seq study (Y. Zhang et al., 2014).

The field of nonvesicular lipid transport is still emerging, which raises the possibility that proteins not currently identified for ER-plasma membrane transport could indeed play a role. Additionally, proteins implicated in lipid export from the plasma membrane might also participate in import during myelination, as directionality is not fully clear and may reverse under certain conditions. Also, while I identified GLTP based on its abundance, I believe a low expression of a lipid transfer protein doesn't mean it is not important. This is especially true for bridge-like transfer proteins since one copy is enough to let numerous lipid molecules pass. Therefore, these listed candidates may not be known to be involved in transport to the plasma membrane, or they may not be very abundant. Furthermore, because endosomes are present in developing myelin, I will also include endosome-to-plasma membrane trafficking.

(1) Class II PITP (phosphatidylinositol transfer protein) family. It contains cytosolic proteins Nir2 and Nir3, which act as membrane editors and are unlikely to contribute to bulk transport. Upon phospholipase C activation, they can be recruited to ER-plasma membrane contact sites to clear phosphatidic acids from the plasma

membrane and to supply new phosphoinositides. Additionally, although Nir1 does not possess the transfer function, it is included in Fig 4.3 due to its reported role as a positive regulator of Nir2 (Quintanilla et al., 2022).

(2) SMP (synaptotagmin-like mitochondrial-lipid binding protein) domain-containing protein family. Four mammalian members from this family have been characterized: Extended synaptotagmin (E-syt) 1/2/3 and TMEM24 (also known as C2CD2L). All of these are ER membrane proteins. Biochemical studies suggested E-syts can transfer glycerolipids and diglyceride (Saheki et al., 2016; Schauder et al., 2014), while TMEM24 prefers to transfer phosphoinositides (Lees et al., 2017). Interestingly, both E-syt1 and TMEM24 operate in different modes dependent on intracellular Ca^{2+} level.

(3) OSBP (oxysterol-binding protein) and ORP (OSBP-related protein) family. ORP5 and ORP8 from this family have been shown to transfer phosphotidylserine from the ER to plasma membrane and exchange phosphatidylinositol 4-phosphate (PI4P) from plasma membrane to the ER (Chung et al., 2015).

(4) StART (steroidogenic acute regulatory transfer) and StART-like protein family. There are 15 human StART proteins and a few StART-like proteins. The StART domain can bind various lipids, including sterols and phospholipids, and these proteins are involved in lipid transport across various membrane contact sites, not necessary limited to ER-plasma membrane contact sites (Clark, 2012). Regarding the StART-like proteins, two recent studies (Besprozvannaya et al., 2018; Sandhu et al., 2018) have suggested that GRAMD1/Aster proteins can transfer cholesterol from plasma membrane back to the ER, following the concentration gradient. During myelination, oligodendrocyte synthesize large amounts of cholesterol in the ER, creating an opposite gradient. How GRAMD/Aster proteins operate under this condition warrants further investigations.

(5) Sec22b-Stx1 (syntaxin 1). Sec22b is an ER-anchored SNARE protein and Stx1 is a plasma membrane-anchored SNARE protein. This pair can interact without mediating membrane fusion, thereby stabilizing ER-plasma membrane contacts. Although they lack a lipid transfer function, their associated ER-plasma membrane contact is important for membrane expansion (Gallo et al., 2020; Petkovic et al., 2014).

(6) Mospd2 (motile sperm domain-containing protein 2). Mospd2 is an ER-anchored protein involved in lipid transfer at a number of membrane contact sites (Di Mattia et al., 2018).

(7) NPC (Niemann–Pick type C). NPC1 and NPC2 are localized to late endosomes and lysosome. They may work to transport cholesterol from endosomes that are present in myelin, to the myelin.

(8) Gltp. Gltp expression is specifically high in oligodendrocytes. Another member from this family, FAPP2, is involved in glycolipid transfer between the ER and Golgi (D'Angelo et al., 2007; Halter et al., 2007), but is expressed at a very low level in the brain.

(9) Bltp (Bridge-like transfer protein). This family is recently characterized to form a hydrophobic tunnel and mediate bulk lipid transport at various membrane contact sites. Some members, such as VPS13s, are present in cells at very low levels. However, due to their efficient operation, they are believed to play an important role in intracellular lipid transport. While proteins from this family remain largely unexplored, there is already some evidence suggesting the involvement of some members in plasma membrane expansion (Cheng & Bezanilla, 2021; Neuman & Bashirullah, 2018; Neuman et al., 2022).

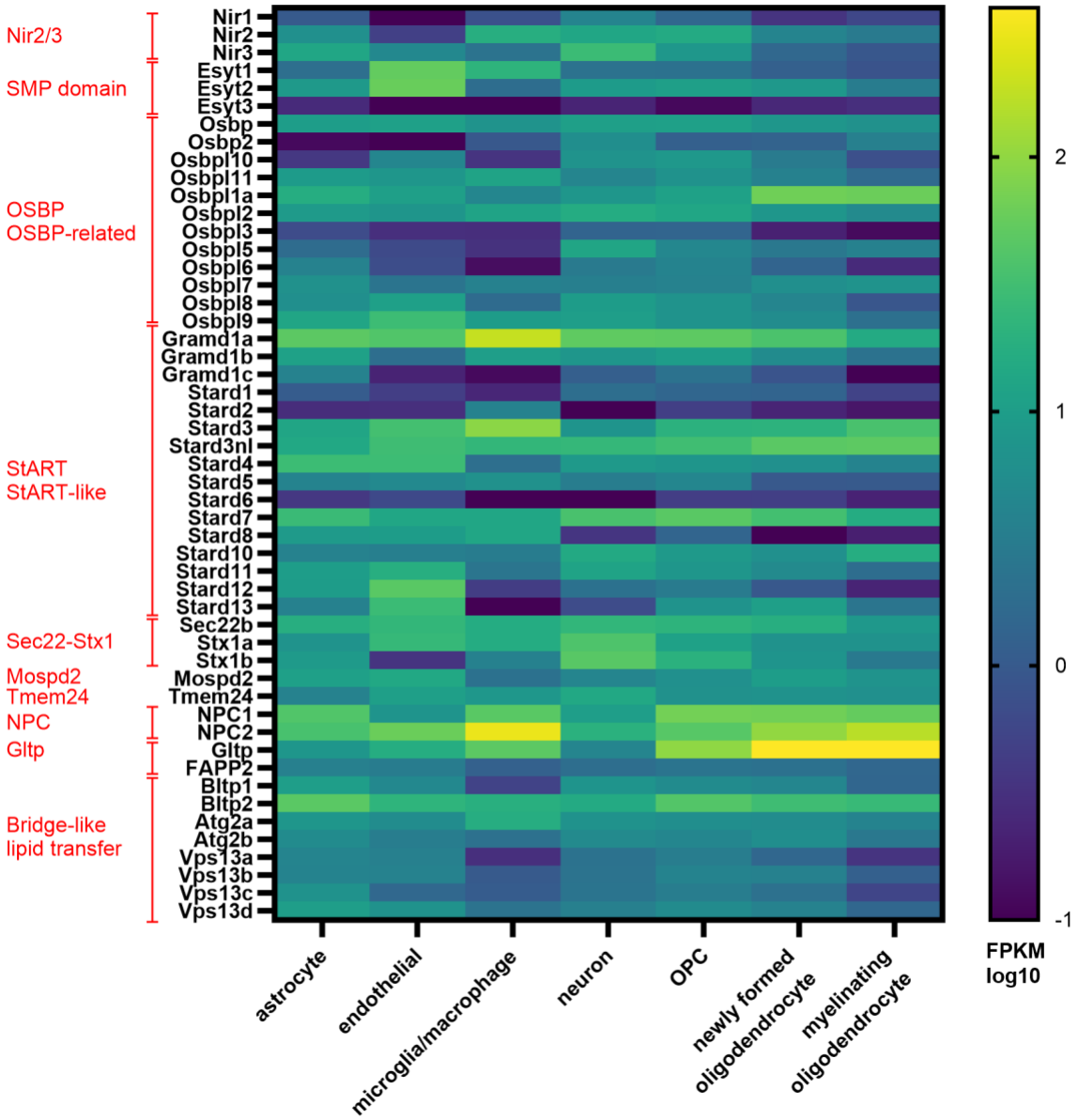

Figure 4.2 Expression pattern of nonvesicular transport protein families across brain cell types in mouse: A heatmap analysis of Zhang et al.'s RNA-Seq data.

4.3.4 Nonvesicular lipid transport for remyelination

GLTP translation is increased during remyelination in a cuprizone-induced mouse model for Multiple Sclerosis, detected by Ribo-Seq screen (Voskuhl et al., 2019). Like developmental myelination, remyelination may also involves nonvesicular transport. Given its superiority in terms of efficiency, boosting nonvesicular transport could potentially enhance remyelination in neurodegenerative diseases.

4.3.5 Other lipid transport for myelination

Beyond vesicular and nonvesicular transport, a recent report (Plochberger et al., 2020) showed that Apolipoproteins may directly fuse with the membrane. Although myelin mainly grows from the inside at the inner tongue, it would be interesting to test this possibility. Perhaps astrocytes or other cell types can facilitate the burden on oligodendrocytes in making myelin by supplying cholesterol directly to the myelin.

4.4 Cell biology of myelination

4.4.1 Other roles the ER might play in myelin

One critical function of the ER is to serve as a reservoir for calcium storage. Many studies have shown calcium is important for myelination (Baraban et al., 2018; Krasnow et al., 2018). It is very likely ER is playing a role here.

4.4.2 Cell biology of cytoplasmic channels

Developing myelin contains cytoplasmic channels that serve as highways for the transport of materials necessary for myelin biogenesis. These channels are highly curved and complex, raising many intriguing cell biology questions. For instance, how can microtubules sustain such high curvature? How are the ER and other organelles transported along microtubules? Additionally, how are extracellular vesicles released in developing myelin? These questions could be interesting directions for future investigations.

4.5 Limitation of the study

Although confocal images of immunocytochemistry provide some evidence that GLTP is adjacent to the plasma membrane, a limitation of this study is the absence of unambiguous evidence demonstrating GLTP's operation between ER-plasma membrane contact sites. This is challenging for many cytosolic lipid transfer proteins. For example, the lipid transfer protein, Oxysterol-binding protein (OSBP) is well-established to function at ER-Golgi contact sites, yet its distribution is largely cytosolic (Mesmin et al., 2013). One potential method to address this is by generating a mutated GLTP that halts in the working state: mutating the glycolipid binding site of GLTP may enhance its interaction with the lipid, thereby allowing

visualization of where GLTP acquires lipids. However, such a mutation has yet to be identified, and its effectiveness remains uncertain.

Another limitation involves the methodology for testing if tubular ER is required for myelination. In this study, *Rtn4* mutation is used to investigate the influence of tubular ER. But RTN4 may have functions beyond stabilizing tubular ER. A more precise approach would involve preventing tubular ER from entering developing myelin, for instance, by mutating adaptors on the ER that link the ER to motor to prevent the tubular ER from entering the myelin.

In general, the limitations of this study stem from the technical challenges inherent in myelin research. Obtaining primary oligodendrocyte cultures is difficult, with cells that are challenging to culture, transfect, and mutate. In this study, I utilized cell-permeable RNAi, but these reagents are costly, and not every knockdown is effective. For example, attempts to knock down *Reep5* were unsuccessful. To circumvent these issues, I conducted what I refer to as "in-cell reconstitution" experiments, by overexpressing *Ugt8*, the enzyme responsible for GalCer synthesis, in a cell line such as U2OS (Fig 3.13s). At the organismal level, challenges are even greater. Attempts to use AAVs for labeling and mutating oligodendrocytes in mouse pups were particularly challenging (data not shown). A zebrafish model could offer a better alternative, which I have begun to explore, with results presented in Appendix.

As a cell biologist, I aspire to conduct more comprehensive biochemical and cell biological studies on oligodendrocytes. I am hopeful that the development of more sophisticated tools in the future will enable deeper investigations into the molecular mechanisms underlying myelin.

4.6 Significance of the study

This study, for the first time, systematically characterize the ER in developing myelin using volume EM and examine its association with myelination. Furthermore, it unveils the involvement of a novel protein, GLTP, in myelination. This study brings a 3D perspective and cell biology concepts to the field of myelination and lipid biology. A special achievement is, as a study using mouse models, it has implications at the molecular scale, such as insights into membrane leaflets.

Although GLTP is one of the first lipid transfer proteins identified, its function *in vivo* remains elusive. The ambiguity can be attributed largely to the lack of studies within its natural environment. By examining GLTP in oligodendrocytes, a cell type expressing substantial amount of GLTP, my study sheds light to the long-standing mystery regarding GLTP's function.

The findings of this study are novel not only in neuroscience but also in cell biology, aligning with my aspirations to contribute to both fields during my PhD.

Reference

Aggarwal, S., Yurlova, L., & Simons, M. (2011). Central nervous system myelin: structure, synthesis and assembly. *Trends in Cell Biology*, *21*(10), 585–593. https://doi.org/10.1016/j.tcb.2011.06.004

Alberts, B., Johnson, A., Lewis, J., Morgan, D., Raff, M., Roberts, K., & Walter, P. (2017). *Molecular biology of the cell* (J. Wilson & T. Hunt, Eds.; pp. 1297–1342). Garland Science, New York, NY. https://doi.org/10.1201/9781315735368

Almeida, A. R., & Macklin, W. B. (2023). Early myelination involves the dynamic and repetitive ensheathment of axons which resolves through a low and consistent stabilization rate. *ELife*, *12*. https://doi.org/10.7554/eLife.82111

Balla, T., Kim, Y. J., Alvarez-Prats, A., & Pemberton, J. (2019). Lipid dynamics at contact sites between the endoplasmic reticulum and other organelles. *Annual Review of Cell and Developmental Biology*, *35*, 85–109. https://doi.org/10.1146/annurev-cellbio-100818-125251

Baraban, M., Koudelka, S., & Lyons, D. A. (2018). Ca 2+ activity signatures of myelin sheath formation and growth in vivo. *Nature Neuroscience*, *21*(1), 19–23. https://doi.org/10.1038/s41593-017-0040-x

Baron, W., & Hoekstra, D. (2010). On the biogenesis of myelin membranes: sorting, trafficking and cell polarity. *FEBS Letters*, *584*(9), 1760–1770. https://doi.org/10.1016/j.febslet.2009.10.085

Baron, W., Ozgen, H., Klunder, B., de Jonge, J. C., Nomden, A., Plat, A., Trifilieff, E., de Vries, H., & Hoekstra, D. (2015). The major myelin-resident protein PLP is transported to myelin membranes via a transcytotic mechanism: involvement of sulfatide. *Molecular and Cellular Biology*, *35*(1), 288–302. https://doi.org/10.1128/MCB.00848-14

Baumann, N. A., Sullivan, D. P., Ohvo-Rekilä, H., Simonot, C., Pottekat, A., Klaassen, Z., Beh, C. T., & Menon, A. K. (2005). Transport of newly synthesized sterol to the sterol-enriched plasma membrane occurs via nonvesicular equilibration. *Biochemistry*, *44*(15), 5816–5826. https://doi.org/10.1021/bi048296z

Reference

Berger, D. R., Seung, H. S., & Lichtman, J. W. (2018). VAST (Volume Annotation and Segmentation Tool): Efficient Manual and Semi-Automatic Labeling of Large 3D Image Stacks. *Frontiers in Neural Circuits*, *12*, 88. https://doi.org/10.3389/fncir.2018.00088

Besprozvannaya, M., Dickson, E., Li, H., Ginburg, K. S., Bers, D. M., Auwerx, J., & Nunnari, J. (2018). GRAM domain proteins specialize functionally distinct ER-PM contact sites in human cells. *ELife*, *7*. https://doi.org/10.7554/eLife.31019

Boggs, J. M. (2014). Role of galactosylceramide and sulfatide in oligodendrocytes and CNS myelin: formation of a glycosynapse. *Advances in Neurobiology*, *9*, 263–291. https://doi.org/10.1007/978-1-4939-1154-7_12

Bonetto, G., Belin, D., & Káradóttir, R. T. (2021). Myelin: A gatekeeper of activity-dependent circuit plasticity? *Science*, *374*(6569), eaba6905. https://doi.org/10.1126/science.aba6905

Bonifacino, J. S., & Glick, B. S. (2004). The mechanisms of vesicle budding and fusion. *Cell*, *116*(2), 153–166. https://doi.org/10.1016/s0092-8674(03)01079-1

Bosio, A., Binczek, E., & Stoffel, W. (1996). Functional breakdown of the lipid bilayer of the myelin membrane in central and peripheral nervous system by disrupted galactocerebroside synthesis. *Proceedings of the National Academy of Sciences of the United States of America*, *93*(23), 13280–13285. https://doi.org/10.1073/pnas.93.23.13280

Braschi, B., Bruford, E. A., Cavanagh, A. T., Neuman, S. D., & Bashirullah, A. (2022). The bridge-like lipid transfer protein (BLTP) gene group: introducing new nomenclature based on structural homology indicating shared function. *Human Genomics*, *16*(1), 66. https://doi.org/10.1186/s40246-022-00439-3

Brito, A. (2018). *Blender Quick Start Guide: 3D Modeling, Animation, and Render with Eevee in Blender 2.8*. Packt Publishing Ltd.

Burger, K. N., van der Bijl, P., & van Meer, G. (1996). Topology of sphingolipid galactosyltransferases in ER and Golgi: transbilayer movement of monohexosyl sphingolipids is required for higher glycosphingolipid biosynthesis. *The Journal of Cell Biology*, *133*(1), 15–28. https://doi.org/10.1083/jcb.133.1.15

Reference

Buton, X, Morrot, G., Fellmann, P., & Seigneuret, M. (1996). Ultrafast glycerophospholipid-selective transbilayer motion mediated by a protein in the endoplasmic reticulum membrane. *The Journal of Biological Chemistry*, *271*(12), 6651–6657. https://doi.org/10.1074/jbc.271.12.6651

Buton, Xavier, Hervé, P., Kubelt, J., Tannert, A., Burger, K. N. J., Fellmann, P., Müller, P., Herrmann, A., Seigneuret, M., & Devaux, P. F. (2002). Transbilayer movement of monohexosylsphingolipids in endoplasmic reticulum and Golgi membranes. *Biochemistry*, *41*(43), 13106–13115. https://doi.org/10.1021/bi020385t

Chen, C. Z., Neumann, B., Förster, S., & Franklin, R. J. M. (2021). Schwann cell remyelination of the central nervous system: why does it happen and what are the benefits? *Open Biology*, *11*(1), 200352. https://doi.org/10.1098/rsob.200352

Cheng, X., & Bezanilla, M. (2021). SABRE populates ER domains essential for cell plate maturation and cell expansion influencing cell and tissue patterning. *ELife*, *10*. https://doi.org/10.7554/eLife.65166

Chen, Y.-J., Quintanilla, C. G., & Liou, J. (2019). Recent insights into mammalian ER-PM junctions. *Current Opinion in Cell Biology*, *57*, 99–105. https://doi.org/10.1016/j.ceb.2018.12.011

Chong, S. Y. C., Rosenberg, S. S., Fancy, S. P. J., Zhao, C., Shen, Y.-A. A., Hahn, A. T., McGee, A. W., Xu, X., Zheng, B., Zhang, L. I., Rowitch, D. H., Franklin, R. J. M., Lu, Q. R., & Chan, J. R. (2012). Neurite outgrowth inhibitor Nogo-A establishes spatial segregation and extent of oligodendrocyte myelination. *Proceedings of the National Academy of Sciences of the United States of America*, *109*(4), 1299–1304. https://doi.org/10.1073/pnas.1113540109

Chung, J., Torta, F., Masai, K., Lucast, L., Czapla, H., Tanner, L. B., Narayanaswamy, P., Wenk, M. R., Nakatsu, F., & De Camilli, P. (2015). INTRACELLULAR TRANSPORT. PI4P/phosphatidylserine countertransport at ORP5- and ORP8-mediated ER-plasma membrane contacts. *Science*, *349*(6246), 428–432. https://doi.org/10.1126/science.aab1370

Clark, B. J. (2012). The mammalian START domain protein family in lipid transport in health and disease. *The Journal of Endocrinology*, *212*(3), 257–275. https://doi.org/10.1530/JOE-11-0313

Reference

Coetzee, T., Fujita, N., Dupree, J., Shi, R., Blight, A., Suzuki, K., Suzuki, K., & Popko, B. (1996). Myelination in the absence of galactocerebroside and sulfatide: normal structure with abnormal function and regional instability. *Cell*, *86*(2), 209–219. https://doi.org/10.1016/s0092-8674(00)80093-8

Concordet, J.-P., & Haeussler, M. (2018). CRISPOR: intuitive guide selection for CRISPR/Cas9 genome editing experiments and screens. *Nucleic Acids Research*, *46*(W1), W242–W245. https://doi.org/10.1093/nar/gky354

Czopka, T., Ffrench-Constant, C., & Lyons, D. A. (2013). Individual oligodendrocytes have only a few hours in which to generate new myelin sheaths in vivo. *Developmental Cell*, *25*(6), 599–609. https://doi.org/10.1016/j.devcel.2013.05.013

D'Angelo, G., Polishchuk, E., Di Tullio, G., Santoro, M., Di Campli, A., Godi, A., West, G., Bielawski, J., Chuang, C.-C., van der Spoel, A. C., Platt, F. M., Hannun, Y. A., Polishchuk, R., Mattjus, P., & De Matteis, M. A. (2007). Glycosphingolipid synthesis requires FAPP2 transfer of glucosylceramide. *Nature*, *449*(7158), 62–67. https://doi.org/10.1038/nature06097

Decker, L., & ffrench-Constant, C. (2004). Lipid rafts and integrin activation regulate oligodendrocyte survival. *The Journal of Neuroscience*, *24*(15), 3816–3825. https://doi.org/10.1523/JNEUROSCI.5725-03.2004

Di Mattia, T., Wilhelm, L. P., Ikhlef, S., Wendling, C., Spehner, D., Nominé, Y., Giordano, F., Mathelin, C., Drin, G., Tomasetto, C., & Alpy, F. (2018). Identification of MOSPD2, a novel scaffold for endoplasmic reticulum membrane contact sites. *EMBO Reports*, *19*(7). https://doi.org/10.15252/embr.201745453

Djannatian, M., Radha, S., Weikert, U., Safaiyan, S., Wrede, C., Deichsel, C., Kislinger, G., Rhomberg, A., Ruhwedel, T., Campbell, D. S., van Ham, T., Schmid, B., Hegermann, J., Möbius, W., Schifferer, M., & Simons, M. (2023). Myelination generates aberrant ultrastructure that is resolved by microglia. *The Journal of Cell Biology*, *222*(3). https://doi.org/10.1083/jcb.202204010

Doktorova, M., Symons, J. L., & Levental, I. (2020). Structural and functional consequences of reversible lipid asymmetry in living membranes. *Nature Chemical Biology*, *16*(12), 1321–1330. https://doi.org/10.1038/s41589-020-00688-0

Reference

Edgar, J. M., McGowan, E., Chapple, K. J., Möbius, W., Lemgruber, L., Insall, R. H., Nave, K.-A., & Boullerne, A. (2021). Río-Hortega's drawings revisited with fluorescent protein defines a cytoplasm-filled channel system of CNS myelin. *Journal of Anatomy*, *239*(6), 1241–1255. https://doi.org/10.1111/joa.13577

Ejsing, C. S., Sampaio, J. L., Surendranath, V., Duchoslav, E., Ekroos, K., Klemm, R. W., Simons, K., & Shevchenko, A. (2009). Global analysis of the yeast lipidome by quantitative shotgun mass spectrometry. *Proceedings of the National Academy of Sciences of the United States of America*, *106*(7), 2136–2141. https://doi.org/10.1073/pnas.0811700106

Emery, B., & Dugas, J. C. (2013). Purification of oligodendrocyte lineage cells from mouse cortices by immunopanning. *Cold Spring Harbor Protocols*, *2013*(9), 854–868. https://doi.org/10.1101/pdb.prot073973

Erwig, M. S., Hesse, D., Jung, R. B., Uecker, M., Kusch, K., Tenzer, S., Jahn, O., & Werner, H. B. (2019). Myelin: methods for purification and proteome analysis. *Methods in Molecular Biology*, *1936*, 37–63. https://doi.org/10.1007/978-1-4939-9072-6_3

Fahy, E., Sud, M., Cotter, D., & Subramaniam, S. (2007). LIPID MAPS online tools for lipid research. *Nucleic Acids Research*, *35*(Web Server issue), W606-12. https://doi.org/10.1093/nar/gkm324

Fancy, S. P. J., Chan, J. R., Baranzini, S. E., Franklin, R. J. M., & Rowitch, D. H. (2011). Myelin regeneration: a recapitulation of development? *Annual Review of Neuroscience*, *34*, 21–43. https://doi.org/10.1146/annurev-neuro-061010-113629

Fard, M. K., van der Meer, F., Sánchez, P., Cantuti-Castelvetri, L., Mandad, S., Jäkel, S., Fornasiero, E. F., Schmitt, S., Ehrlich, M., Starost, L., Kuhlmann, T., Sergiou, C., Schultz, V., Wrzos, C., Brück, W., Urlaub, H., Dimou, L., Stadelmann, C., & Simons, M. (2017). BCAS1 expression defines a population of early myelinating oligodendrocytes in multiple sclerosis lesions. *Science Translational Medicine*, *9*(419). https://doi.org/10.1126/scitranslmed.aam7816

Farías, G. G., Fréal, A., Tortosa, E., Stucchi, R., Pan, X., Portegies, S., Will, L., Altelaar, M., & Hoogenraad, C. C. (2019). Feedback-Driven Mechanisms between Microtubules and the Endoplasmic Reticulum Instruct Neuronal Polarity. *Neuron*, *102*(1), 184-201.e8. https://doi.org/10.1016/j.neuron.2019.01.030

Reference

Fekete, C. D., Horning, R. Z., Doron, M. S., & Nishiyama, A. (2023). Cleavage of VAMP2/3 affects oligodendrocyte lineage development in the developing mouse spinal cord. *The Journal of Neuroscience*, *43*(39), 6592–6608. https://doi.org/10.1523/JNEUROSCI.2206-21.2023

Feldmann, A., Amphornrat, J., Schönherr, M., Winterstein, C., Möbius, W., Ruhwedel, T., Danglot, L., Nave, K.-A., Galli, T., Bruns, D., Trotter, J., & Krämer-Albers, E.-M. (2011). Transport of the major myelin proteolipid protein is directed by VAMP3 and VAMP7. *The Journal of Neuroscience*, *31*(15), 5659–5672. https://doi.org/10.1523/JNEUROSCI.6638-10.2011

Foran, D. R., & Peterson, A. C. (1992). Myelin acquisition in the central nervous system of the mouse revealed by an MBP-Lac Z transgene. *The Journal of Neuroscience*, *12*(12), 4890–4897. https://doi.org/10.1523/JNEUROSCI.12-12-04890.1992

Fu, M.-M., McAlear, T. S., Nguyen, H., Oses-Prieto, J. A., Valenzuela, A., Shi, R. D., Perrino, J. J., Huang, T.-T., Burlingame, A. L., Bechstedt, S., & Barres, B. A. (2019). The golgi outpost protein TPPP nucleates microtubules and is critical for myelination. *Cell*, *179*(1), 132-146.e14. https://doi.org/10.1016/j.cell.2019.08.025

Fünfschilling, U., Supplie, L. M., Mahad, D., Boretius, S., Saab, A. S., Edgar, J., Brinkmann, B. G., Kassmann, C. M., Tzvetanova, I. D., Möbius, W., Diaz, F., Meijer, D., Suter, U., Hamprecht, B., Sereda, M. W., Moraes, C. T., Frahm, J., Goebbels, S., & Nave, K.-A. (2012). Glycolytic oligodendrocytes maintain myelin and long-term axonal integrity. *Nature*, *485*(7399), 517–521. https://doi.org/10.1038/nature11007

Gallo, A., Danglot, L., Giordano, F., Hewlett, B., Binz, T., Vannier, C., & Galli, T. (2020). Role of the Sec22b-E-Syt complex in neurite growth and ramification. *Journal of Cell Science*, *133*(18). https://doi.org/10.1242/jcs.247148

Ghosh, T., Almeida, R. G., Zhao, C., Mannioui, A., Martin, E., Fleet, A., Chen, C. Z., Assinck, P., Ellams, S., Gonzalez, G. A., Graham, S. C., Rowitch, D. H., Stott, K., Adams, I., Zalc, B., Goldman, N., Lyons, D. A., & Franklin, R. J. M. (2024). A retroviral link to vertebrate myelination through retrotransposon-RNA-mediated control of myelin gene expression. *Cell*, *187*(4), 814-830.e23. https://doi.org/10.1016/j.cell.2024.01.011

Reference

Gibson, E. M., Purger, D., Mount, C. W., Goldstein, A. K., Lin, G. L., Wood, L. S., Inema, I., Miller, S. E., Bieri, G., Zuchero, J. B., Barres, B. A., Woo, P. J., Vogel, H., & Monje, M. (2014). Neuronal activity promotes oligodendrogenesis and adaptive myelination in the mammalian brain. *Science*, *344*(6183), 1252304. https://doi.org/10.1126/science.1252304

Gouna, G., Klose, C., Bosch-Queralt, M., Liu, L., Gokce, O., Schifferer, M., Cantuti-Castelvetri, L., & Simons, M. (2021). TREM2-dependent lipid droplet biogenesis in phagocytes is required for remyelination. *The Journal of Experimental Medicine*, *218*(10). https://doi.org/10.1084/jem.20210227

Halter, D., Neumann, S., van Dijk, S. M., Wolthoorn, J., de Mazière, A. M., Vieira, O. V., Mattjus, P., Klumperman, J., van Meer, G., & Sprong, H. (2007). Pre- and post-Golgi translocation of glucosylceramide in glycosphingolipid synthesis. *The Journal of Cell Biology*, *179*(1), 101–115. https://doi.org/10.1083/jcb.200704091

Hanna, M., Guillén-Samander, A., & De Camilli, P. (2023). RBG Motif Bridge-Like Lipid Transport Proteins: Structure, Functions, and Open Questions. *Annual Review of Cell and Developmental Biology*, *39*, 409–434. https://doi.org/10.1146/annurev-cellbio-120420-014634

Hayashi, T., & Su, T.-P. (2004). Sigma-1 receptors at galactosylceramide-enriched lipid microdomains regulate oligodendrocyte differentiation. *Proceedings of the National Academy of Sciences of the United States of America*, *101*(41), 14949–14954. https://doi.org/10.1073/pnas.0402890101

Heino, S., Lusa, S., Somerharju, P., Ehnholm, C., Olkkonen, V. M., & Ikonen, E. (2000). Dissecting the role of the golgi complex and lipid rafts in biosynthetic transport of cholesterol to the cell surface. *Proceedings of the National Academy of Sciences of the United States of America*, *97*(15), 8375–8380. https://doi.org/10.1073/pnas.140218797

Heinrich, L., Bennett, D., Ackerman, D., Park, W., Bogovic, J., Eckstein, N., Petruncio, A., Clements, J., Pang, S., Xu, C. S., Funke, J., Korff, W., Hess, H. F., Lippincott-Schwartz, J., Saalfeld, S., Weigel, A. V., & COSEM Project Team. (2021). Whole-cell organelle segmentation in volume electron microscopy. *Nature*, *599*(7883), 141–146. https://doi.org/10.1038/s41586-021-03977-3

Reference

Herzog, R., Schuhmann, K., Schwudke, D., Sampaio, J. L., Bornstein, S. R., Schroeder, M., & Shevchenko, A. (2012). LipidXplorer: a software for consensual cross-platform lipidomics. *Plos One*, *7*(1), e29851. https://doi.org/10.1371/journal.pone.0029851

Herzog, R., Schwudke, D., Schuhmann, K., Sampaio, J. L., Bornstein, S. R., Schroeder, M., & Shevchenko, A. (2011). A novel informatics concept for high-throughput shotgun lipidomics based on the molecular fragmentation query language. *Genome Biology*, *12*(1), R8. https://doi.org/10.1186/gb-2011-12-1-r8

Hoffmann, P. C., Giandomenico, S. L., Ganeva, I., Wozny, M. R., Sutcliffe, M., Lancaster, M. A., & Kukulski, W. (2021). Electron cryo-tomography reveals the subcellular architecture of growing axons in human brain organoids. *ELife*, *10*. https://doi.org/10.7554/eLife.70269

Honke, K., Hirahara, Y., Dupree, J., Suzuki, K., Popko, B., Fukushima, K., Fukushima, J., Nagasawa, T., Yoshida, N., Wada, Y., & Taniguchi, N. (2002). Paranodal junction formation and spermatogenesis require sulfoglycolipids. *Proceedings of the National Academy of Sciences of the United States of America*, *99*(7), 4227–4232. https://doi.org/10.1073/pnas.032068299

Hughes, E. G., Orthmann-Murphy, J. L., Langseth, A. J., & Bergles, D. E. (2018). Myelin remodeling through experience-dependent oligodendrogenesis in the adult somatosensory cortex. *Nature Neuroscience*, *21*(5), 696–706. https://doi.org/10.1038/s41593-018-0121-5

Jahn, R., & Scheller, R. H. (2006). SNAREs--engines for membrane fusion. *Nature Reviews. Molecular Cell Biology*, *7*(9), 631–643. https://doi.org/10.1038/nrm2002

Kaiser, T., Allen, H. M., Kwon, O., Barak, B., Wang, J., He, Z., Jiang, M., & Feng, G. (2021). MyelTracer: A Semi-Automated Software for Myelin g-Ratio Quantification. *ENeuro*, *8*(4). https://doi.org/10.1523/ENEURO.0558-20.2021

Kaplan, M. R., & Simoni, R. D. (1985a). Intracellular transport of phosphatidylcholine to the plasma membrane. *The Journal of Cell Biology*, *101*(2), 441–445. https://doi.org/10.1083/jcb.101.2.441

Kaplan, M. R., & Simoni, R. D. (1985b). Transport of cholesterol from the endoplasmic reticulum to the plasma membrane. *The Journal of Cell Biology*, *101*(2), 446–453. https://doi.org/10.1083/jcb.101.2.446

Kasthuri, N., Hayworth, K. J., Berger, D. R., Schalek, R. L., Conchello, J. A., Knowles-Barley, S., Lee, D., Vázquez-Reina, A., Kaynig, V., Jones, T. R., Roberts, M., Morgan, J. L., Tapia, J. C., Seung, H. S., Roncal, W. G., Vogelstein, J. T., Burns, R., Sussman, D. L., Priebe, C. E., … Lichtman, J. W. (2015). Saturated reconstruction of a volume of neocortex. *Cell*, *162*(3), 648–661. https://doi.org/10.1016/j.cell.2015.06.054

Kim, W. S., Weickert, C. S., & Garner, B. (2008). Role of ATP-binding cassette transporters in brain lipid transport and neurological disease. *Journal of Neurochemistry*, *104*(5), 1145–1166. https://doi.org/10.1111/j.1471-4159.2007.05099.x

Kislinger, G., Fabig, G., Wehn, A., Rodriguez, L., Jiang, H., Niemann, C., Klymchenko, A. S., Plesnila, N., Misgeld, T., Müller-Reichert, T., Khalin, I., & Schifferer, M. (2023). *ATUM-Tomo: A multi-scale approach to cellular ultrastructure by combined volume scanning electron microscopy and electron tomography*. https://doi.org/10.7554/eLife.90565.1

Kislinger, G., Gnägi, H., Kerschensteiner, M., Simons, M., Misgeld, T., & Schifferer, M. (2020). ATUM-FIB microscopy for targeting and multiscale imaging of rare events in mouse cortex. *STAR Protocols*, *1*(3), 100232. https://doi.org/10.1016/j.xpro.2020.100232

Kislinger, G., Niemann, C., Rodriguez, L., Jiang, H., Fard, M. K., Snaidero, N., Schumacher, A.-M., Kerschensteiner, M., Misgeld, T., & Schifferer, M. (2023). Neurons on tape: Automated Tape Collecting Ultramicrotomy-mediated volume EM for targeting neuropathology. *Methods in Cell Biology*, *177*, 125–170. https://doi.org/10.1016/bs.mcb.2023.01.012

Krämer-Albers, E.-M., & Werner, H. B. (2023). Mechanisms of axonal support by oligodendrocyte-derived extracellular vesicles. *Nature Reviews. Neuroscience*, *24*(8), 474–486. https://doi.org/10.1038/s41583-023-00711-y

Krasnow, A. M., Ford, M. C., Valdivia, L. E., Wilson, S. W., & Attwell, D. (2018). Regulation of developing myelin sheath elongation by oligodendrocyte calcium transients in vivo. *Nature Neuroscience*, *21*(1), 24–28. https://doi.org/10.1038/s41593-017-0031-y

Kulkarni, K., Snyder, D. S., & McIntosh, T. J. (1999). Adhesion between cerebroside bilayers. *Biochemistry*, *38*(46), 15264–15271. https://doi.org/10.1021/bi991725m

Reference

Lam, M., Takeo, K., Almeida, R. G., Cooper, M. H., Wu, K., Iyer, M., Kantarci, H., & Zuchero, J. B. (2022). CNS myelination requires VAMP2/3-mediated membrane expansion in oligodendrocytes. *Nature Communications*, *13*(1), 5583. https://doi.org/10.1038/s41467-022-33200-4

Lappe-Siefke, C., Goebbels, S., Gravel, M., Nicksch, E., Lee, J., Braun, P. E., Griffiths, I. R., & Nave, K.-A. (2003). Disruption of Cnp1 uncouples oligodendroglial functions in axonal support and myelination. *Nature Genetics*, *33*(3), 366–374. https://doi.org/10.1038/ng1095

Lees, J. A., Messa, M., Sun, E. W., Wheeler, H., Torta, F., Wenk, M. R., De Camilli, P., & Reinisch, K. M. (2017). Lipid transport by TMEM24 at ER-plasma membrane contacts regulates pulsatile insulin secretion. *Science*, *355*(6326). https://doi.org/10.1126/science.aah6171

Lee, Y., Morrison, B. M., Li, Y., Lengacher, S., Farah, M. H., Hoffman, P. N., Liu, Y., Tsingalia, A., Jin, L., Zhang, P.-W., Pellerin, L., Magistretti, P. J., & Rothstein, J. D. (2012). Oligodendroglia metabolically support axons and contribute to neurodegeneration. *Nature*, *487*(7408), 443–448. https://doi.org/10.1038/nature11314

Mack, J. T., Beljanski, V., Soulika, A. M., Townsend, D. M., Brown, C. B., Davis, W., & Tew, K. D. (2007). "Skittish" Abca2 knockout mice display tremor, hyperactivity, and abnormal myelin ultrastructure in the central nervous system. *Molecular and Cellular Biology*, *27*(1), 44–53. https://doi.org/10.1128/MCB.01824-06

Maeda, S., Otomo, C., & Otomo, T. (2019). The autophagic membrane tether ATG2A transfers lipids between membranes. *ELife*, *8*. https://doi.org/10.7554/eLife.45777

Maier, O., Hoekstra, D., & Baron, W. (2008). Polarity development in oligodendrocytes: sorting and trafficking of myelin components. *Journal of Molecular Neuroscience*, *35*(1), 35–53. https://doi.org/10.1007/s12031-007-9024-8

McKenzie, I. A., Ohayon, D., Li, H., de Faria, J. P., Emery, B., Tohyama, K., & Richardson, W. D. (2014). Motor skill learning requires active central myelination. *Science*, *346*(6207), 318–322. https://doi.org/10.1126/science.1254960

Melia, T. J., & Reinisch, K. M. (2022). A possible role for VPS13-family proteins in bulk lipid transfer, membrane expansion and organelle biogenesis. *Journal of Cell Science*, *135*(5). https://doi.org/10.1242/jcs.259357

Meschkat, M., Steyer, A. M., Weil, M.-T., Kusch, K., Jahn, O., Piepkorn, L., Agüi-Gonzalez, P., Phan, N. T. N., Ruhwedel, T., Sadowski, B., Rizzoli, S. O., Werner, H. B., Ehrenreich, H., Nave, K.-A., & Möbius, W. (2022). White matter integrity in mice requires continuous myelin synthesis at the inner tongue. *Nature Communications*, *13*(1), 1163. https://doi.org/10.1038/s41467-022-28720-y

Mesmin, B., Bigay, J., Moser von Filseck, J., Lacas-Gervais, S., Drin, G., & Antonny, B. (2013). A four-step cycle driven by PI(4)P hydrolysis directs sterol/PI(4)P exchange by the ER-Golgi tether OSBP. *Cell*, *155*(4), 830–843. https://doi.org/10.1016/j.cell.2013.09.056

Mishra, S. K., Gao, Y.-G., Zou, X., Stephenson, D. J., Malinina, L., Hinchcliffe, E. H., Chalfant, C. E., & Brown, R. E. (2020). Emerging roles for human glycolipid transfer protein superfamily members in the regulation of autophagy, inflammation, and cell death. *Progress in Lipid Research*, *78*, 101031. https://doi.org/10.1016/j.plipres.2020.101031

Mukherjee, C., Kling, T., Russo, B., Miebach, K., Kess, E., Schifferer, M., Pedro, L. D., Weikert, U., Fard, M. K., Kannaiyan, N., Rossner, M., Aicher, M.-L., Goebbels, S., Nave, K.-A., Krämer-Albers, E.-M., Schneider, A., & Simons, M. (2020). Oligodendrocytes provide antioxidant defense function for neurons by secreting ferritin heavy chain. *Cell Metabolism*, *32*(2), 259-272.e10. https://doi.org/10.1016/j.cmet.2020.05.019

Nave, K.-A., & Werner, H. B. (2014). Myelination of the nervous system: mechanisms and functions. *Annual Review of Cell and Developmental Biology*, *30*, 503–533. https://doi.org/10.1146/annurev-cellbio-100913-013101

Nave, K.-A., & Werner, H. B. (2021). Ensheathment and myelination of axons: evolution of glial functions. *Annual Review of Neuroscience*, *44*, 197–219. https://doi.org/10.1146/annurev-neuro-100120-122621

Nawaz, S., Sánchez, P., Schmitt, S., Snaidero, N., Mitkovski, M., Velte, C., Brückner, B. R., Alexopoulos, I., Czopka, T., Jung, S. Y., Rhee, J. S., Janshoff, A., Witke, W., Schaap, I. A. T., Lyons, D. A., & Simons, M. (2015). Actin filament turnover drives leading edge growth during myelin sheath formation in the

central nervous system. *Developmental Cell*, *34*(2), 139–151. https://doi.org/10.1016/j.devcel.2015.05.013

Neuman, S. D., & Bashirullah, A. (2018). Hobbit regulates intracellular trafficking to drive insulin-dependent growth during Drosophila development. *Development*, *145*(11). https://doi.org/10.1242/dev.161356

Neuman, S. D., Jorgensen, J. R., Cavanagh, A. T., Smyth, J. T., Selegue, J. E., Emr, S. D., & Bashirullah, A. (2022). The Hob proteins are novel and conserved lipid-binding proteins at ER-PM contact sites. *Journal of Cell Science*, *135*(5). https://doi.org/10.1242/jcs.259086

Ni, Z., Wölk, M., Jukes, G., Mendivelso Espinosa, K., Ahrends, R., Aimo, L., Alvarez-Jarreta, J., Andrews, S., Andrews, R., Bridge, A., Clair, G. C., Conroy, M. J., Fahy, E., Gaud, C., Goracci, L., Hartler, J., Hoffmann, N., Kopczyinki, D., Korf, A., … Fedorova, M. (2023). Guiding the choice of informatics software and tools for lipidomics research applications. *Nature Methods*, *20*(2), 193–204. https://doi.org/10.1038/s41592-022-01710-0

Norton, W. T., & Poduslo, S. E. (1973). Myelination in rat brain: method of myelin isolation. *Journal of Neurochemistry*, *21*(4), 749–757. https://doi.org/10.1111/j.1471-4159.1973.tb07519.x

Nurmi, H., Backman, A. P. E., Halin, J., Lönnfors, M., Blom, T., Roos-Mattjus, P., & Mattjus, P. (2023). Glycolipid transfer protein knockout disrupts vesicle trafficking to the plasma membrane. *The Journal of Biological Chemistry*, *299*(4), 104607. https://doi.org/10.1016/j.jbc.2023.104607

Omoto, S., Ueno, M., Mochio, S., Takai, T., & Yamashita, T. (2010). Genetic deletion of paired immunoglobulin-like receptor B does not promote axonal plasticity or functional recovery after traumatic brain injury. *The Journal of Neuroscience*, *30*(39), 13045–13052. https://doi.org/10.1523/JNEUROSCI.3228-10.2010

Osawa, T., Kotani, T., Kawaoka, T., Hirata, E., Suzuki, K., Nakatogawa, H., Ohsumi, Y., & Noda, N. N. (2019). Atg2 mediates direct lipid transfer between membranes for autophagosome formation. *Nature Structural & Molecular Biology*, *26*(4), 281–288. https://doi.org/10.1038/s41594-019-0203-4

Reference

Pan, L., Trimarco, A., Zhang, A. J., Fujimori, K., Urade, Y., Sun, L. O., Taveggia, C., & Zhang, Y. (2023). Oligodendrocyte-lineage cell exocytosis and L-type prostaglandin D synthase promote oligodendrocyte development and myelination. *ELife*, *12*. https://doi.org/10.7554/eLife.77441

Park, G. (2023). *Using Amira to manually segment organelles in vEM for machine learning v2*. https://doi.org/10.17504/protocols.io.bp2l61rb5vqe/v2

Petkovic, M., Jemaiel, A., Daste, F., Specht, C. G., Izeddin, I., Vorkel, D., Verbavatz, J.-M., Darzacq, X., Triller, A., Pfenninger, K. H., Tareste, D., Jackson, C. L., & Galli, T. (2014). The SNARE Sec22b has a non-fusogenic function in plasma membrane expansion. *Nature Cell Biology*, *16*(5), 434–444. https://doi.org/10.1038/ncb2937

Pfeiffer, S. E., Warrington, A. E., & Bansal, R. (1993). The oligodendrocyte and its many cellular processes. *Trends in Cell Biology*, *3*(6), 191–197. https://doi.org/10.1016/0962-8924(93)90213-k

Pfenninger, K. H. (2009). Plasma membrane expansion: a neuron's Herculean task. *Nature Reviews. Neuroscience*, *10*(4), 251–261. https://doi.org/10.1038/nrn2593

Plochberger, B., Sych, T., Weber, F., Novacek, J., Axmann, M., Stangl, H., & Sezgin, E. (2020). Lipoprotein Particles Interact with Membranes and Transfer Their Cargo without Receptors. *Biochemistry*, *59*(45), 4421–4428. https://doi.org/10.1021/acs.biochem.0c00748

Prinz, W. A. (2010). Lipid trafficking sans vesicles: where, why, how? *Cell*, *143*(6), 870–874. https://doi.org/10.1016/j.cell.2010.11.031

Quintanilla, C. G., Lee, W.-R., & Liou, J. (2022). Nir1 constitutively localizes at ER-PM junctions and promotes Nir2 recruitment for PIP2 homeostasis. *Molecular Biology of the Cell*, *33*(3), br2. https://doi.org/10.1091/mbc.E21-07-0356

Raiborg, C., Wenzel, E. M., & Stenmark, H. (2015). ER-endosome contact sites: molecular compositions and functions. *The EMBO Journal*, *34*(14), 1848–1858. https://doi.org/10.15252/embj.201591481

Reinisch, K. M., & Prinz, W. A. (2021). Mechanisms of nonvesicular lipid transport. *The Journal of Cell Biology*, *220*(3). https://doi.org/10.1083/jcb.202012058

Reference

Saheki, Y., Bian, X., Schauder, C. M., Sawaki, Y., Surma, M. A., Klose, C., Pincet, F., Reinisch, K. M., & De Camilli, P. (2016). Control of plasma membrane lipid homeostasis by the extended synaptotagmins. *Nature Cell Biology*, *18*(5), 504–515. https://doi.org/10.1038/ncb3339

Saheki, Y., & De Camilli, P. (2017). Endoplasmic Reticulum-Plasma Membrane Contact Sites. *Annual Review of Biochemistry*, *86*, 659–684. https://doi.org/10.1146/annurev-biochem-061516-044932

Sakai, H., Tanaka, Y., Tanaka, M., Ban, N., Yamada, K., Matsumura, Y., Watanabe, D., Sasaki, M., Kita, T., & Inagaki, N. (2007). ABCA2 deficiency results in abnormal sphingolipid metabolism in mouse brain. *The Journal of Biological Chemistry*, *282*(27), 19692–19699. https://doi.org/10.1074/jbc.M611056200

Sandhu, J., Li, S., Fairall, L., Pfisterer, S. G., Gurnett, J. E., Xiao, X., Weston, T. A., Vashi, D., Ferrari, A., Orozco, J. L., Hartman, C. L., Strugatsky, D., Lee, S. D., He, C., Hong, C., Jiang, H., Bentolila, L. A., Gatta, A. T., Levine, T. P., … Tontonoz, P. (2018). Aster proteins facilitate nonvesicular plasma membrane to ER cholesterol transport in mammalian cells. *Cell*, *175*(2), 514-529.e20. https://doi.org/10.1016/j.cell.2018.08.033

Schauder, C. M., Wu, X., Saheki, Y., Narayanaswamy, P., Torta, F., Wenk, M. R., De Camilli, P., & Reinisch, K. M. (2014). Structure of a lipid-bound extended synaptotagmin indicates a role in lipid transfer. *Nature*, *510*(7506), 552–555. https://doi.org/10.1038/nature13269

Schindelin, J., Arganda-Carreras, I., Frise, E., Kaynig, V., Longair, M., Pietzsch, T., Preibisch, S., Rueden, C., Saalfeld, S., Schmid, B., Tinevez, J.-Y., White, D. J., Hartenstein, V., Eliceiri, K., Tomancak, P., & Cardona, A. (2012). Fiji: an open-source platform for biological-image analysis. *Nature Methods*, *9*(7), 676–682. https://doi.org/10.1038/nmeth.2019

Scorrano, L., De Matteis, M. A., Emr, S., Giordano, F., Hajnóczky, G., Kornmann, B., Lackner, L. L., Levine, T. P., Pellegrini, L., Reinisch, K., Rizzuto, R., Simmen, T., Stenmark, H., Ungermann, C., & Schuldiner, M. (2019). Coming together to define membrane contact sites. *Nature Communications*, *10*(1), 1287. https://doi.org/10.1038/s41467-019-09253-3

Sharma, K., Schmitt, S., Bergner, C. G., Tyanova, S., Kannaiyan, N., Manrique-Hoyos, N., Kongi, K., Cantuti, L., Hanisch, U.-K., Philips, M.-A., Rossner, M. J., Mann, M., & Simons, M. (2015). Cell type- and

brain region-resolved mouse brain proteome. *Nature Neuroscience*, *18*(12), 1819–1831. https://doi.org/10.1038/nn.4160

Sleight, R. G., & Pagano, R. E. (1983). Rapid appearance of newly synthesized phosphatidylethanolamine at the plasma membrane. *The Journal of Biological Chemistry*, *258*(15), 9050–9058. https://doi.org/10.1016/S0021-9258(17)44630-8

Snaidero, N., Möbius, W., Czopka, T., Hekking, L. H. P., Mathisen, C., Verkleij, D., Goebbels, S., Edgar, J., Merkler, D., Lyons, D. A., Nave, K.-A., & Simons, M. (2014). Myelin membrane wrapping of CNS axons by PI(3,4,5)P3-dependent polarized growth at the inner tongue. *Cell*, *156*(1–2), 277–290. https://doi.org/10.1016/j.cell.2013.11.044

Snaidero, N., & Simons, M. (2014). Myelination at a glance. *Journal of Cell Science*, *127*(Pt 14), 2999–3004. https://doi.org/10.1242/jcs.151043

Snaidero, N., & Simons, M. (2017). The logistics of myelin biogenesis in the central nervous system. *Glia*, *65*(7), 1021–1031. https://doi.org/10.1002/glia.23116

Snaidero, N., Velte, C., Myllykoski, M., Raasakka, A., Ignatev, A., Werner, H. B., Erwig, M. S., Möbius, W., Kursula, P., Nave, K.-A., & Simons, M. (2017). Antagonistic functions of MBP and CNP establish cytosolic channels in CNS myelin. *Cell Reports*, *18*(2), 314–323. https://doi.org/10.1016/j.celrep.2016.12.053

Snapp, E. L., Hegde, R. S., Francolini, M., Lombardo, F., Colombo, S., Pedrazzini, E., Borgese, N., & Lippincott-Schwartz, J. (2003). Formation of stacked ER cisternae by low affinity protein interactions. *The Journal of Cell Biology*, *163*(2), 257–269. https://doi.org/10.1083/jcb.200306020

Stadelmann, C., Timmler, S., Barrantes-Freer, A., & Simons, M. (2019). Myelin in the central nervous system: structure, function, and pathology. *Physiological Reviews*, *99*(3), 1381–1431. https://doi.org/10.1152/physrev.00031.2018

Subra, M., Grimanelli, Z., Gautier, R., & Mesmin, B. (2023). Stranger twins: A tale of resemblance and contrast between VAP proteins. *Contact (Thousand Oaks (Ventura County, Calif.))*, *6*, 25152564231183896. https://doi.org/10.1177/25152564231183897

Reference

Surma, Michał A, Gerl, M. J., Herzog, R., Helppi, J., Simons, K., & Klose, C. (2021). Mouse lipidomics reveals inherent flexibility of a mammalian lipidome. *Scientific Reports*, *11*(1), 19364. https://doi.org/10.1038/s41598-021-98702-5

Surma, Michal A, Herzog, R., Vasilj, A., Klose, C., Christinat, N., Morin-Rivron, D., Simons, K., Masoodi, M., & Sampaio, J. L. (2015). An automated shotgun lipidomics platform for high throughput, comprehensive, and quantitative analysis of blood plasma intact lipids. *European Journal of Lipid Science and Technology : EJLST*, *117*(10), 1540–1549. https://doi.org/10.1002/ejlt.201500145

Suzuki, S. W., West, M., Zhang, Y., Fan, J. S., Roberts, R. T., Odorizzi, G., & Emr, S. D. (2024). A role for Vps13-mediated lipid transfer at the ER-endosome contact site in ESCRT-mediated sorting. *The Journal of Cell Biology*, *223*(4). https://doi.org/10.1083/jcb.202307094

Tanaka, Y., Yamada, K., Zhou, C.-J., Ban, N., Shioda, S., & Inagaki, N. (2003). Temporal and spatial profiles of ABCA2-expressing oligodendrocytes in the developing rat brain. *The Journal of Comparative Neurology*, *455*(3), 353–367. https://doi.org/10.1002/cne.10493

Terasaki, M. (2018). Axonal endoplasmic reticulum is very narrow. *Journal of Cell Science*, *131*(4). https://doi.org/10.1242/jcs.210450

Trajkovic, K., Dhaunchak, A. S., Goncalves, J. T., Wenzel, D., Schneider, A., Bunt, G., Nave, K.-A., & Simons, M. (2006). Neuron to glia signaling triggers myelin membrane exocytosis from endosomal storage sites. *The Journal of Cell Biology*, *172*(6), 937–948. https://doi.org/10.1083/jcb.200509022

Tuuf, J., Wistbacka, L., & Mattjus, P. (2009). The glycolipid transfer protein interacts with the vesicle-associated membrane protein-associated protein VAP-A. *Biochemical and Biophysical Research Communications*, *388*(2), 395–399. https://doi.org/10.1016/j.bbrc.2009.08.023

Urbani, L., & Simoni, R. D. (1990). Cholesterol and vesicular stomatitis virus G protein take separate routes from the endoplasmic reticulum to the plasma membrane. *The Journal of Biological Chemistry*, *265*(4), 1919–1923. https://doi.org/10.1016/S0021-9258(19)39918-1

Reference

Valverde, D. P., Yu, S., Boggavarapu, V., Kumar, N., Lees, J. A., Walz, T., Reinisch, K. M., & Melia, T. J. (2019). ATG2 transports lipids to promote autophagosome biogenesis. *The Journal of Cell Biology*, *218*(6), 1787–1798. https://doi.org/10.1083/jcb.201811139

Vance, J. E., Aasman, E. J., & Szarka, R. (1991). Brefeldin A does not inhibit the movement of phosphatidylethanolamine from its sites for synthesis to the cell surface. *The Journal of Biological Chemistry*, *266*(13), 8241–8247. https://doi.org/10.1016/S0021-9258(18)92968-6

van Meer, G. (2011). Dynamic transbilayer lipid asymmetry. *Cold Spring Harbor Perspectives in Biology*, *3*(5). https://doi.org/10.1101/cshperspect.a004671

Voeltz, G K, Sawyer, E. M., Hajnóczky, G., & Prinz, W. A. (2024). Making the connection: How membrane contact sites have changed our view of organelle biology. *Cell*, *187*(2), 257–270. https://doi.org/10.1016/j.cell.2023.11.040

Voeltz, Gia K, Prinz, W. A., Shibata, Y., Rist, J. M., & Rapoport, T. A. (2006). A class of membrane proteins shaping the tubular endoplasmic reticulum. *Cell*, *124*(3), 573–586. https://doi.org/10.1016/j.cell.2005.11.047

Voskuhl, R. R., Itoh, N., Tassoni, A., Matsukawa, M. A., Ren, E., Tse, V., Jang, E., Suen, T. T., & Itoh, Y. (2019). Gene expression in oligodendrocytes during remyelination reveals cholesterol homeostasis as a therapeutic target in multiple sclerosis. *Proceedings of the National Academy of Sciences of the United States of America*, *116*(20), 10130–10139. https://doi.org/10.1073/pnas.1821306116

Warnock, D. E., Lutz, M. S., Blackburn, W. A., Young, W. W., & Baenziger, J. U. (1994). Transport of newly synthesized glucosylceramide to the plasma membrane by a non-Golgi pathway. *Proceedings of the National Academy of Sciences of the United States of America*, *91*(7), 2708–2712. https://doi.org/10.1073/pnas.91.7.2708

Wefers, B., Wurst, W., & Kühn, R. (2023). Gene editing in mouse zygotes using the crispr/cas9 system. *Methods in Molecular Biology*, *2631*, 207–230. https://doi.org/10.1007/978-1-0716-2990-1_8

Winterstein, C., Trotter, J., & Krämer-Albers, E.-M. (2008). Distinct endocytic recycling of myelin proteins promotes oligodendroglial membrane remodeling. *Journal of Cell Science*, *121*(Pt 6), 834–842. https://doi.org/10.1242/jcs.022731

Wolf, A., Bauer, B., & Hartz, A. M. S. (2012). ABC Transporters and the Alzheimer's Disease Enigma. *Frontiers in Psychiatry*, *3*, 54. https://doi.org/10.3389/fpsyt.2012.00054

Wu, Y., Whiteus, C., Xu, C. S., Hayworth, K. J., Weinberg, R. J., Hess, H. F., & De Camilli, P. (2017). Contacts between the endoplasmic reticulum and other membranes in neurons. *Proceedings of the National Academy of Sciences of the United States of America*, *114*(24), E4859–E4867. https://doi.org/10.1073/pnas.1701078114

Xin, W., & Chan, J. R. (2020). Myelin plasticity: sculpting circuits in learning and memory. *Nature Reviews. Neuroscience*, *21*(12), 682–694. https://doi.org/10.1038/s41583-020-00379-8

Yang, F., Guan, Y., Feng, X., Rolfs, A., Schlüter, H., & Luo, J. (2019). Proteomics of the corpus callosum to identify novel factors involved in hypomyelinated Niemann-Pick Type C disease mice. *Molecular Brain*, *12*(1), 17. https://doi.org/10.1186/s13041-019-0440-9

Yurlova, L., Kahya, N., Aggarwal, S., Kaiser, H.-J., Chiantia, S., Bakhti, M., Pewzner-Jung, Y., Ben-David, O., Futerman, A. H., Brügger, B., & Simons, M. (2011). Self-segregation of myelin membrane lipids in model membranes. *Biophysical Journal*, *101*(11), 2713–2720. https://doi.org/10.1016/j.bpj.2011.10.026

Zhang, C., Chen, Z., Zhang, D., Wang, X., Qiu, M., & Tan, Z. (2023). Role of gltp in maturation of oligodendrocytes under the regulation of nkx2.2. *Molecular Neurobiology*, *60*(9), 4897–4908. https://doi.org/10.1007/s12035-023-03383-y

Zhang, H., & Hu, J. (2016). Shaping the Endoplasmic Reticulum into a Social Network. *Trends in Cell Biology*, *26*(12), 934–943. https://doi.org/10.1016/j.tcb.2016.06.002

Zhang, Y., Chen, K., Sloan, S. A., Bennett, M. L., Scholze, A. R., O'Keeffe, S., Phatnani, H. P., Guarnieri, P., Caneda, C., Ruderisch, N., Deng, S., Liddelow, S. A., Zhang, C., Daneman, R., Maniatis, T., Barres, B. A., & Wu, J. Q. (2014). An RNA-sequencing transcriptome and splicing database of glia, neurons, and

vascular cells of the cerebral cortex. *The Journal of Neuroscience*, *34*(36), 11929–11947. https://doi.org/10.1523/JNEUROSCI.1860-14.2014

Zuchero, J. B., Fu, M.-M., Sloan, S. A., Ibrahim, A., Olson, A., Zaremba, A., Dugas, J. C., Wienbar, S., Caprariello, A. V., Kantor, C., Leonoudakis, D., Lariosa-Willingham, K., Kronenberg, G., Gertz, K., Soderling, S. H., Miller, R. H., & Barres, B. A. (2015). CNS myelin wrapping is driven by actin disassembly. *Developmental Cell*, *34*(2), 152–167. https://doi.org/10.1016/j.devcel.2015.06.011

Appendix I. Using zebrafish to investigate oligodendroglial ER during live myelination.

Method

All zebrafish experimental protocols involving zebrafish were approved and conducted in compliance with the guidelines set by the District Government of Upper Bavaria. The zebrafish were maintained in the DZNE fish facility located in Munich, adhering to local guidelines for animal welfare.

To visualize myelin, I utilized transgenic line Tg(Sox10:mRFP). To express ER markers, I generated the following pDestCG2 Tol2 plasmids: (1) “JWC099”: Myrf promoter-ERmoxGFP. The construction is based on pERmoxGFP (Addgene #68072); (2) “JWC101”: Myrf promoter-mEGFP-Sec61b; (3) “JWC106”: Myrf promoter-Rtn4b-mEGFP; (4) “JWC107”: Myrf promoter-Reep5-mEGFP. The process of microinjection into zebrafish involved the injection of a 1:1 mixture of plasmid DNA (25 ng/µl) and transposase mRNA (ranging from 25 to 200 ng/µl) directly into early-stage embryos. To inhibit pigmentation and enhance imaging, embryos designated for imaging were treated with PTU starting from 8 to 24h post-fertilization (hpf). Injected eggs were analyzed 3–5 days post-fertilization.

Results

I utilized zebrafish to investigate oligodendroglial ER during live myelination. The oligodendroglial ER was visualized by ER-luminal, monomeric and oxidizing environment-optimized GFP, which was expressed under the control of the Myrf promoter. Myelin was marked by membrane-targeted RFP, which was expressed under the Sox10 promoter. The oligodendroglial ER was in the oligodendroglial cell body, cell processes, and extended into the developing myelin, where it appeared spiral. This spiral appearance indicates its localization within the cytoplasmic channels (Fig A1, Movie A1). Similar results were observed with other ER markers driven by the Myrf promoter, such as mEGFP-Sec61b, Rtn4b-mEGFP, and Reep5-mEGFP (data not shown). Consistent with findings in mice, the ER extends into developing myelin in zebrafish as well, highlighting a conserved mechanism across species.

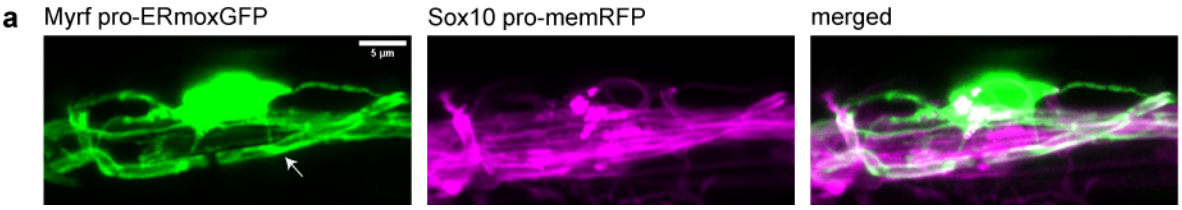

Fig A1 Oligodendroglial ER during live myelination

a Maximum intensity projection of z stack of myelinating oligodendrocyte in zebrafish at 4 days post fertilization (4 dpf). Green: oligodendroglial ER-luminal monomeric GFP; Magenta: oligodendroglial membrane-targeted RFP; Arrow: ER-moxGFP appears spiral in myelin. Scale bar: 5 µm (a)

Movie A1: 3D stack of Oligodendroglial ER in live myelination, 8.88 µm-thick (38 slices with 240 nm interval) related to Fig A1.1.

Discussion

Employing zebrafish as a model organism offers a unique opportunity to observe oligodendroglial ER dynamics in real-time during the process of myelination. However, the ER signal did not show the typical fine structure due to the lack of resolution. A high-resolution microscopy would greatly improve this study.

Copyright of figures taken from publication

Fig 1.2: from Snaidero et al. 2014

End Page	290
Type of Use	reuse in a thesis/dissertation
Portion	figures/tables/illustrations
Number of figures/tables/illustrations	1
Format	both print and electronic
Are you the author of this Elsevier article?	No
Will you be translating?	No
Title of new work	CNS MYELINATION INVOLVES NONVESICULAR GLYCOLIPID TRANSPORT FROM ENDOPLASMIC RETICULUM TO PLASMA MEMBRANE IN OLIGODENDROCYTES
Institution name	LMU Munich
Expected presentation date	Apr 2024
Portions	Figure 7
Requestor Location	Jianping Wu Siegesstr. 15 Munich, 80802 Germany Attn: Jianping Wu
Publisher Tax ID	GB 494 6272 12
Total	0.00 EUR

Copyright of figures taken from publication

Terms and Conditions

INTRODUCTION

1. The publisher for this copyrighted material is Elsevier. By clicking "accept" in connection with completing this licensing transaction, you agree that the following terms and conditions apply to this transaction (along with the Billing and Payment terms and conditions established by Copyright Clearance Center, Inc. ("CCC"), at the time that you opened your RightsLink account and that are available at any time at https://myaccount.copyright.com).

GENERAL TERMS

2. Elsevier hereby grants you permission to reproduce the aforementioned material subject to the terms and conditions indicated.

3. Acknowledgement: If any part of the material to be used (for example, figures) has appeared in our publication with credit or acknowledgement to another source, permission must also be sought from that source. If such permission is not obtained then that material may not be included in your publication/copies. Suitable acknowledgement to the source must be made, either as a footnote or in a reference list at the end of your publication, as follows:

"Reprinted from Publication title, Vol /edition number, Author(s), Title of article / title of chapter, Pages No., Copyright (Year), with permission from Elsevier [OR APPLICABLE SOCIETY COPYRIGHT OWNER]." Also Lancet special credit - "Reprinted from The Lancet, Vol. number, Author(s), Title of article, Pages No., Copyright (Year), with permission from Elsevier."

4. Reproduction of this material is confined to the purpose and/or media for which permission is hereby given. The material may not be reproduced or used in any other way, including use in combination with an artificial intelligence tool (including to train an algorithm, test, process, analyse, generate output and/or develop any form of artificial intelligence tool), or to create any derivative work and/or service (including resulting from the use of artificial intelligence tools).

5. Altering/Modifying Material: Not Permitted. However figures and illustrations may be altered/adapted minimally to serve your work. Any other abbreviations, additions, deletions and/or any other alterations shall be made only with prior written authorization of Elsevier Ltd. (Please contact Elsevier's permissions helpdesk here). No modifications can be made to any Lancet figures/tables and they must be reproduced in full.

6. If the permission fee for the requested use of our material is waived in this instance, please be advised that your future requests for Elsevier materials may attract a fee.

7. Reservation of Rights: Publisher reserves all rights not specifically granted in the combination of (i) the license details provided by you and accepted in the course of this licensing transaction, (ii) these terms and conditions and (iii) CCC's Billing and Payment terms and conditions.

8. License Contingent Upon Payment: While you may exercise the rights licensed immediately upon issuance of the license at the end of the licensing process for the transaction, provided that you have disclosed complete and accurate details of your

proposed use, no license is finally effective unless and until full payment is received from you (either by publisher or by CCC) as provided in CCC's Billing and Payment terms and conditions. If full payment is not received on a timely basis, then any license preliminarily granted shall be deemed automatically revoked and shall be void as if never granted. Further, in the event that you breach any of these terms and conditions or any of CCC's Billing and Payment terms and conditions, the license is automatically revoked and shall be void as if never granted. Use of materials as described in a revoked license, as well as any use of the materials beyond the scope of an unrevoked license, may constitute copyright infringement and publisher reserves the right to take any and all action to protect its copyright in the materials.

9. Warranties: Publisher makes no representations or warranties with respect to the licensed material.

10. Indemnity: You hereby indemnify and agree to hold harmless publisher and CCC, and their respective officers, directors, employees and agents, from and against any and all claims arising out of your use of the licensed material other than as specifically authorized pursuant to this license.

11. No Transfer of License: This license is personal to you and may not be sublicensed, assigned, or transferred by you to any other person without publisher's written permission.

12. No Amendment Except in Writing: This license may not be amended except in a writing signed by both parties (or, in the case of publisher, by CCC on publisher's behalf).

13. Objection to Contrary Terms: Publisher hereby objects to any terms contained in any purchase order, acknowledgment, check endorsement or other writing prepared by you, which terms are inconsistent with these terms and conditions or CCC's Billing and Payment terms and conditions. These terms and conditions, together with CCC's Billing and Payment terms and conditions (which are incorporated herein), comprise the entire agreement between you and publisher (and CCC) concerning this licensing transaction. In the event of any conflict between your obligations established by these terms and conditions and those established by CCC's Billing and Payment terms and conditions, these terms and conditions shall control.

14. Revocation: Elsevier or Copyright Clearance Center may deny the permissions described in this License at their sole discretion, for any reason or no reason, with a full refund payable to you. Notice of such denial will be made using the contact information provided by you. Failure to receive such notice will not alter or invalidate the denial. In no event will Elsevier or Copyright Clearance Center be responsible or liable for any costs, expenses or damage incurred by you as a result of a denial of your permission request, other than a refund of the amount(s) paid by you to Elsevier and/or Copyright Clearance Center for denied permissions.

LIMITED LICENSE

The following terms and conditions apply only to specific license types:

15. **Translation**: This permission is granted for non-exclusive world **English** rights only unless your license was granted for translation rights. If you licensed translation rights you may only translate this content into the languages you requested. A professional translator must perform all translations and reproduce the content word for word preserving the integrity of the article.

16. **Posting licensed content on any Website**: The following terms and conditions apply as follows: Licensing material from an Elsevier journal: All content posted to the web site must maintain the copyright information line on the bottom of each image; A hyper-text must be included to the Homepage of the journal from which you are licensing at http://www.sciencedirect.com/science/journal/xxxxx or the Elsevier homepage for books at http://www.elsevier.com; Central Storage: This license does not include permission for a scanned version of the material to be stored in a central repository such as that provided by Heron/XanEdu.

Licensing material from an Elsevier book: A hyper-text link must be included to the Elsevier homepage at http://www.elsevier.com . All content posted to the web site must maintain the copyright information line on the bottom of each image.

Posting licensed content on Electronic reserve: In addition to the above the following clauses are applicable: The web site must be password-protected and made available only to bona fide students registered on a relevant course. This permission is granted for 1 year only. You may obtain a new license for future website posting.

17. **For journal authors:** the following clauses are applicable in addition to the above:

Preprints:

A preprint is an author's own write-up of research results and analysis, it has not been peer-reviewed, nor has it had any other value added to it by a publisher (such as formatting, copyright, technical enhancement etc.).

Authors can share their preprints anywhere at any time. Preprints should not be added to or enhanced in any way in order to appear more like, or to substitute for, the final versions of articles however authors can update their preprints on arXiv or RePEc with their Accepted Author Manuscript (see below).

If accepted for publication, we encourage authors to link from the preprint to their formal publication via its DOI. Millions of researchers have access to the formal publications on ScienceDirect, and so links will help users to find, access, cite and use the best available version. Please note that Cell Press, The Lancet and some society-owned have different preprint policies. Information on these policies is available on the journal homepage.

Accepted Author Manuscripts: An accepted author manuscript is the manuscript of an article that has been accepted for publication and which typically includes author-incorporated changes suggested during submission, peer review and editor-author communications.

Authors can share their accepted author manuscript:

- immediately
  - via their non-commercial person homepage or blog
  - by updating a preprint in arXiv or RePEc with the accepted manuscript
  - via their research institute or institutional repository for internal institutional uses or as part of an invitation-only research collaboration work-group
  - directly by providing copies to their students or to research collaborators for their personal use
  - for private scholarly sharing as part of an invitation-only work group on commercial sites with which Elsevier has an agreement
- After the embargo period

- via non-commercial hosting platforms such as their institutional repository
- via commercial sites with which Elsevier has an agreement

In all cases accepted manuscripts should:

- link to the formal publication via its DOI
- bear a CC-BY-NC-ND license - this is easy to do
- if aggregated with other manuscripts, for example in a repository or other site, be shared in alignment with our hosting policy not be added to or enhanced in any way to appear more like, or to substitute for, the published journal article.

Published journal article (JPA): A published journal article (PJA) is the definitive final record of published research that appears or will appear in the journal and embodies all value-adding publishing activities including peer review co-ordination, copy-editing, formatting, (if relevant) pagination and online enrichment.

Policies for sharing publishing journal articles differ for subscription and gold open access articles:

Subscription Articles: If you are an author, please share a link to your article rather than the full-text. Millions of researchers have access to the formal publications on ScienceDirect, and so links will help your users to find, access, cite, and use the best available version.

Theses and dissertations which contain embedded PJAs as part of the formal submission can be posted publicly by the awarding institution with DOI links back to the formal publications on ScienceDirect.

If you are affiliated with a library that subscribes to ScienceDirect you have additional private sharing rights for others' research accessed under that agreement. This includes use for classroom teaching and internal training at the institution (including use in course packs and courseware programs), and inclusion of the article for grant funding purposes.

Gold Open Access Articles: May be shared according to the author-selected end-user license and should contain a CrossMark logo, the end user license, and a DOI link to the formal publication on ScienceDirect.

Please refer to Elsevier's posting policy for further information.

18. **For book authors** the following clauses are applicable in addition to the above: Authors are permitted to place a brief summary of their work online only. You are not allowed to download and post the published electronic version of your chapter, nor may you scan the printed edition to create an electronic version. **Posting to a repository:** Authors are permitted to post a summary of their chapter only in their institution's repository.

19. **Thesis/Dissertation**: If your license is for use in a thesis/dissertation your thesis may be submitted to your institution in either print or electronic form. Should your thesis be published commercially, please reapply for permission. These requirements include permission for the Library and Archives of Canada to supply single copies, on demand, of the complete thesis and include permission for Proquest/UMI to supply single copies, on demand, of the complete thesis. Should your thesis be published commercially, please reapply for permission. Theses and dissertations which contain embedded PJAs as part of the formal submission can be posted publicly by the awarding institution with DOI links back to the formal publications on ScienceDirect.

Copyright of figures taken from publication

Elsevier Open Access Terms and Conditions

You can publish open access with Elsevier in hundreds of open access journals or in nearly 2000 established subscription journals that support open access publishing. Permitted third party re-use of these open access articles is defined by the author's choice of Creative Commons user license. See our open access license policy for more information.

Terms & Conditions applicable to all Open Access articles published with Elsevier:

Any reuse of the article must not represent the author as endorsing the adaptation of the article nor should the article be modified in such a way as to damage the author's honour or reputation. If any changes have been made, such changes must be clearly indicated.

The author(s) must be appropriately credited and we ask that you include the end user license and a DOI link to the formal publication on ScienceDirect.

If any part of the material to be used (for example, figures) has appeared in our publication with credit or acknowledgement to another source it is the responsibility of the user to ensure their reuse complies with the terms and conditions determined by the rights holder.

Additional Terms & Conditions applicable to each Creative Commons user license:

CC BY: The CC-BY license allows users to copy, to create extracts, abstracts and new works from the Article, to alter and revise the Article and to make commercial use of the Article (including reuse and/or resale of the Article by commercial entities), provided the user gives appropriate credit (with a link to the formal publication through the relevant DOI), provides a link to the license, indicates if changes were made and the licensor is not represented as endorsing the use made of the work. The full details of the license are available at http://creativecommons.org/licenses/by/4.0.

CC BY NC SA: The CC BY-NC-SA license allows users to copy, to create extracts, abstracts and new works from the Article, to alter and revise the Article, provided this is not done for commercial purposes, and that the user gives appropriate credit (with a link to the formal publication through the relevant DOI), provides a link to the license, indicates if changes were made and the licensor is not represented as endorsing the use made of the work. Further, any new works must be made available on the same conditions. The full details of the license are available at http://creativecommons.org/licenses/by-nc-sa/4.0.

CC BY NC ND: The CC BY-NC-ND license allows users to copy and distribute the Article, provided this is not done for commercial purposes and further does not permit distribution of the Article if it is changed or edited in any way, and provided the user gives appropriate credit (with a link to the formal publication through the relevant DOI), provides a link to the license, and that the licensor is not represented as endorsing the use made of the work. The full details of the license are available at http://creativecommons.org/licenses/by-nc-nd/4.0. Any commercial reuse of Open Access articles published with a CC BY NC SA or CC BY NC ND license requires permission from Elsevier and will be subject to a fee.

Commercial reuse includes:

- Associating advertising with the full text of the Article
- Charging fees for document delivery or access
- Article aggregation
- Systematic distribution via e-mail lists or share buttons

Posting or linking by commercial companies for use by customers of those companies.

20. **Other Conditions**:

v1.10

Questions? customercare@copyright.com.

Fig 1.3: from Baron and Hoekstra 2010

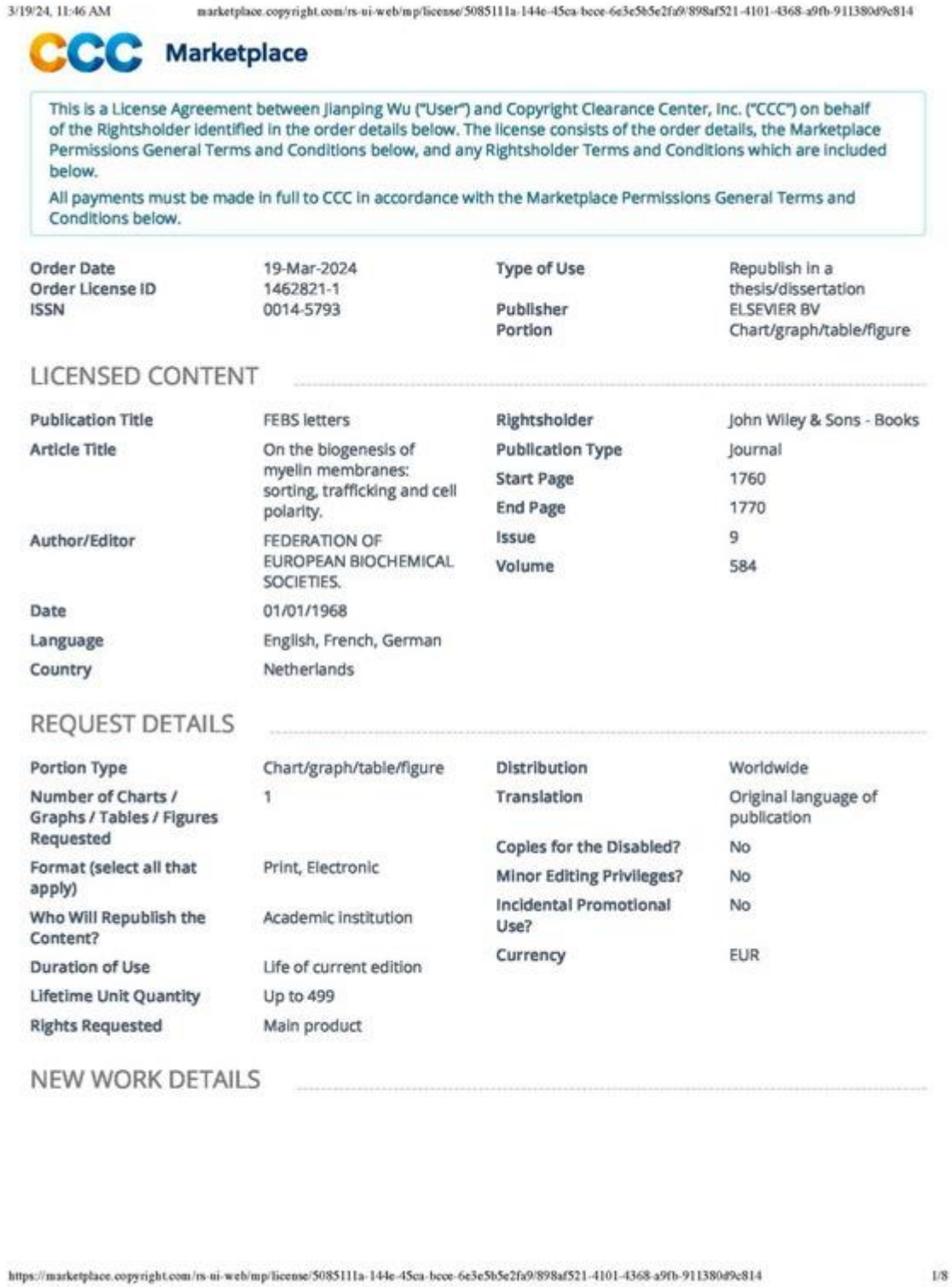

3/19/24, 11:46 AM marketplace.copyright.com/rs-ui-web/mp/license/5085111a-144e-45ca-bcce-6e3e5b5e2fa9/898af521-4101-4368-a9fb-911380d9c814

CCC Marketplace

This is a License Agreement between Jianping Wu ("User") and Copyright Clearance Center, Inc. ("CCC") on behalf of the Rightsholder identified in the order details below. The license consists of the order details, the Marketplace Permissions General Terms and Conditions below, and any Rightsholder Terms and Conditions which are included below.

All payments must be made in full to CCC in accordance with the Marketplace Permissions General Terms and Conditions below.

Order Date	19-Mar-2024	Type of Use	Republish in a thesis/dissertation
Order License ID	1462821-1		
ISSN	0014-5793	Publisher	ELSEVIER BV
		Portion	Chart/graph/table/figure

LICENSED CONTENT

Publication Title	FEBS letters	Rightsholder	John Wiley & Sons - Books
Article Title	On the biogenesis of myelin membranes: sorting, trafficking and cell polarity.	Publication Type	Journal
		Start Page	1760
		End Page	1770
Author/Editor	FEDERATION OF EUROPEAN BIOCHEMICAL SOCIETIES.	Issue	9
		Volume	584
Date	01/01/1968		
Language	English, French, German		
Country	Netherlands		

REQUEST DETAILS

Portion Type	Chart/graph/table/figure	Distribution	Worldwide
Number of Charts / Graphs / Tables / Figures Requested	1	Translation	Original language of publication
		Copies for the Disabled?	No
Format (select all that apply)	Print, Electronic	Minor Editing Privileges?	No
Who Will Republish the Content?	Academic institution	Incidental Promotional Use?	No
Duration of Use	Life of current edition	Currency	EUR
Lifetime Unit Quantity	Up to 499		
Rights Requested	Main product		

NEW WORK DETAILS

https://marketplace.copyright.com/rs-ui-web/mp/license/5085111a-144e-45ca-bcce-6e3e5b5e2fa9/898af521-4101-4368-a9fb-911380d9c814 1/8

Title	CNS MYELINATION INVOLVES NONVESICULARGLYCOLIPID TRANSPORT FROM ENDOPLASMICRETICULUM TO PLASMA MEMBRANE INOLIGODENDROCYTES	**Institution Name**	LMU Munich
		Expected Presentation Date	2024-06-15
Instructor Name	Mikael Simons		

ADDITIONAL DETAILS

The Requesting Person / Organization to Appear on the License	Jianping Wu

REQUESTED CONTENT DETAILS

Title, Description or Numeric Reference of the Portion(s)	Fig 2	**Title of the Article / Chapter the Portion Is From**	On the biogenesis of myelin membranes: sorting, trafficking and cell polarity.
Editor of Portion(s)	Baron, Wia; Hoekstra, Dick		
Volume / Edition	584	**Author of Portion(s)**	Baron, Wia; Hoekstra, Dick
Page or Page Range of Portion	1760-1770	**Publication Date of Portion**	2010-05-03

RIGHTSHOLDER TERMS AND CONDITIONS

No right, license or interest to any trademark, trade name, service mark or other branding ("Marks") of WILEY or its licensors is granted hereunder, and you agree that you shall not assert any such right, license or interest with respect thereto. You may not alter, remove or suppress in any manner any copyright, trademark or other notices displayed by the Wiley material. This Agreement will be void if the Type of Use, Format, Circulation, or Requestor Type was misrepresented during the licensing process. In no instance may the total amount of Wiley Materials used in any Main Product, Compilation or Collective work comprise more than 5% (if figures/tables) or 15% (if full articles/chapters) of the (entirety of the) Main Product, Compilation or Collective Work. Some titles may be available under an Open Access license. It is the Licensors' responsibility to identify the type of Open Access license on which the requested material was published, and comply fully with the terms of that license for the type of use specified Further details can be found on Wiley Online Library http://olabout.wiley.com/WileyCDA/Section/id-410895.html.

Marketplace Permissions General Terms and Conditions

The following terms and conditions ("General Terms"), together with any applicable Publisher Terms and Conditions, govern User's use of Works pursuant to the Licenses granted by Copyright Clearance Center, Inc. ("CCC") on behalf of the applicable Rightsholders of such Works through CCC's applicable Marketplace transactional licensing services (each, a "Service").

1) **Definitions.** For purposes of these General Terms, the following definitions apply:

"License" is the licensed use the User obtains via the Marketplace platform in a particular licensing transaction, as set forth in the Order Confirmation.

"Order Confirmation" is the confirmation CCC provides to the User at the conclusion of each Marketplace transaction. "Order Confirmation Terms" are additional terms set forth on specific Order Confirmations not set forth in the General Terms that can include terms applicable to a particular CCC transactional licensing service and/or any Rightsholder-specific terms.

"Rightsholder(s)" are the holders of copyright rights in the Works for which a User obtains licenses via the Marketplace platform, which are displayed on specific Order Confirmations.

"Terms" means the terms and conditions set forth in these General Terms and any additional Order Confirmation Terms collectively.

"User" or "you" is the person or entity making the use granted under the relevant License. Where the person accepting the Terms on behalf of a User is a freelancer or other third party who the User authorized to accept the General Terms on the User's behalf, such person shall be deemed jointly a User for purposes of such Terms.

"Work(s)" are the copyright protected works described in relevant Order Confirmations.

2) **Description of Service.** CCC's Marketplace enables Users to obtain Licenses to use one or more Works in accordance with all relevant Terms. CCC grants Licenses as an agent on behalf of the copyright rightsholder identified in the relevant Order Confirmation.

3) **Applicability of Terms.** The Terms govern User's use of Works in connection with the relevant License. In the event of any conflict between General Terms and Order Confirmation Terms, the latter shall govern. User acknowledges that Rightsholders have complete discretion whether to grant any permission, and whether to place any limitations on any grant, and that CCC has no right to supersede or to modify any such discretionary act by a Rightsholder.

4) **Representations; Acceptance.** By using the Service, User represents and warrants that User has been duly authorized by the User to accept, and hereby does accept, all Terms.

5) **Scope of License; Limitations and Obligations.** All Works and all rights therein, including copyright rights, remain the sole and exclusive property of the Rightsholder. The License provides only those rights expressly set forth in the terms and conveys no other rights in any Works

6) **General Payment Terms.** User may pay at time of checkout by credit card or choose to be invoiced. If the User chooses to be invoiced, the User shall: (i) remit payments in the manner identified on specific invoices, (ii) unless otherwise specifically stated in an Order Confirmation or separate written agreement, Users shall remit payments upon receipt of the relevant invoice from CCC, either by delivery or notification of availability of the invoice via the Marketplace platform, and (iii) if the User does not pay the invoice within 30 days of receipt, the User may incur a service charge of 1.5% per month or the maximum rate allowed by applicable law, whichever is less. While User may exercise the rights in the License immediately upon receiving the Order Confirmation, the License is automatically revoked and is null and void, as if it had never been issued, if CCC does not receive complete payment on a timely basis.

7) **General Limits on Use.** Unless otherwise provided in the Order Confirmation, any grant of rights to User (i) involves only the rights set forth in the Terms and does not include subsequent or additional uses, (ii) is non-exclusive and non-transferable, and (iii) is subject to any and all limitations and restrictions (such as, but not limited to, limitations on duration of use or circulation) included in the Terms. Upon completion of the licensed use as set forth in the Order Confirmation, User shall either secure a new permission for further use of the Work(s) or immediately cease any new use of the Work(s) and shall render inaccessible (such as by deleting or by removing or severing links or other locators) any further copies of the Work. User may only make alterations to the Work if and as expressly set forth in the Order Confirmation. No Work may be used in any way that is unlawful, including without limitation if such use would violate applicable sanctions laws or regulations, would be defamatory, violate the rights of third parties (including such third parties' rights of copyright, privacy, publicity, or other tangible or intangible property), or is otherwise illegal, sexually explicit, or obscene. In addition, User may not conjoin a Work with any other material that may result in damage to the reputation of the Rightsholder. Any unlawful use will render any licenses hereunder null and void. User agrees to inform CCC if it becomes aware of any infringement of any rights in a Work and to cooperate with any reasonable request of CCC or the Rightsholder in connection therewith.

8) **Third Party Materials.** In the event that the material for which a License is sought includes third party materials (such as photographs, illustrations, graphs, inserts and similar materials) that are identified in such material as having been used by permission (or a similar indicator), User is responsible for identifying, and seeking separate licenses (under this Service, if available, or otherwise) for any of such third party materials; without a separate license, User may not use such third party materials via the License.

9) **Copyright Notice.** Use of proper copyright notice for a Work is required as a condition of any License granted under the Service. Unless otherwise provided in the Order Confirmation, a proper copyright notice will read substantially as

follows: "Used with permission of [Rightsholder's name], from [Work's title, author, volume, edition number and year of copyright]; permission conveyed through Copyright Clearance Center, Inc." Such notice must be provided in a reasonably legible font size and must be placed either on a cover page or in another location that any person, upon gaining access to the material which is the subject of a permission, shall see, or in the case of republication Licenses, immediately adjacent to the Work as used (for example, as part of a by-line or footnote) or in the place where substantially all other credits or notices for the new work containing the republished Work are located. Failure to include the required notice results in loss to the Rightsholder and CCC, and the User shall be liable to pay liquidated damages for each such failure equal to twice the use fee specified in the Order Confirmation, in addition to the use fee itself and any other fees and charges specified.

10) **Indemnity.** User hereby indemnifies and agrees to defend the Rightsholder and CCC, and their respective employees and directors, against all claims, liability, damages, costs, and expenses, including legal fees and expenses, arising out of any use of a Work beyond the scope of the rights granted herein and in the Order Confirmation, or any use of a Work which has been altered in any unauthorized way by User, including claims of defamation or infringement of rights of copyright, publicity, privacy, or other tangible or intangible property.

11) **Limitation of Liability.** UNDER NO CIRCUMSTANCES WILL CCC OR THE RIGHTSHOLDER BE LIABLE FOR ANY DIRECT, INDIRECT, CONSEQUENTIAL, OR INCIDENTAL DAMAGES (INCLUDING WITHOUT LIMITATION DAMAGES FOR LOSS OF BUSINESS PROFITS OR INFORMATION, OR FOR BUSINESS INTERRUPTION) ARISING OUT OF THE USE OR INABILITY TO USE A WORK, EVEN IF ONE OR BOTH OF THEM HAS BEEN ADVISED OF THE POSSIBILITY OF SUCH DAMAGES. In any event, the total liability of the Rightsholder and CCC (including their respective employees and directors) shall not exceed the total amount actually paid by User for the relevant License. User assumes full liability for the actions and omissions of its principals, employees, agents, affiliates, successors, and assigns.

12) **Limited Warranties.** THE WORK(S) AND RIGHT(S) ARE PROVIDED "AS IS." CCC HAS THE RIGHT TO GRANT TO USER THE RIGHTS GRANTED IN THE ORDER CONFIRMATION DOCUMENT. CCC AND THE RIGHTSHOLDER DISCLAIM ALL OTHER WARRANTIES RELATING TO THE WORK(S) AND RIGHT(S), EITHER EXPRESS OR IMPLIED, INCLUDING WITHOUT LIMITATION IMPLIED WARRANTIES OF MERCHANTABILITY OR FITNESS FOR A PARTICULAR PURPOSE. ADDITIONAL RIGHTS MAY BE REQUIRED TO USE ILLUSTRATIONS, GRAPHS, PHOTOGRAPHS, ABSTRACTS, INSERTS, OR OTHER PORTIONS OF THE WORK (AS OPPOSED TO THE ENTIRE WORK) IN A MANNER CONTEMPLATED BY USER; USER UNDERSTANDS AND AGREES THAT NEITHER CCC NOR THE RIGHTSHOLDER MAY HAVE SUCH ADDITIONAL RIGHTS TO GRANT.

13) **Effect of Breach.** Any failure by User to pay any amount when due, or any use by User of a Work beyond the scope of the License set forth in the Order Confirmation and/or the Terms, shall be a material breach of such License. Any breach not cured within 10 days of written notice thereof shall result in immediate termination of such License without further notice. Any unauthorized (but licensable) use of a Work that is terminated immediately upon notice thereof may be liquidated by payment of the Rightsholder's ordinary license price therefor; any unauthorized (and unlicensable) use that is not terminated immediately for any reason (including, for example, because materials containing the Work cannot reasonably be recalled) will be subject to all remedies available at law or in equity, but in no event to a payment of less than three times the Rightsholder's ordinary license price for the most closely analogous licensable use plus Rightsholder's and/or CCC's costs and expenses incurred in collecting such payment.

14) **Additional Terms for Specific Products and Services.** If a User is making one of the uses described in this Section 14, the additional terms and conditions apply:

a) ***Print Uses of Academic Course Content and Materials (photocopies for academic coursepacks or classroom handouts).*** For photocopies for academic coursepacks or classroom handouts the following additional terms apply:

i) The copies and anthologies created under this License may be made and assembled by faculty members individually or at their request by on-campus bookstores or copy centers, or by off-campus copy shops and other similar entities.

ii) No License granted shall in any way: (i) include any right by User to create a substantively non-identical copy of the Work or to edit or in any other way modify the Work (except by means of deleting material immediately preceding or following the entire portion of the Work copied) (ii) permit "publishing ventures" where any particular anthology would be systematically marketed at multiple institutions.

iii) Subject to any Publisher Terms (and notwithstanding any apparent contradiction in the Order Confirmation arising from data provided by User), any use authorized under the academic pay-per-use service is limited as follows:

A) any License granted shall apply to only one class (bearing a unique identifier as assigned by the institution, and thereby including all sections or other subparts of the class) at one institution;

B) use is limited to not more than 25% of the text of a book or of the items in a published collection of essays, poems or articles;

C) use is limited to no more than the greater of (a) 25% of the text of an issue of a journal or other periodical or (b) two articles from such an issue;

D) no User may sell or distribute any particular anthology, whether photocopied or electronic, at more than one institution of learning;

E) in the case of a photocopy permission, no materials may be entered into electronic memory by User except in order to produce an identical copy of a Work before or during the academic term (or analogous period) as to which any particular permission is granted. In the event that User shall choose to retain materials that are the subject of a photocopy permission in electronic memory for purposes of producing identical copies more than one day after such retention (but still within the scope of any permission granted), User must notify CCC of such fact in the applicable permission request and such retention shall constitute one copy actually sold for purposes of calculating permission fees due; and

F) any permission granted shall expire at the end of the class. No permission granted shall in any way include any right by User to create a substantively non-identical copy of the Work or to edit or in any other way modify the Work (except by means of deleting material immediately preceding or following the entire portion of the Work copied).

iv) Books and Records; Right to Audit. As to each permission granted under the academic pay-per-use Service, User shall maintain for at least four full calendar years books and records sufficient for CCC to determine the numbers of copies made by User under such permission. CCC and any representatives it may designate shall have the right to audit such books and records at any time during User's ordinary business hours, upon two days' prior notice. If any such audit shall determine that User shall have underpaid for, or underreported, any photocopies sold or by three percent (3%) or more, then User shall bear all the costs of any such audit; otherwise, CCC shall bear the costs of any such audit. Any amount determined by such audit to have been underpaid by User shall immediately be paid to CCC by User, together with interest thereon at the rate of 10% per annum from the date such amount was originally due. The provisions of this paragraph shall survive the termination of this License for any reason.

b) ***Digital Pay-Per-Uses of Academic Course Content and Materials (e-coursepacks, electronic reserves, learning management systems, academic institution intranets).*** For uses in e-coursepacks, posts in electronic reserves, posts in learning management systems, or posts on academic institution intranets, the following additional terms apply:

i) The pay-per-uses subject to this Section 14(b) include:

A) **Posting e-reserves, course management systems, e-coursepacks for text-based content,** which grants authorizations to import requested material in electronic format, and allows electronic access to this material to members of a designated college or university class, under the direction of an instructor designated by the college or university, accessible only under appropriate electronic controls (e.g., password);

B) **Posting e-reserves, course management systems, e-coursepacks for material consisting of photographs or other still images not embedded in text,** which grants not only the authorizations described in Section 14(b)(i)(A) above, but also the following authorization: to include the requested material in course materials for use consistent with Section 14(b)(i)(A) above, including any necessary resizing, reformatting or modification of the resolution of such requested material (provided that such modification does not alter the underlying editorial content or meaning of the requested material, and provided that the resulting modified content is used solely within the scope of, and in a manner consistent with, the particular authorization described in the Order Confirmation and the Terms), but not including any other form of manipulation, alteration or editing of the requested material;

C) **Posting e-reserves, course management systems, e-coursepacks or other academic distribution for audiovisual content,** which grants not only the authorizations described in Section 14(b)(i)(A) above, but also the following authorizations: (i) to include the requested material in course materials for use consistent with

Section 14(b)(i)(A) above; (ii) to display and perform the requested material to such members of such class in the physical classroom or remotely by means of streaming media or other video formats; and (iii) to "clip" or reformat the requested material for purposes of time or content management or ease of delivery, provided that such "clipping" or reformatting does not alter the underlying editorial content or meaning of the requested material and that the resulting material is used solely within the scope of, and in a manner consistent with, the particular authorization described in the Order Confirmation and the Terms. Unless expressly set forth in the relevant Order Conformation, the License does not authorize any other form of manipulation, alteration or editing of the requested material.

ii) Unless expressly set forth in the relevant Order Confirmation, no License granted shall in any way: (i) include any right by User to create a substantively non-identical copy of the Work or to edit or in any other way modify the Work (except by means of deleting material immediately preceding or following the entire portion of the Work copied or, in the case of Works subject to Sections 14(b)(1)(B) or (C) above, as described in such Sections) (ii) permit "publishing ventures" where any particular course materials would be systematically marketed at multiple institutions.

iii) Subject to any further limitations determined in the Rightsholder Terms (and notwithstanding any apparent contradiction in the Order Confirmation arising from data provided by User), any use authorized under the electronic course content pay-per-use service is limited as follows:

A) any License granted shall apply to only one class (bearing a unique identifier as assigned by the institution, and thereby including all sections or other subparts of the class) at one institution;

B) use is limited to not more than 25% of the text of a book or of the items in a published collection of essays, poems or articles;

C) use is limited to not more than the greater of (a) 25% of the text of an issue of a journal or other periodical or (b) two articles from such an issue;

D) no User may sell or distribute any particular materials, whether photocopied or electronic, at more than one institution of learning;

E) electronic access to material which is the subject of an electronic-use permission must be limited by means of electronic password, student identification or other control permitting access solely to students and instructors in the class;

F) User must ensure (through use of an electronic cover page or other appropriate means) that any person, upon gaining electronic access to the material, which is the subject of a permission, shall see:

- a proper copyright notice, identifying the Rightsholder in whose name CCC has granted permission,
- a statement to the effect that such copy was made pursuant to permission,
- a statement identifying the class to which the material applies and notifying the reader that the material has been made available electronically solely for use in the class, and
- a statement to the effect that the material may not be further distributed to any person outside the class, whether by copying or by transmission and whether electronically or in paper form, and User must also ensure that such cover page or other means will print out in the event that the person accessing the material chooses to print out the material or any part thereof.

G) any permission granted shall expire at the end of the class and, absent some other form of authorization, User is thereupon required to delete the applicable material from any electronic storage or to block electronic access to the applicable material.

iv) Uses of separate portions of a Work, even if they are to be included in the same course material or the same university or college class, require separate permissions under the electronic course content pay-per-use Service. Unless otherwise provided in the Order Confirmation, any grant of rights to User is limited to use completed no later than the end of the academic term (or analogous period) as to which any particular permission is granted.

Copyright of figures taken from publication

v) Books and Records; Right to Audit. As to each permission granted under the electronic course content Service, User shall maintain for at least four full calendar years books and records sufficient for CCC to determine the numbers of copies made by User under such permission. CCC and any representatives it may designate shall have the right to audit such books and records at any time during User's ordinary business hours, upon two days' prior notice. If any such audit shall determine that User shall have underpaid for, or underreported, any electronic copies used by three percent (3%) or more, then User shall bear all the costs of any such audit; otherwise, CCC shall bear the costs of any such audit. Any amount determined by such audit to have been underpaid by User shall immediately be paid to CCC by User, together with interest thereon at the rate of 10% per annum from the date such amount was originally due. The provisions of this paragraph shall survive the termination of this license for any reason.

c) ***Pay-Per-Use Permissions for Certain Reproductions (Academic photocopies for library reserves and interlibrary loan reporting) (Non-academic internal/external business uses and commercial document delivery).*** The License expressly excludes the uses listed in Section (c)(i)-(v) below (which must be subject to separate license from the applicable Rightsholder) for: academic photocopies for library reserves and interlibrary loan reporting; and non-academic internal/external business uses and commercial document delivery.

i) electronic storage of any reproduction (whether in plain-text, PDF, or any other format) other than on a transitory basis;

ii) the input of Works or reproductions thereof into any computerized database;

iii) reproduction of an entire Work (cover-to-cover copying) except where the Work is a single article;

iv) reproduction for resale to anyone other than a specific customer of User;

v) republication in any different form. Please obtain authorizations for these uses through other CCC services or directly from the rightsholder.

Any license granted is further limited as set forth in any restrictions included in the Order Confirmation and/or in these Terms.

d) ***Electronic Reproductions in Online Environments (Non-Academic-email, intranet, internet and extranet).*** For "electronic reproductions", which generally includes e-mail use (including instant messaging or other electronic transmission to a defined group of recipients) or posting on an intranet, extranet or intranet site (including any display or performance incidental thereto), the following additional terms apply:

i) Unless otherwise set forth in the Order Confirmation, the License is limited to use completed within 30 days for any use on the Internet, 60 days for any use on an intranet or extranet and one year for any other use, all as measured from the "republication date" as identified in the Order Confirmation, if any, and otherwise from the date of the Order Confirmation.

ii) User may not make or permit any alterations to the Work, unless expressly set forth in the Order Confirmation (after request by User and approval by Rightsholder); provided, however, that a Work consisting of photographs or other still images not embedded in text may, if necessary, be resized, reformatted or have its resolution modified without additional express permission, and a Work consisting of audiovisual content may, if necessary, be "clipped" or reformatted for purposes of time or content management or ease of delivery (provided that any such resizing, reformatting, resolution modification or "clipping" does not alter the underlying editorial content or meaning of the Work used, and that the resulting material is used solely within the scope of, and in a manner consistent with, the particular License described in the Order Confirmation and the Terms.

15) **Miscellaneous.**

a) User acknowledges that CCC may, from time to time, make changes or additions to the Service or to the Terms, and that Rightsholder may make changes or additions to the Rightsholder Terms. Such updated Terms will replace the prior terms and conditions in the order workflow and shall be effective as to any subsequent Licenses but shall not apply to Licenses already granted and paid for under a prior set of terms.

b) Use of User-related information collected through the Service is governed by CCC's privacy policy, available online at www.copyright.com/about/privacy-policy/.

c) The License is personal to User. Therefore, User may not assign or transfer to any other person (whether a natural person or an organization of any kind) the License or any rights granted thereunder; provided, however, that, where applicable, User may assign such License in its entirety on written notice to CCC in the event of a transfer of all or substantially all of User's rights in any new material which includes the Work(s) licensed under this Service.

d) No amendment or waiver of any Terms is binding unless set forth in writing and signed by the appropriate parties, including, where applicable, the Rightsholder. The Rightsholder and CCC hereby object to any terms contained in any writing prepared by or on behalf of the User or its principals, employees, agents or affiliates and purporting to govern or otherwise relate to the License described in the Order Confirmation, which terms are in any way inconsistent with any Terms set forth in the Order Confirmation, and/or in CCC's standard operating procedures, whether such writing is prepared prior to, simultaneously with or subsequent to the Order Confirmation, and whether such writing appears on a copy of the Order Confirmation or in a separate instrument.

e) The License described in the Order Confirmation shall be governed by and construed under the law of the State of New York, USA, without regard to the principles thereof of conflicts of law. Any case, controversy, suit, action, or proceeding arising out of, in connection with, or related to such License shall be brought, at CCC's sole discretion, in any federal or state court located in the County of New York, State of New York, USA, or in any federal or state court whose geographical jurisdiction covers the location of the Rightsholder set forth in the Order Confirmation. The parties expressly submit to the personal jurisdiction and venue of each such federal or state court.

Last updated October 2022

Fig 1.4: from Prinz 2010

ELSEVIER LICENSE TERMS AND CONDITIONS

Mar 14, 2024

This Agreement between Jianping Wu ("You") and Elsevier ("Elsevier") consists of your license details and the terms and conditions provided by Elsevier and Copyright Clearance Center.

License Number	5747690781232
License date	Mar 14, 2024
Licensed Content Publisher	Elsevier
Licensed Content Publication	Cell
Licensed Content Title	Lipid Trafficking sans Vesicles: Where, Why, How?
Licensed Content Author	William A. Prinz
Licensed Content Date	Dec 10, 2010
Licensed Content Volume	143
Licensed Content Issue	6
Licensed Content Pages	5
Start Page	870
End Page	874
Type of Use	reuse in a thesis/dissertation
Portion	figures/tables/illustrations
Number of figures/tables/illustrations	1
Format	both print and electronic
Are you the author of this Elsevier article?	No
Will you be translating?	No
Title of new work	CNS MYELINATION INVOLVES NONVESICULAR GLYCOLIPID TRANSPORT FROM ENDOPLASMIC RETICULUM TO PLASMA MEMBRANE IN OLIGODENDROCYTES
Institution name	LMU Munich
Expected presentation date	Apr 2024
Portions	Figure 1
Requestor Location	Jianping Wu Siegesstr. 15 Munich, 80802 Germany Attn: Jianping Wu
Publisher Tax ID	GB 494 6272 12
Total	**0.00 EUR**
Terms and Conditions	

INTRODUCTION

1. The publisher for this copyrighted material is Elsevier. By clicking "accept" in connection with completing this licensing transaction, you agree that the following terms and conditions apply to this transaction (along with the Billing and Payment terms and conditions established by Copyright Clearance Center, Inc. ("CCC"), at the time that you opened your RightsLink account and that are available at any time at https://myaccount.copyright.com).

GENERAL TERMS

2. Elsevier hereby grants you permission to reproduce the aforementioned material subject to the terms and conditions indicated.

3. Acknowledgement: If any part of the material to be used (for example, figures) has appeared in our publication with credit or acknowledgement to another source, permission must also be sought from that source. If such permission is not obtained then that material may not be included in your publication/copies. Suitable acknowledgement to the source must be made, either as a footnote or in a reference list at the end of your publication, as follows:
"Reprinted from Publication title, Vol /edition number, Author(s), Title of article / title of chapter, Pages No., Copyright (Year), with permission from Elsevier [OR APPLICABLE SOCIETY COPYRIGHT OWNER]." Also Lancet special credit - "Reprinted from The Lancet, Vol. number, Author(s), Title of article, Pages No., Copyright (Year), with permission from Elsevier."
4. Reproduction of this material is confined to the purpose and/or media for which permission is hereby given. The material may not be reproduced or used in any other way, including use in combination with an artificial intelligence tool (including to train an algorithm, test, process, analyse, generate output and/or develop any form of artificial intelligence tool), or to create any derivative work and/or service (including resulting from the use of artificial intelligence tools).
5. Altering/Modifying Material: Not Permitted. However figures and illustrations may be altered/adapted minimally to serve your work. Any other abbreviations, additions, deletions and/or any other alterations shall be made only with prior written authorization of Elsevier Ltd. (Please contact Elsevier's permissions helpdesk here). No modifications can be made to any Lancet figures/tables and they must be reproduced in full.
6. If the permission fee for the requested use of our material is waived in this instance, please be advised that your future requests for Elsevier materials may attract a fee.
7. Reservation of Rights: Publisher reserves all rights not specifically granted in the combination of (i) the license details provided by you and accepted in the course of this licensing transaction, (ii) these terms and conditions and (iii) CCC's Billing and Payment terms and conditions.
8. License Contingent Upon Payment: While you may exercise the rights licensed immediately upon issuance of the license at the end of the licensing process for the transaction, provided that you have disclosed complete and accurate details of your proposed use, no license is finally effective unless and until full payment is received from you (either by publisher or by CCC) as provided in CCC's Billing and Payment terms and conditions. If full payment is not received on a timely basis, then any license preliminarily granted shall be deemed automatically revoked and shall be void as if never granted. Further, in the event that you breach any of these terms and conditions or any of CCC's Billing and Payment terms and conditions, the license is automatically revoked and shall be void as if never granted. Use of materials as described in a revoked license, as well as any use of the materials beyond the scope of an unrevoked license, may constitute copyright infringement and publisher reserves the right to take any and all action to protect its copyright in the materials.
9. Warranties: Publisher makes no representations or warranties with respect to the licensed material.
10. Indemnity: You hereby indemnify and agree to hold harmless publisher and CCC, and their respective officers, directors, employees and agents, from and against any and all claims arising out of your use of the licensed material other than as specifically authorized pursuant to this license.
11. No Transfer of License: This license is personal to you and may not be sublicensed, assigned, or transferred by you to any other person without publisher's written permission.
12. No Amendment Except in Writing: This license may not be amended except in a writing signed by both parties (or, in the case of publisher, by CCC on publisher's behalf).
13. Objection to Contrary Terms: Publisher hereby objects to any terms contained in any purchase order, acknowledgment, check endorsement or other writing prepared by you, which terms are inconsistent with these terms and conditions or CCC's Billing and Payment terms and conditions. These terms and conditions, together with CCC's Billing and Payment terms and conditions (which are incorporated herein), comprise the entire agreement between you and publisher (and CCC) concerning this licensing transaction. In the event of any conflict between your obligations established by these terms and conditions and those established by CCC's Billing and Payment terms and conditions, these terms and conditions shall control.
14. Revocation: Elsevier or Copyright Clearance Center may deny the permissions described in this License at their sole discretion, for any reason or no reason, with a full refund payable to you. Notice of such denial will be made using the contact information provided by you. Failure to receive such notice will not alter or invalidate the denial. In no event will Elsevier or Copyright Clearance Center be responsible or liable for any costs, expenses or damage incurred by you as a result of a denial of your permission request, other than a refund of the amount(s) paid by you to Elsevier and/or Copyright Clearance Center for denied permissions.

LIMITED LICENSE

The following terms and conditions apply only to specific license types:
15. **Translation**: This permission is granted for non-exclusive world English rights only unless your license was granted for translation rights. If you licensed translation rights you may only translate this content into the languages you requested. A professional translator must perform all translations and reproduce the content word for word preserving the integrity of the article.
16. **Posting licensed content on any Website**: The following terms and conditions apply as follows: Licensing material from an Elsevier journal: All content posted to the web site must maintain the copyright information line on the bottom of each image; A hyper-text must be included to the Homepage of the journal from which you are licensing at http://www.sciencedirect.com/science/journal/xxxxx or the Elsevier homepage for books at http://www.elsevier.com; Central Storage: This license does not include permission for a scanned version of the material to be stored in a central repository such as that provided by Heron/XanEdu.

Licensing material from an Elsevier book: A hyper-text link must be included to the Elsevier homepage at http://www.elsevier.com . All content posted to the web site must maintain the copyright information line on the bottom of each image.

Posting licensed content on Electronic reserve: In addition to the above the following clauses are applicable: The web site must be password-protected and made available only to bona fide students registered on a relevant course. This permission is granted for 1 year only. You may obtain a new license for future website posting.

17. **For journal authors:** the following clauses are applicable in addition to the above:

Preprints:

A preprint is an author's own write-up of research results and analysis, it has not been peer-reviewed, nor has it had any other value added to it by a publisher (such as formatting, copyright, technical enhancement etc.).

Authors can share their preprints anywhere at any time. Preprints should not be added to or enhanced in any way in order to appear more like, or to substitute for, the final versions of articles however authors can update their preprints on arXiv or RePEc with their Accepted Author Manuscript (see below).

If accepted for publication, we encourage authors to link from the preprint to their formal publication via its DOI. Millions of researchers have access to the formal publications on ScienceDirect, and so links will help users to find, access, cite and use the best available version. Please note that Cell Press, The Lancet and some society-owned have different preprint policies. Information on these policies is available on the journal homepage.

Accepted Author Manuscripts: An accepted author manuscript is the manuscript of an article that has been accepted for publication and which typically includes author-incorporated changes suggested during submission, peer review and editor-author communications.

Authors can share their accepted author manuscript:

- immediately
  - via their non-commercial person homepage or blog
  - by updating a preprint in arXiv or RePEc with the accepted manuscript
  - via their research institute or institutional repository for internal institutional uses or as part of an invitation-only research collaboration work-group
  - directly by providing copies to their students or to research collaborators for their personal use
  - for private scholarly sharing as part of an invitation-only work group on commercial sites with which Elsevier has an agreement
- After the embargo period
  - via non-commercial hosting platforms such as their institutional repository
  - via commercial sites with which Elsevier has an agreement

In all cases accepted manuscripts should:

- link to the formal publication via its DOI
- bear a CC-BY-NC-ND license - this is easy to do
- if aggregated with other manuscripts, for example in a repository or other site, be shared in alignment with our hosting policy not be added to or enhanced in any way to appear more like, or to substitute for, the published journal article.

Published journal article (JPA): A published journal article (PJA) is the definitive final record of published research that appears or will appear in the journal and embodies all value-adding publishing activities including peer review co-ordination, copy-editing, formatting, (if relevant) pagination and online enrichment.

Policies for sharing publishing journal articles differ for subscription and gold open access articles:

Subscription Articles: If you are an author, please share a link to your article rather than the full-text. Millions of researchers have access to the formal publications on ScienceDirect, and so links will help your users to find, access, cite, and use the best available version.

Theses and dissertations which contain embedded PJAs as part of the formal submission can be posted publicly by the awarding institution with DOI links back to the formal publications on ScienceDirect.

If you are affiliated with a library that subscribes to ScienceDirect you have additional private sharing rights for others' research accessed under that agreement. This includes use for classroom teaching and internal training at the institution (including use in course packs and courseware programs), and inclusion of the article for grant funding purposes.

Gold Open Access Articles: May be shared according to the author-selected end-user license and should contain a CrossMark logo, the end user license, and a DOI link to the formal publication on ScienceDirect.

Please refer to Elsevier's posting policy for further information.

18. **For book authors** the following clauses are applicable in addition to the above: Authors are permitted to place a brief summary of their work online only. You are not allowed to download and post the published electronic version of your chapter, nor may you scan the printed edition to create an electronic version. **Posting to a repository:** Authors are permitted to post a summary of their chapter only in their institution's repository.

19. **Thesis/Dissertation**: If your license is for use in a thesis/dissertation your thesis may be submitted to your institution in either print or electronic form. Should your thesis be published commercially, please reapply for permission. These requirements include

permission for the Library and Archives of Canada to supply single copies, on demand, of the complete thesis and include permission for Proquest/UMI to supply single copies, on demand, of the complete thesis. Should your thesis be published commercially, please reapply for permission. Theses and dissertations which contain embedded PJAs as part of the formal submission can be posted publicly by the awarding institution with DOI links back to the formal publications on ScienceDirect.

Elsevier Open Access Terms and Conditions

You can publish open access with Elsevier in hundreds of open access journals or in nearly 2000 established subscription journals that support open access publishing. Permitted third party re-use of these open access articles is defined by the author's choice of Creative Commons user license. See our open access license policy for more information.

Terms & Conditions applicable to all Open Access articles published with Elsevier:

Any reuse of the article must not represent the author as endorsing the adaptation of the article nor should the article be modified in such a way as to damage the author's honour or reputation. If any changes have been made, such changes must be clearly indicated.

The author(s) must be appropriately credited and we ask that you include the end user license and a DOI link to the formal publication on ScienceDirect.

If any part of the material to be used (for example, figures) has appeared in our publication with credit or acknowledgement to another source it is the responsibility of the user to ensure their reuse complies with the terms and conditions determined by the rights holder.

Additional Terms & Conditions applicable to each Creative Commons user license:

CC BY: The CC-BY license allows users to copy, to create extracts, abstracts and new works from the Article, to alter and revise the Article and to make commercial use of the Article (including reuse and/or resale of the Article by commercial entities), provided the user gives appropriate credit (with a link to the formal publication through the relevant DOI), provides a link to the license, indicates if changes were made and the licensor is not represented as endorsing the use made of the work. The full details of the license are available at http://creativecommons.org/licenses/by/4.0.

CC BY NC SA: The CC BY-NC-SA license allows users to copy, to create extracts, abstracts and new works from the Article, to alter and revise the Article, provided this is not done for commercial purposes, and that the user gives appropriate credit (with a link to the formal publication through the relevant DOI), provides a link to the license, indicates if changes were made and the licensor is not represented as endorsing the use made of the work. Further, any new works must be made available on the same conditions. The full details of the license are available at http://creativecommons.org/licenses/by-nc-sa/4.0.

CC BY NC ND: The CC BY-NC-ND license allows users to copy and distribute the Article, provided this is not done for commercial purposes and further does not permit distribution of the Article if it is changed or edited in any way, and provided the user gives appropriate credit (with a link to the formal publication through the relevant DOI), provides a link to the license, and that the licensor is not represented as endorsing the use made of the work. The full details of the license are available at http://creativecommons.org/licenses/by-nc-nd/4.0. Any commercial reuse of Open Access articles published with a CC BY NC SA or CC BY NC ND license requires permission from Elsevier and will be subject to a fee.

Commercial reuse includes:

- Associating advertising with the full text of the Article
- Charging fees for document delivery or access
- Article aggregation
- Systematic distribution via e-mail lists or share buttons

Posting or linking by commercial companies for use by customers of those companies.

20. **Other Conditions**:

v1.10

Questions? E-mail us at customercare@copyright.com.

Acknowledgements

I would like to thank my advisor Prof. Mikael Simons who gave me the opportunity to work on this exciting project. I appreciate his insight and resources. I would also thank co-authors of my papers and the supporting facilities, including the animal facilities in TUM Biederstein campus and DZNE, and the SyNergy EM facility. My PhD research won't be possible without their contributions.

I thank people that gave critical feedback to the research: my TAC members (Prof. Thomas Misgeld and Prof. Christian Behrends), and Prof. Volker Haucke. I also thank Prof. Shujun Cai (Southern University of Science and Technology, Shenzhen, China) and Dr. Jennifer Lippincott-Schwartz (Janelia Research Campus, HHMI) for inputs on the EM.

I would like to thank the Simons lab. I don't have a senior lab member as my supervisor when I joined the lab, and many people generously offered to teach me something out of their busy schedule without getting authorship or help from me. They are Liliana Pedro that showed me the primary oligodendrocyte culture and oli-neu culture, Chaitali Mukherjee that showed me perfusion, slice culture and floating section, Janos Groh that advised me on quantification of myelin degeneration, Minou Djannatian and Martina Arends that showed me optic nerve dissection and zebrafish injection, Seiji Kaji that helped me to troubleshoot biochemistry experiments. In addition to research, I thank my lovely friends in the lab for their personal support and the laughter we shared.

I also thank the organizations that provided me with training opportunities: my graduate school - Graduate School of Systemic Neuroscience (GSN), and SyNergy for the travel grant to Cell Bio 23 conference, and for the mentoring program for female scientists.

I would like to express my gratitude to my former mentor, Prof. Charlie Barlowe, and my former school Dartmouth's cell biology community for providing a solid foundation for my PhD studies. Charlie introduced me to the field of membrane biology and taught me endoplasmic reticulum and nonvesicular lipid transport, which became the primary focus of my doctoral work. At Dartmouth, I not only received an excellent education—learning extensively about microscopy and cell biology—but also

experienced tremendous support throughout and even after my studies. Prof. Bill Wickner is an example. Whenever I encountered challenges in Munich, I always sought advice from him. Additionally, my classmate Thomas Torng has become my best science friend. Whenever I got cool results, he is the first person I share them with.

Last but not least, I would like to thank my family: my parents, my sister, and my husband, Julian Heger. Pursuing a PhD is a challenging journey, filled with back pains, hunger, and mental stress. I am grateful I can come home, laugh and refresh. I could not have persisted without Julian's love and support.

Declaration of author contributions

We hereby declare author contributions as follows:

Majority of the contents in the results section has been submitted as a research article:

Jianping Wu, Georg Kislinger, Ayşe Damla Durmaz, Benedikt Wefers, Karsten Nalbach, Christian Behrends, Wolfgang Wurst, Martina Schifferer, Mikael Simons. "Nonvesicular lipid transfer drives myelin growth in the central nervous system"

Jianping Wu (J.W.)'s detailed contributions are:

- J.W. proposed to study nonvesicular lipid transport and GLTP, and co-designed experiments with Mikael Simons (M.S.).
- J.W. conducted experiments except for the following:
    (1) Electron microscopy samples were processed and imaged by SyNergy EM facility (Georg Kislinger and Martina Schifferer).
    (2) J.W. trained master student Ayşe Damla Durmaz and conducted experiments together for Fig 3.2.1a-g, Fig 3.2.2 a-c, Fig 3.3.1a-d.
    (3) Shortgun lipidomics analysis were performed by Lipotype.
    (4) Karsten Nalbach and Christian Behrends provided technical support to search for GLTP interactors.
    (5) The *Gltp* KO and *Gltp flox* mouse lines were generated by DZNE transgenic facility (Benedikt Wefers and Wolfgang Wurst).
- J.W. quantified all resulting data and generated all the figures.
- J.W. and M.S. together interpreted the results and wrote the manuscript.

The discussion section of this dissertation primarily reflects J.W.'s personal views, with some inputs from M.S. The working model and the graph depicting GalCer distribution across various leaflets in both wildtype and knockout samples were developed by J.W.

Yours truly,

Jianping Wu

Mikael Simons